Multi-imaging approach to analyze bioactive compounds in *Abelmoschus moschatus* and *Cinnamomum zeylanicum* via planar chromatography hyphenated with effect–directed assays and high-resolution mass spectrometry

Cumulative dissertation

for the degree of

Doctor rerum naturalium (*Dr. rer. nat.*)

by

N.G.A.S. Sumudu Chandana

Submitted to

Faculty of Agricultural Science, Nutritional Science,

and Environmental Management

Prepared at

Department of Food Science

Institute of Nutritional Science

Justus Liebig University Giessen, Germany

Giessen, March 2022

Multi-imaging approach to analyze bioactive compounds in *Abelmoschus moschatus* and *Cinnamomum zeylanicum* via planar chromatography hyphenated with effect–directed assays and high-resolution mass spectrometry

Cumulative dissertation

for the degree of

Doctor rerum naturalium (*Dr. rer. nat.*)

by

N.G.A.S. Sumudu Chandana

Index No:7049891

Submitted to

Faculty of Agricultural Science, Nutritional Science,

and Environmental Management

Prepared at

Department of Food Science

Institute of Nutritional Science

Justus Liebig University Giessen, Germany

Giessen, March 2022

TABLE OF CONTENT

DECLARATION

Declaration

I declare that the dissertation submitted is a work of my own, written without any illegitimate help by any third party and only with materials indicated in the dissertation. I have indicated in the text where I have used texts from already published sources, either word for word or in substance, and where I have made statements based on oral information given to me. At any times during the investigations carried out by me and described in the dissertation, I followed the principles of good scientific practice as defined in the "Statutes of the Justus Liebig University Giessen for the safeguarding of Good Scientific Practice".

N.G.A.S. Sumudu Chandana

Giessen, March 2022

REVIEWERS AND EXAMINERS

1st Reviewer

Professor Dr. Gertrud Morlock

Department of Food Science

Institute of Nutritional Science, Justus Liebig Giessen University

2nd Reviewer

Professor Dr. Sylvia Schnell

Department of General and Soil Microbiology

Institute of Applied Microbiology, Justus Liebig Giessen University

1st Examiner

Professor Dr. Wolfgang Schwack

Department of Food Science

Institute of Nutritional Sciences, Justus Liebig University Giessen

2nd Examiner

Professor Dr. Anika Wagner

Department of Nutrition and Immune System

Institute of Nutritional Sciences, Justus Liebig University Giessen

ACKNOWLEDGEMENTS

I am greatly indebted to my supervisor Professor Dr. Gertrud Morlock, who gave me a valuable opportunity to join her laboratory and continue my higher education. Her advice, guidance, expertise, and support were instrumental in the success of my studies. I am also grateful to my co-supervisor Professor Dr. Sylvia Schnell for her great support of my PhD study. I acknowledge Prof. Dr. Wolfgang Schwack, Dr. Ines Klingelhöfer and Dr. Ebrahim Azadniya who provided advice, and in particular, Annabel Mehl, who assisted for mass spectrometry recording. Further, I would like to thank the Food Science group of Prof. Dr. Morlock, especially Daniel Meyer, Stefanie Kruse, Tamara Schreiner, Isabel Mueller, Julia Heil, Simone Cutts and Elke Balzer for kind support and help during my studies.

DEDICATION

To my mother and father

To all teachers during my education

To my brother and his family

To my sister and her family

SCIENTIFIC CONTRIBUTION

Peer-reviewed original research papers

1) Chandana, NGASS, Morlock, GE (2021) Comprehensive bioanalytical multi-imaging by planar chromatography *in situ* combined with biological and biochemical assays highlights bioactive fatty acids in abelmosk, *Talanta*, 223, 121701
https://doi.org/10.1016/j.talanta.2020.121701

Contribution of Chandana, NGASS: performance of the experiments supported by the Food Science group and writing of the initial draft.

2) Chandana, NGASS, Morlock, GE (2021) Eight different bioactivity profiles of 40 cinnamons to discover multipotent compounds by multi-imaging planar chromatography hyphenated with effect-directed analysis and high-resolution mass spectrometry, *Food Chemistry*, 357, 129135
https://doi.org/10.1016/j.foodchem.2021.129135

Contribution of Chandana, NGASS: performance of the experiments supported by the Food Science group and writing of the initial draft.

List of Figures

List of Abbreviations

AChE	Acetylcholinesterase
AD	Alzheimer's disease
ADC2	Automatic Development Chamber 2
BChE	Butyrylcholinesterase
DPPH•	2,2-Diphenyl-1-picrylhydrazyl
EFSA	European Food Safety Authority
EDA	Effect-directed analysis
GC	Gas chromatography
GPC	Gel permeation chromatography
HILIC	Hydrophilic interaction liquid chromatography
HPLC	High-performance liquid chromatography
HPTLC	High-performance thin-layer chromatography
L-DOPA	L-3,4-Dihydroxyphenylalanine
MS	Mass spectrometry
NMR	Nuclear magnetic resonance spectroscopy
PC	Positive control
PPOs	Polyphenoloxidases
ROS	Reactive oxygen species
T2DM	Type 2 diabetes mellitus
TLC	Thin-layer chromatography
TRP	Tyrosinase-related protein
WHO	World Health Organization

1 Introduction

1.1 Bioactive compounds

Bioactive compounds or natural products are molecules with biological activity derived from natural sources such as plants, animals and microorganisms (Abdel-Razek et al. 2020). People are now paying more attention to natural products to improve living standards and strengthen health awareness (Zhang et al. 2020). According to the history of bioactive compounds, the earliest documentation reported from Mesopotamia`s medicinal system is from 2900 to 2600 BCE, and by the early 1900s, regarding the application of natural products to improve human health, 80% of all medicine was obtained from plant sources (Pham et al. 2019). Natural products have been extensively used in food, healthcare, perfume, cosmetics and pharmaceutical fields (Zhang et al. 2020). For instance, natural products play a significant role in the current discovery and development of drugs (Medina-Franco 2019), because of their incomparable structural diversity, relatively smaller size molecules (<2000 Da) and drug-like properties such as their ability to be absorbed and metabolized (Sticher 2008). In addition, natural products are less toxic compared to synthetic products (Kotha and Luthria 2019).

In the past decades, natural products have become more popular in the western world as they have high pharmacological activities and rare complications (Rab et al. 2020). The reason for the fewer complications from natural products is that it is assumed that natural products are more compatible with biological systems (Ahmad et al. 2020). As popularity has been increasing for the application of natural products in dietary supplements, cosmetics, and treatments, rapid authentication and standardization seem to be essential for these products (Ebrahimi-Najafabadi et al. 2019).

1.2 Herbal extracts

Eighty percent of the world population depend on traditional medicine as primary healthcare (Osathanunkul et al. 2018). The herbal sources used in traditional medicine consist of significant amounts of bioactive compounds with valuable health effects. A single plant may contain one or more bioactive compounds, and traditional medicine uses combinational approaches to enhance therapeutic effects (Kuruppu et al. 2019). Several drawbacks influence the quality of herbal drugs, such as the source of raw material, chemical constituents, part of the plant collected, harvesting season, plant origin, drying process, active principles mostly unknown, and selective analytical methods or references may not be commercially available.

Therefore, quality assurance of herbal medicine has become an important factor for the herbal drug manufacturing sector and other drug development organizations (Shivatare R.S et al. 2013).

There is a growing interest in the identification of compounds responsible for health-promoting effects from botanicals (Krüger et al. 2017). Natural products from medicinal plants provide extensive opportunities for new drugs because of the unparalleled accessibility of diverse chemical compounds (Gul et al. 2011). Although many of these compounds have been identified as therapeutic agents, there are many more that need to be investigated as potential therapeutic agents for novel drug discovery (Agatonovic-Kustrin and Morton 2020a). Herbal extracts are more affordable, clinically effective, and have fewer side effects than modern drugs (Tran et al. 2020). In addition, in comparison to synthetic drugs, herbal products have been used by humans over centuries and have time-proven safety (Jayasinghe and Jayawardena 2019). Herbal drugs with fewer side effects and safer pharmacological profiles for various diseases are becoming of interest (Sahoo and S 2019). Major pharmaceutical companies are currently conducting a wide range of research on plant materials to assess their medicinal value. The annual global market for herbal medicine stays at over $60 billion (Itankar et al. 2015). Several medicines have been produced by the origin of medicinal plants. Salicylates (willow bark), digitalis (from foxglove), and quinine (from cinchona) are some examples of plant-derived medicinal drugs (Sen and Samanta 2015). Plant secondary metabolites are used as an important source of active traditional medicine, perfume, industrial raw material, pharmaceutics, cosmetics, fine chemicals, or more recently nutraceuticals, due to their remarkable activity. Some examples for plant secondary metabolites are as follows and they have been classified according to chemical structure: phenolic acid, flavonoids, terpenoids, steroids, and alkaloids, etc. (Yang et al. 2018).

Extraction, pharmacological screening, isolation and characterization of the bioactive substances with beneficial biological activity is highly important for the use of alternative medicine (Ozaslan and Oguzkan 2018). In the analytical method development process, for the analysis of botanicals and herbal products, the sample preparation step is important. The basic procedure steps include prewashing, drying of plant materials or freeze-drying, grinding to obtain a homogenous sample, and common methods such as sonication, heating under reflux, and Soxhlet extraction are used (Ong 2004). The extraction method should be simple, fast, efficient, selective, reproducible, and following the principles of green chemistry and Environment Protection Agency guidelines. However, meeting all these criteria is challenging, due to the high sample complexity, low concentrations of target compounds, and

matrix interference effects, and some compounds are unstable (Liang et al. 2020). Suboptimal sample preparation and analytical methods are needed for the accurate evaluation of bioactivities and their clinical efficacy (Kotha and Luthria 2019). The primary processing step of medicinal plants for herbal drug preparation directly influences the active pharmaceutical ingredients. Because of the hereditary complex nature of growing medicinal plants, and the available definite number of simple analytical techniques to identify active ingredients, there is a need for an adequate quality assurance system for herbal drugs (Kunle 2012). Due to the lack of a well-organized regulation and legislation system for traditional medicine and herbal products, the world health organization (WHO) and other regulatory bodies are concerned about the efficacy and safety of herbal medicine (Ebrahimi-Najafabadi et al. 2019).

1.3 Separation of bioactive compounds

Identification of pharmacologically active compounds from natural sources is a challenging task (Medina-Franco 2019). For instance, botanicals contain hundreds of chemical constituents, and among them a few components are bioactive. Therefore, the use of separation and detection methods for rapid analysis of the chemical composition presents a significant challenge, due to the variability and complexity of botanical extracts (Wu et al. 2013). The complex nature of extracts obstructs the separation and determination of a single component, which is difficult (Migas et al. 2020). The analytical techniques need to continually improve to overcome problems such as matric effects and to detect low abundance analytes in complex mixtures (Laub et al. 2020). The discovery of a new drug is a multidisciplinary, expensive task and major steps are the identification of a lead compound (a certain degree of potency), metabolic properties, and pharmacokinetics profiles (Ntie-Kang and Svozil 2020). The phytochemical profile of the medicinal plant, which describes its therapeutic value, provides valuable information for the discovery of new drugs. The discovery of new chemical structures with pharmacological effects mainly depends on chance, and therefore there is a probable need to screen a large number of compounds (Gupta et al. 2019). According to the literature, various analytical techniques are described to separate complex mixtures and each technique has its restrictions (Kharat et al. 2017).

From the point of view of separation, chromatographic methods are highly efficient for the analysis of natural products (Wu et al. 2013). Therefore, natural product researchers are more concerned with chromatography techniques for the separation of chemical components in complex extracts, to evaluate chemicals of natural origin in biological activity assays and

clinical trials (Friesen et al. 2015). Chromatography-based techniques are accepted internationally to determine the efficacy and authenticity of herbal drugs (Kaur et al. 2020). As per modern research parameters, standardization of polyherbal formulations for quality has become an essential requirement and chromatography is recommended by the WHO as an accepted tool for the quality assessment (Abraham et al. 2020).

According to the nature of stationary or mobile phases and the mechanism of distribution involved, chromatographic techniques can be classified as (1) high-performance liquid chromatography (HPLC), (2) gas chromatography (GC), (3) thin-layer chromatography (TLC), (4) gel permeation chromatography (GPC), (5) partition chromatography (PC), (6) counter-current chromatography (CCC), (7) supercritical fluid chromatography (SCFC), (8) and ion-exchange chromatography, etc. (Ullah and Mohammad 2020). TLC is the first choice for phytochemical analysis, and this technique is trustworthy, rapid and simple, and can be hyphenated for multi-detection. High-performance thin-layer liquid chromatography (HPTLC) is the development of conventional TLC and this is the preferred method for tracing bioactivity in extracts (Chaita et al. 2017). The main differences between TLC and HPTLC are the particle size and pore size of sorbent (Ullah and Mohammad 2020). HPLC and HPTLC are established techniques (Singh et al. 2015). HPTLC has been accepted as an effective and suitable analytical platform because of its high accuracy, adaptability, flexibility and reproducibility, and it can generate a quick fingerprint of diverse samples in a unique analysis (Maldini et al. 2019). On the one hand, HPLC uses large quantities of solvent with a high concentration of buffers, which requires a lot of time for the analyte detection and may lead to some restrictions. On the other hand, the HPTLC technique uses smaller quantities of solvents, is cost-effective and can analyze a large number of samples in a short period (Ganorkar and Shirkhedkar 2017). For HPTLC there exist facilities to optimize operational parameters, such as sample application, plate development, documentation and derivatization, and these are the main advantages of this technique (Mulaudzi et al. 2021). In comparison to TLC, the HPTLC technique produces better resolution, sensitivity, and reproducible results, and combining with digital scanning and documentation software is able to obtain complete information (Mulaudzi et al. 2021). After separation, the same analyte can be observed under different wavelengths in HPTLC, and this provides a more complete profile picture of constituents of plant extracts rather than a more specific type of analysis (Kunle 2012). HPTLC provides a high sample throughout with the in-situ recording of spectra, thus enabling simple and reliable identification and quantification of components (Dubey et al.

2012). However, HPTLC has a few restrictions, such as a low plate efficiency and narrow developing distance compared with GC and HPLC (Kharat et al. 2017).

Basic steps in HPTLC method development include: selection of stationary phase, mobile phase selection, mobile phase optimization, sample preparation, sample application, chromatogram development and detection (Shivatare R.S et al. 2013). The HPTLC technique uses automated application devices to spray extracts as thin bands and this dramatically improves the application procedure (Urbain and Simões-Pires 2006). The chromatography separation technique separates compounds between two phases. One phase is fixed on a plate (stationary phase) and the other phase is mobile and known as the mobile phase. Silica gel is the dominant stationary phase used in HPTLC. The most common is silica gel 60, which has a pore size of 6 nm (60° A), and the average surface concentration of OH groups is about 8 µmol/m^2 (Spangenberg et al. 2011). The interaction between the analyte and the silanol groups in the unmodified silica, where the mobile phase is apolar, is known as a normal phase chromatography system. The interaction between analyte with the apolar modified silica gel layer, where the mobile phase is polar is referred to as reversed-phase chromatography (Shewiyo et al. 2012). In normal phase chromatography, retention increases as the polarity of the mobile phase decreases and polar analytes are more strongly retained than nonpolar ones. The opposite situation occurs in reversed-phase liquid chromatography (Buszewski and Noga 2012). The interaction of analytes with polar (modified) layers, as in normal phase chromatography but in which the mobile phases are polar (e.g. methanol-based), is called HILIC (hydrophilic interaction liquid chromatography) (Shewiyo et al. 2012).

In the development, the sample component interacts with both the stationary and mobile phase according to the dominated mechanism by the absorption process. The forces, which are van der Waal´s forces, dipole-type interactions, and complexation interactions such as hydrogen bonding, are involved in adsorption chromatography. For chromatographic separations, the adsorption process must be reversible and only involves physical interactions (Spangenberg et al. 2011). A compound structure and the system temperature play a role in adsorption. Under constant temperature, the balance of adsorption interaction depends on the solute concentration at the adsorbent surface and its concentration in the mobile phase. Chromatographic results can be seriously influenced by the polarity of the stationary phase, mobile phase selection, and composition of the vapour phase (Spangenberg et al. 2011). Using an automatic developing chamber avoids irregular curve-like elution in chromatogram in the development process by controlling the humidity (Urbain and Simões-Pires 2006). The separated compounds detected can be plotted with separation distance and namely as

densitogram. In the densitogram, the retardation factor (R_f factor) is the outcome of the distance of the substance zone from sample origin to the front of the mobile phase (Spangenberg et al. 2011). After the multifaction Rf value by 100, the hR_f value is obtained. HPTLC is based on R_F-values, provides information about the analyte, such as polarity, spectral properties, such as absorbance, fluorescence etc. (Dimkić et al. 2017). The chromatographic separation process by fractionation reduced the complexity of the sample matrix and this easily allows chemical analysis and better identification of unknown compounds (Agatonovic-Kustrin et al. 2019). TLC and HPTLC can include processing samples and standards at the same time and with versatile detection including different post-chromatographic derivatization reagents (combined with derivatization reagent, allowed to react with sample compounds, and transformed them into detectable derivatives) (Biringanine et al. 2006). The use of proper standardization of HPTLC methods allows for reliable, precise and reproducible quantitative results (Morlock and Schwack 2010).

1.4 Multi-imaging

HPTLC is an adaptability system for comprehensive detection, which can combine UV/Vis absorption and fluorescence measurements, detection of functional groups using derivatization reagents, and can also be coupled with a mass spectrometer (MS) for compound identification (Weiss et al. 2017). Recently, HPTLC-based multi-imaging profiling studies have been under development. Under this technique via effect-directed profiling, individual activity profiles are visualized as images and capture important information. This comprehensive detection plus nontargeted bio-profiling allows for fast detection of target compounds (Morlock and Heil 2020). Using HPTLC can rapidly screen authenticate the herbal product and differentiate related herbal species (Mulaudzi et al. 2021). This chromatographic fingerprint investigation is a realistic and practical approach for quality assessment and species authentication, and using this method can identify the presence or absence of markers of concern as well as the ratio of all detectable compounds (Kharat et al. 2017).

In this process, the HPTLC tool is used after being combined with suitable reference material for comparison. Comprehensive fingerprinting concept images are converted into peak profiles and intensities of selected zones compared to corresponding zones of the reference material. This comparison is more objective than the simple visual comparison of zone intensities. A single HPTLC analysis provides information about identity, purity and minimum content of markers of an herbal drug (Frommenwiler et al. 2018), using dynamic

reference standards or pooled reference samples, which can better capture seasonal, geographical, environmental, or processing variations (Islam et al. 2021). Herbal diet food adulteration with unsafe drugs is growing in market products, and to solve this problem simple and rapid methods are needed to detect adulterants. HPTLC is proved to be a well-fitted method for routine quality control to handle the problem of the adulteration of foodstuffs with drugs (Mathon et al. 2014). This is because, in HPTLC fingerprints, chromatograms can be compared between authentic samples and unknowns for the identification of drugs or adulterants (Hazra et al. 2004). Open source web packages (for example rTLC software) are available for image processing and a combination of HPTLC with this technology is able to perform chemometric analysis and explore differences and similarities within individual samples (Mulaudzi et al. 2021).

Validation is the performance characteristics of an analytical method that meets the requirement for the intended applications and characterizations achieved through a statistical approach of accuracy, precision, specificity, detection limit, quantification limit and linearity. The idea of validation used for the densitometric evaluation on HPTLC varies according to the goal of the analysis (Biringanine et al. 2006).

1.5 Effect-directed analysis

HPTLC is a cost-effective, simple, and fast technique for fingerprint separation, such as complex samples of phytochemicals (Kroslakova et al. 2016). In recent decades, the traditional approaches used to discover therapeutic activity have been challenged, due to difficult and expensive methods, and the bioactivity was studied after the isolation of compounds (Agatonovic-Kustrin and Morton 2020a). Effect-directed analysis (EDA) is a combined strategy of HPTLC linked bioassays, biochemical assays, and chemical assays. In this approach, the aim is to identify the compounds in the sample with significant biological effects, using direct chemical analysis. In the process, a complex sample (plant extract) is separated by chromatography (chemical fractionation), detection of bioactivity and chemical class, and finally by identifying the individual bioactive compounds (Agatonovic-Kustrin and Morton 2020a). EDA can be design target and nontarget analysis. Under target analysis, most bioactive compounds were left undiscovered, due to focused only known target compounds. However, the use of nontargeted EDA analysis enables the identification of a huge list of compounds that are responsible for a certain biological effect (Agatonovic-Kustrin and Morton 2020a). In effect-directed profiling, the individual activity profiles are visualized as images, and the important individual substances can be identified (Morlock and Heil 2020).

Compounds identification is based on chromatographic-spectroscopic hyphenated techniques. The bioactive zones of interest can be eluted from the HPTLC plate with a suitable solvent and either transferred online to the MS or collected in a sample vial for further offline analysis (Agatonovic-Kustrin and Morton 2020b).

There are many advantages in HPTLC linked EDA and these are proved in the literature (described as follows) (Morlock and Schwack 2010). False results are minimal compared to other high-throughput systems, which can occur due to interferences in a cuvette or microtiter plates. The sample clean-up step is minimal due to the single-use of the stationary phase and matrix-robustness of HPTLC. While providing a comprehensive view of bioactive compounds for discovering new compounds, and low-cost, fast, and rapid response time especially for bioactivity, are some of the other advantages. The organic solvents used in mobile phases for development are removed or evaporated before bio-detection, which does not affect the enzyme or bioassays. In the separation step, the number of substances is reduced from the complex mixture and allows more effective decisions and further analysis or evaluations. The detection limits are typically within the ng to pg range. Using digital image evaluation systems detected compounds can be quantified. Effect-directed profiling and multi-imaging can identify known functional food ingredients, but also detect compounds such as bioactive contaminants, residues, or adulterations (Morlock et al. 2021). Using HPTLC-based densitometric measurements, prominent spots can be detected using a plate scanner operated by software that is capable of converting the spots under spectroscopic detection into densitograms. This approach provides analytical results of herbal product evaluation similar to HPLC (Urbain and Simões-Pires 2006).

Diabetes mellites, Alzheimer's disease, and the increasing of multi-resistant bacteria are prominent global health problems and need novel effective therapeutic agents. Antioxidants, skin whitening agents, and inhibitors for enzymatic browning of fruit and vegetables from natural sources are also interesting research areas for the pharmacy, cosmetic, and food industries, respectively. EDA can be used to screen antidiabetic, antibacterial, acetylcholine esterase inhibitors, tyrosinase inhibitors, and antioxidant compounds from plant extracts.

1.5.1 Screening antidiabetic compounds

The incidence of global type 2 diabetes mellitus (T2DM) is increasing (Bharti et al. 2012) and is predicted to be 693 million by 2045 (Cole and Florez 2020). In past decades, antidiabetic agents screening research have become interested and natural products are one of the probable sources of drug discovery (Jugran et al. 2020). Some plant-derived drugs have

shown more antidiabetic activity than the currently used oral hypoglycaemic agents (Tran et al. 2020). For the treatment of diabetes, medicinal plant different species are used. Before the discovery of insulin for diabetes treatment, the only options were based on traditional practices (herbal products). Metformin is one of the major accepted drugs for type 2 diabetes mellites and this drug is derived from a medicinal plant *Galega officinalis* (Bailey 2017). Glucosidases are involved in different metabolic disorders, and inhibition of glucosidase, including β-D-glucosidase has many promising applications (Abu Khalaf et al. 2011). Alpha-glucosidase inhibitors screening via HPTLC bioautography provides a simple and effective method for the investigation of complex samples, such as plant extracts (Theiler et al. 2017).
According to Jamshidi-Aidji et al. (2019), an HPTLC regarding an α-glucosidase inhibition assay, *α*-D-glucosidase converts 2-naphthyl-*α*-D-glucopyranoside into α-naphthol, in which α-naphthol reacts with fast blue B salt (chromogenic agent) giving a purple-coloured background on the HPTLC plates **(Figure 1)**. *α*-D-glucosidase enzymatic inhibitors inhibit *α*-D-glucosidase and block the conversion of 2-naphthyl-*α*-D-glucopyranoside into α-naphthol, resulting in no reaction with fast B salt. As a result, *α*-D-glucosidase enzymatic inhibitors available position on HPTLC plate, visualized as a whitish zone on the purple colour plate background.

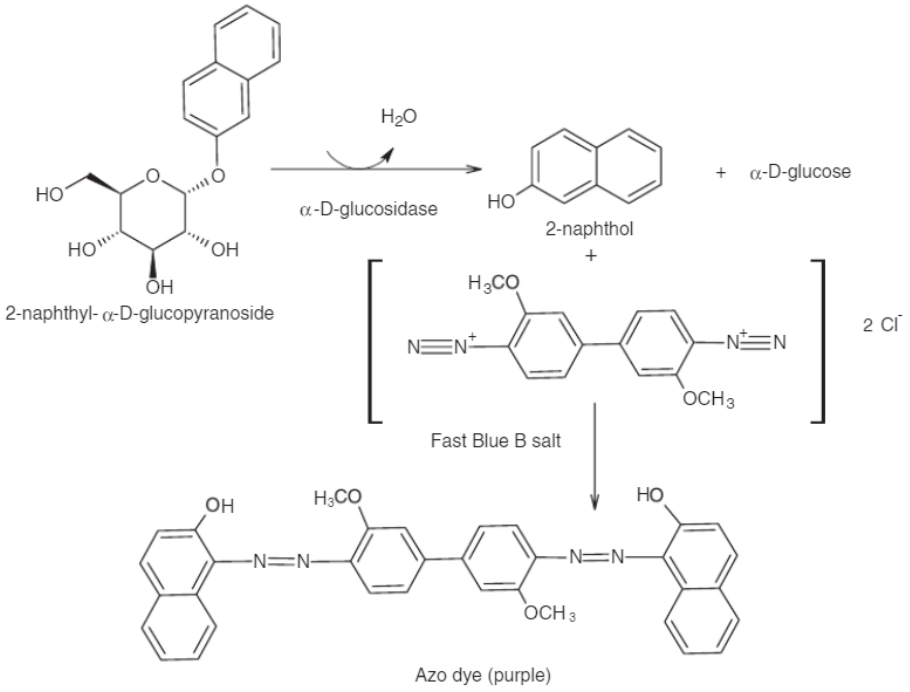

Figure 1. The reaction of *α*-D-glucosidase with 2-naphthyl-*α*-D-glucopyranoside and the subsequent formation of the purple dye between 2-naphthol and Fast Blue B salt in the TLC bioautographic assay (Simões-Pires et al. 2009).

1.5.2 Screening acetylcholinesterase inhibitors

Alzheimer's disease (AD) is the commonest form of dementia. In 2015, 46.8 million people were living with dementia, a number predicted to double every 20 years (Wightman 2017). Scientists are looking for new treatment strategies to improve the quality of life in patients with AD (Trifunović et al. 2017). Neurodegenerative disease is AD-associated with memory and cognition impairment, and acetylcholinesterase (AChE) inhibitors are used as one of the major therapeutic strategies (Dey et al. 2017). In this process, the target drugs inhibit the action of the AChE enzyme, thus decreasing the breakdown of acetylcholine, and as a result increasing cholinergic neurotransmission (Birks 2006). AChE inhibitory compounds already have been reported from the plant; as an example, galantamine is obtained from the *Galanthus* species, which is used to treat symptoms of mild to moderate dementia in AD (Galarce-Bustos et al. 2019). Acetylcholine esterase inhibitors, tacrine, donepezil, rivastigmine, and galantamine have been approved by the Food and Drug Administration in the United States. Synthetic drugs other than galantamine have side effects. In recent studies are prompting a greater focus on finding natural acetylcholinesterase inhibitors with fewer side effects (Yang et al. 2009). In the last two years, an HPTLC linked AChE assay-based piezoelectric spraying method has been introduced to screen AChE inhibitors (Azadniya and Morlock 2019). According to Azadniya and Morlock (2019), regarding the HPTLC AChE inhibitory assay, acetylcholine esterase converts α-naphthyl acetate into α-naphthol, which reacts with fast blue B salt (chromogenic agent) to give a purple-coloured background on the HPTLC plates, while AChE inhibitors produce white spots due to enzyme inhibitors inactivating the acetylcholine esterase and so there is no conversion of α-naphthyl acetate into α-naphthol and hence no purple colouration produced (**Figure 2)**.

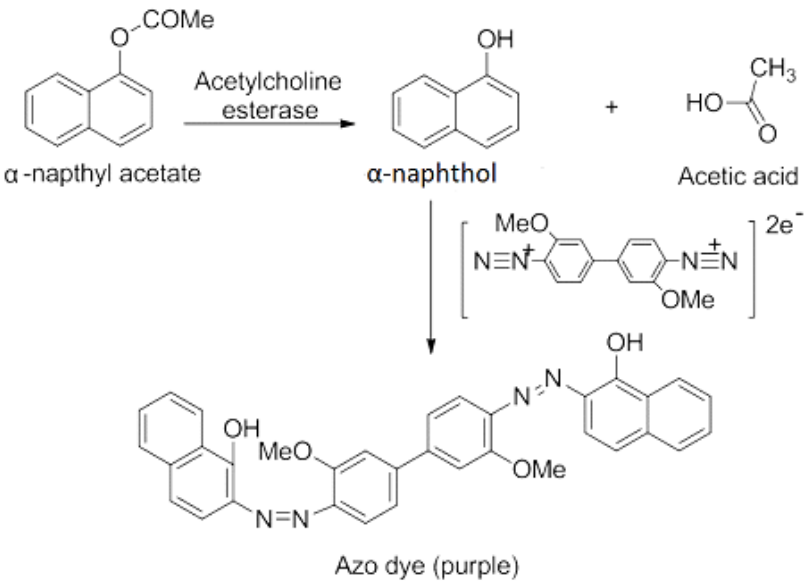

Figure 2. The chemical reaction conversion of α-naphthyl acetate into α-naphthol by acetylcholine esterase and then α-naphthol reacts with fast blue B salt to produce purple-coloured azo dye (Dewanjee et al. 2015).

1.5.3 Screening antibiotics

Infectious diseases are caused by microorganisms recognized as a global health threat by the WHO, and annually about 3.5 million people die from infectious diseases (Ruwizhi and Aderibigbe 2020). Recently, due to the misuse and overuse of antibiotics, the effectiveness of drugs has reduced and increased the development of resistant bacteria (Kostić et al. 2020). The development of new antibiotics is essential to control the increasing threat of multidrug-resistant bacteria (Mühlberg et al. 2020). For the discovery of novel bioactive agents, investigation of medicinal plants is considered as a feasible approach to solve widespread health problems (Sharma et al. 2017). Plant extracts and their isolated pure compounds are necessary sources for the control of current viral infections and useful for future challenges (Mohan et al. 2020). From ancient times, plants have been used for different purposes, such as treating infectious diseases (Sakkas and Papadopoulou 2017). As plants contain plenty of biological and structural different compounds, they are a good source for the discovery of new antibacterial, antifungal, and antiparasitic compounds (Sakkas and Papadopoulou 2017). For instance, several studies have shown cinnamon extracts, cinnamon essential oil, and pure compounds show significant antimicrobial activity against the oral pathogen (Yanakiev 2020).

Antibacterial compounds for gram-negative bacteria can be screened using HPTLC - *Aliivibrio fischeri* bioassay (Azadniya and Morlock 2019). *A. fischeri* is a gram-negative marine bacterium that emits bioluminescence at a critical density. This bioluminescence is associated with bacterial metabolism. Luciferase is the bioluminescence catalyst and it catalyzes an oxidation reaction that releases excess energy in the form of light. In screening antibacterial compounds on HPTLC plate, after introducing *A. fischeri* culture on to HPTLC plate, it decreases light intensity that indicates a disturbance of the bacteria metabolism, and antibacterial compound positions (for gram-negative bacteria) indicate dark zones on a luminescent background.

The HPTLC-*Bacillus subtilis* bioassay (Jamshidi-Aidji et al. 2019) can be used for screening antibacterial compounds for gram-positive bacteria. In the MTT assay, the live bacterial cells contain dehydrogenase reduced MTT (3-(4,5-dimethylthiazol-2-yl)-2,5-diphenyltetrazolium bromide) into coloured formazan **(Figure 3)**. Antibacterial compounds (for gram-positive bacteria) inhibit bacterial dehydrogenase activity, and antibacterial compound positions on the plate were observed as pale-yellow zones on a purple-coloured background.

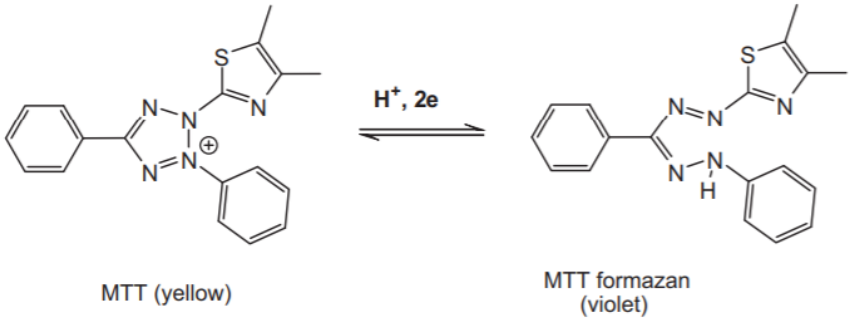

Figure 3. Detection of microorganism dehydrogenase activity by reduction of tetrazolium salts (Marston 2011).

1.5.4 Screening tyrosinase inhibitors

Melanin is the pigment accountable for the colour of hair and skin, and hyperpigmentation of melanin can produce skin problems such as age spots, melasma and melanoma (Iraji et al. 2021). The melanin synthesis process is known as melanogenesis, and the enzymes such as tyrosinase and tyrosinase-related protein-1 (TRP-1) and TRP-2 played a major role in melanin synthesis (Pillaiyar et al. 2017). Reducing skin pigmentation is popular in many cultures and whitening agents such as corticosteroids, tretinoin and hydroquinone are effective for lightening the skin. However, they have a variety of side effects (Desmedt et al. 2016). Therefore, research for new tyrosinase inhibitors for pharmaceutical, cosmetic

industries has become of interest (Bonesi et al. 2019). Plant origin tyrosinase inhibitors are broad and their chemistry and biological activity have been described in the literature (Wu 2014). Enzymatic browning of food and vegetables is caused by polyphenol oxidases (PPOs) and affects the quality of the colour of fruit and vegetables. This enzyme catalyzes the hydroxylation of monophenols to *o*-diphenols and their subsequent oxidation to *o*-quinones (Urbain and Simões-Pires 2006). As currently used synthetic chemical PPO inhibitors have several drawbacks, there is a focus on consumer-oriented, natural and environmentally friendly PPO inhibitors (Moon et al. 2020).

Using an HPTLC-tyrosinase inhibition assay can screen tyrosinase inhibitors from natural sources, according to Jamshidi-Aidji and Morlock (2018). Tyrosinase is involved in catalyzing the reaction of the hydroxylation of L-tyrosinase to L-3,4-dihydroxyphenylalanine (L-DOPA). Then oxidation of L-DOPA involved several steps and the resulting formation of melanin (**Figure 4**). Tyrosinase HPTLC assay tyrosinase inhibitors inhibit tyrosinase and no formation of melanin. As a result, tyrosinase inhibitors containing positions are visualized as a whitish zone against a grey background.

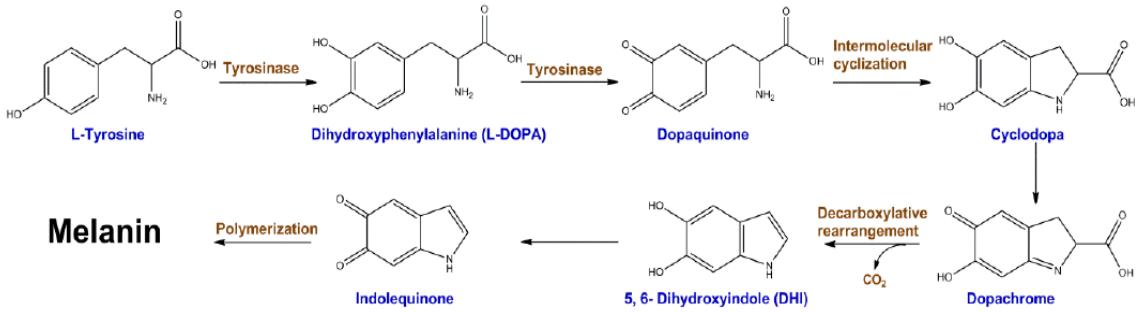

Figure 4. The oxidation of L-DOPA involved several steps and the resulting formation of melanin (Vavricka et al. 2010).

1.5.5 Screening radical scavengers

Free radicals, reactive oxygen species, and reactive nitrogen species are generated as by-products in metabolic processes, and a balance between free radicals and antioxidants is essential for an appropriate physiological function (Lobo et al. 2010). Natural antioxidants play an essential role in protective mechanisms to scavenge these free radicals (Ahmed et al. 2019). Different types of antioxidants are available, such as enzymatic, non-enzymatic and also those from plant sources (Ghosh and Deb 2014). As an example, plant extracts or their secondary metabolites have served as antioxidants to protect against oxidative stress and free radicals of mainly the reactive oxygen species (Nile and Park 2014). In the literature, a high

number of radical-scavenging compounds, such as flavonoids, phenolic acid, carotenoids, tocopherol have been found in herbs, spices and medicinal plants (Krüger et al. 2017). The antioxidant activity can be assessed using different antioxidant assays, such as total antioxidant, reducing power, DPPH• radical scavenging, hydrogen peroxide scavenging, and hydroxyl radical scavenging (Saravanan and Asharani 2016).

Using the HPTLC- DPPH• assay, antioxidant compounds can be screened, according to Krüger et al. (2017). DPPH• (2,2-diphenyl-1-picrylhydrazyl) stable radical has maximum absorption at 517 nm, which decreases upon reduction via reaction with a radical scavenger. Free radical scavengers containing positions on HPTLC plate are visualized as cream or yellow spots against a purple background (**Figure 5**).

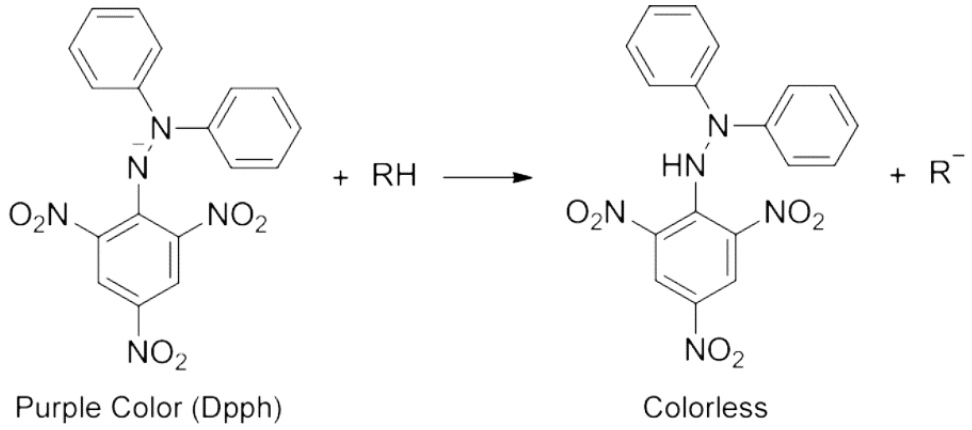

Figure 5. Reaction of DPPH radical with radical scavengers (Dewanjee et al. 2015).

1.6 HPTLC-HRMS

The hyphenation of HPTLC or TLC with mass spectrometry is helpful to determine the molecular weight of separated compounds (Urbain and Simões-Pires 2006). Using these HRMS or NMR allows the structure elucidation of interest bioactive zones. The hyphenation HPTLC/TLC-MS can be archived by elution-based (examples: Elution head-based interface, Micro capillary arrow, surface sampling probe) and desorption-based techniques [examples: atom bombardment (FAB), excited gas beam (DART), laser light beam (MALDI)] (Morlock and Schwack 2010). Elution can be done offline or online. In offline elution, the adsorbent region of interest is scraped off the glass carrier plate, and the residues are dissolved in an appropriate solvent and further analyzed. Online elution-head-based interfaces are allowed direct online elution target zones from the plate and less contamination-prone collection of target zones in vials (Móricz et al. 2020).

2. Scope

About 80% of the population in developing countries depend on traditional medicine, which is mainly based on plant sources (Gunawardana and Jayasuriya 2019). The people in developing countries rely on indigenous knowledge and practices and use locally available medicinal plants for different treatments. Most of these plants have not been investigated for their chemical composition or pharmacological properties. While in some plants, the whole plant extracts have been tested for their bioactivity, and most of the plants' single compounds and their effects have still not been identified. Identification and investigation of individual compounds effects in plant extracts are important for producing pure substances with high specific activity for the wide range of applications in pharmaceutical, food, and cosmetic fields. As pure drugs have fewer impurities, fewer side effects can be expected. Separation of whole extracts into a higher number of single compounds and studying their individual effects allows for the production of more pure drugs. Therefore, it is interesting to study medicinal plants' single compound effects for botany-based drug development. In addition, these findings can be used to substantiate the current traditional medical knowledge and to evaluate their benefits, risks and limitations.

Over the past three decades, usage of herbal medicinal products and supplements has been excessively increased, worldwide. Although these agents have shown promising therapeutic potential, and among them a good number of herbal products have been established, many of them remain untested. Due to a lack of knowledge of these untested products regarding mode of action, potential adverse reactions, contraindications, and interactions with existing pharmaceuticals and functional foods, safety continues to be a major issue with the use of herbal remedies (Ekor 2014). Therefore, it is necessary to evaluate the quality of market products and their bioactivities, impurities, and possible risk factors for the safety of the global food chain.

Sri Lanka has a long history of medicinal plants. This is evidenced by the early 18th-century manuscript, [*Icones Plantarum Malabaricarum, adscriptis omnibus et viribus* (Illustrations of Plants from the Malabar, assigned names and strength) *Vol. I. & II],* which included 262 watercolour drawings of medicinal plants from Sri Lanka, and their information exists in the library of Leiden University in the Netherlands (van Andel et al. 2018). There are 1430 species (out of 3771 flowering plant species) that are considered medicinal plants in Sri Lanka. Out of them, 174 (12%) are endemic and about 250 species are used in Sri Lankan traditional medicine (Gunawardana and Jayasuriya 2019). According to the literature, only a

small number of medicinal plants in Sri Lanka have been tested for their bioactivity for the aim of developing novel drugs and further research is needed (Kuruppu et al. 2019). Traditional medicine systems in Sri Lanka consist of Ayurveda, Unani, and Deshiya Chikitsa, where herbs are used as remedies for treatment (Gunawardana and Jayasuriya 2019). Where a single plant contains one or more active compounds, traditional medicine uses several plants as a combination approach that would deliver an enhanced therapeutic effect (Kuruppu et al. 2019). In the literature, several studies have shown the effects of whole plant extracts of Sri Lankan medicinal plants. For example, *Abelmoschus moschatus, Asparagus falcatus, Barleria prionitis* extracts have been used as kidney therapeutic agents in Sri Lankan traditional medicine and aqueous extracts of these plants have shown high antioxidant activity in vitro (Amarasiri et al. 2020). In the clinical trial phase-I study, aqueous extracts of *Cinnamomum zeylanicum* have shown beneficial anti-hyperlipidaemic and blood pressure lowering effects among healthy adults (Ranasinghe et al. 2017). However, responsible compounds that produce these bioactivities in these extracts mostly have not been identified. Due to limited scientific instrumentation and facilities for chemical characterization and to conduct bioassays, most studies investigating bioactive properties of Sri Lankan medicinal plants rarely progress to the molecular level and typically scientific efforts are limited to reporting the bioactivity of plant extracts (Mohotti et al. 2020).

In HPTLC, using automated equipment for the application, development and detection, as well as using standardized stationary phases, has the ability to powerfully separate in minimum time and can obtain reproducible results for quality analysis (Bräm and Wolfram 2017). TLC (or HPTLC) combined with EDA is an effective and simple technique for the study of multi-compound plant extracts. This procedure provides simultaneously chromatographic separation of a complex multi-component mixture and visualizes the localization of active constituents directly on a TLC plate in a short time (Marston 2011). Conventional microtiter plates or reactions inside a cuvette are only able to investigate whole extract effects. No information of component effects or potential synergistic effects in extracts can be obtained (Morlock and Schwack 2010).

The strategy, to hyphenate HPTLC with EDA and mass spectrometry might open up a faster and low-cost active discovery path in the field of phytochemical analysis research (Klingelhöfer and Morlock 2014). In HPTLC-EDA, the evaporation of organic solvents of the mobile phase, which might cause enzyme inactivation, is advantageous (Marston 2011). The chromatographic separation process reduced the complexity of the sample matrix, and this allows chemical analysis easily and better identification of unknown compounds

(Agatonovic-Kustrin et al. 2019). Both the following studies had a similar approach. After the initial development of the chromatographic system, the samples were subjected to the EDA, whereby a positive control was applied on the same plate. Some separated bioactive compounds were quantified directly via the enzymatic response using an equivalent calculation to known references. Bioactive zones discovered were eluted into the MS, and full scan HESI-HRMS spectra were recorded in the positive and negative ionization modes. The multi-imaging via UV/Vis/FLD and the co-chromatography of the identified reference standards allowed us to confirm the correct bioactive compound preliminary assigned via hR_F values and EDA. Post-chromatographic derivatization reactions helped to further characterize and identify the chemical nature of the main bioactive compounds found in the chromatogram and to improve visualization of separated substances by broadening the detectable compound range. Figure 6. describes the HPTLC-UV/Vis/FLD-EDA-HESI-HRMS analytical platform which was designed to identification of bioactive compounds in *Abelmoschus moschatus* and *Cinnamomum zeylanicum*.

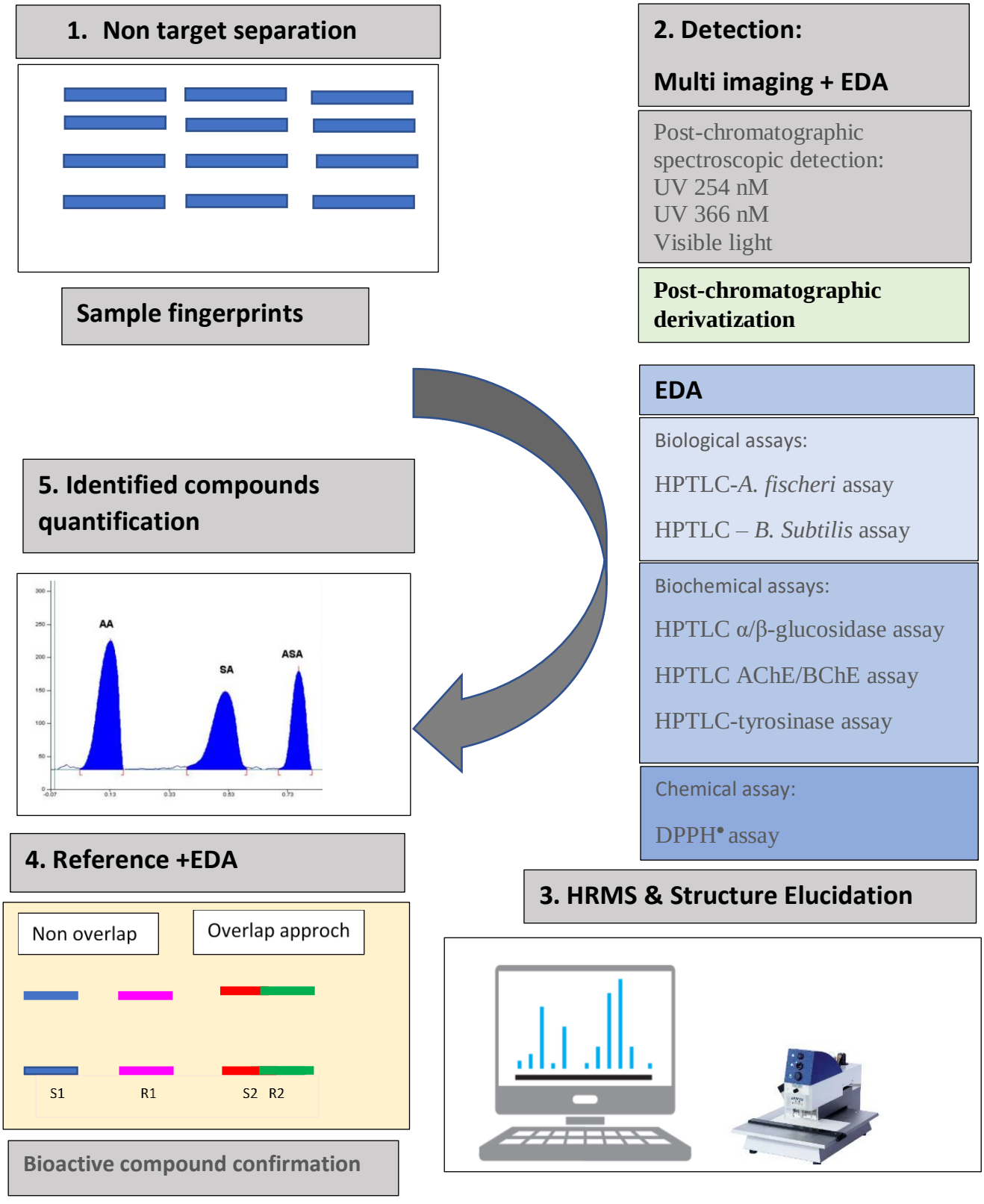

Figure 6. Schematic diagram describes HPTLC-UV/Vis/FLD-EDA-HESI-HRMS analytical platform which was designed to identification of bioactive compounds in *Abelmoschus moschatus* and *Cinnamomum zeylanicum*.

3. Progress achieved

3.1 Paper 1

Abelmoschus moschatus Medik belongs to the family Malvaceae and has been used for a long time in traditional herbal remedies in Sri Lanka (Amarasiri et al. 2020). Multiple bioactivities are reported for *Abelmoschus moschatus*, but the single compounds effects for its antimicrobial, enzyme inhibiting, and antioxidative activities still have not been identified. The first study was focused on the investigation of bioactive compounds in *Abelmoschus moschatus* bark leaf and seed extracts via hyphenated HPTLC. This contribution was attempted to gain a better insight into the curative potential of botanical medicines nowadays in use. The paper has highlighted following outcomes.

1. A multi-potent compound zone in most *Abelmoschus moschatus* extracts was observed at hR_F 75 on the HPTLC plate for the seven different bioassays or enzymatic assays. It consisted of coeluting unsaturated fatty acids (linoleic acid and oleic acid), saturated fatty acids (palmitic acid and, stearic acid, arachidic acid, and behenic acid).
2. *Abelmoschus moschatus* extracts showed antibacterial effects as well as α-glucosidase and tyrosinase inhibitions. The β-glucosidase and AChE responses were comparatively weak.
3. Three different plant parts had comparatively more common bioactivity patterns than were different. The seed extracts were most potent and much richer in bioactivities compared to bark and leaf.
4. Oleic acid was selected as a representative unsaturated fatty acid. Its overlapped application and co-chromatography confirmed its significant activities as an antibacterial agent, free radical scavenger, and inhibitor of α-glucosidase, β-glucosidase, acetylcholinesterase, and tyrosinase.
5. The α-glucosidase and tyrosinase inhibition responses of the bioactive compound zone were equivalently quantified referred to as oleic acid. The comparison of both independent enzymatic quantifications achieved comparable results. Enzymatic quantification by a planar enzyme assay was successfully proven.

In summary, the newly developed hyphenated HPTLC-UV/Vis/FLD-EDA-HESI-HRMS analytical platform demonstrated prominent bio-effective compounds in Abelmosk and further exhibited antimicrobial and antioxidant as well as glucosidase, acetylcholinesterase and tyrosinase inhibiting effects. Future studies are needed for fatty acid separation using HPTLC technology.

Talanta 223 (2021) 121701

Contents lists available at ScienceDirect

Talanta

journal homepage: www.elsevier.com/locate/talanta

Comprehensive bioanalytical multi-imaging by planar chromatography in situ combined with biological and biochemical assays highlights bioactive fatty acids in abelmosk

N.G.A.S. Sumudu Chandana, Gertrud E. Morlock *

Justus Liebig University Giessen, Institute of Nutritional Science, Chair of Food Science, and TransMIT Center for Effect-Directed Analysis, Heinrich-Buff-Ring 26-32, 35392 Giessen, Germany

ARTICLE INFO

Keywords:
Antibacterial
Enzyme inhibitor
Radical scavenger
Bioprofiling
Planar bioassay
HPTLC-UV/Vis/FLD-EDA-HESI-HRMS

ABSTRACT

The identification of the bioactivity of individual compounds in natural products is helpful to understand their therapeutic applications. Thus, a bioanalytical multi-imaging screening was developed and applied to 54 bark, leaf and seed extracts of Sri Lankan *Abelmoschus moschatus* (abelmosk) to find out the most bioactive individual compounds. The focus was laid on a comprehensive bioactivity profiling of its extracts. High-performance thin-layer chromatography (HPTLC) was hyphenated with seven effect-directed assays (EDA), *i. e.* biological (Gram-negative *Aliivibrio fischeri* and Gram-positive *Bacillus subtilis*), biochemical (α-glucosidase, β-glucosidase, acetylcholinesterase and tyrosinase) and chemical (2,2-diphenyl-1-picrylhydrazyl) assays. This multi-imaging was complemented by ultraviolet (UV), white light (Vis), fluorescence detection (FLD) and eight micro-chemical derivatizations. Heated electrospray ionization high-resolution mass spectrometry (HESI-HRMS) was used to characterize the most prominent multi-potent compound zone. It consisted of coeluting unsaturated fatty acids (linoleic acid and oleic acid), but also saturated fatty acids (palmitic acid and to a lower extent stearic acid, arachidic acid and behenic acid). For confirmation of the detected effects (antibacterial, free radical scavenger and inhibitor of α-glucosidase, β-glucosidase, acetylcholinesterase and tyrosinase), oleic acid was exemplarily analyzed by co-development and overlapped application (with sample). The proven effects underlined the beneficial health effects derived from unsaturated fatty acids like oleic acid. Exemplarily, the α-glucosidase and tyrosinase inhibition responses of the multi-potent compound zone were quantified equivalently in reference to oleic acid. The comparable results obtained by two independent enzymatic responses successfully proved the use of biochemical quantification by planar enzyme assays, and thus the new method based on HPTLC-UV/Vis/FLD-EDA-HESI-HRMS.

1. Introduction

Ongoing attention is paid to medicinal plants for the discovery of safe drugs for humans [1], as market expectations for drugs produced by synthetic drug libraries have not been fulfilled [2]. Around 21,000 plant species are possibly used as medicinal plants, whereof the majority is inexpensive, readily available and low in side effects [3]. This huge potential offered by nature needs to be exploited. Latest innovative extraction methods using natural deep eutectic solvents [4] or natural products rich in bioactive compounds or biofortified extracts [5,6] attract interest in the cosmetic, medicinal, nutritional and industrial fields. Plant-derived drugs account for 33% of the total drug production in the industry [7]. In consequence, proof-based strategies for their quality control and unequivocal identification are demanded [8]. In particular, such strategies are treasured which include the evaluation of the bioactivity profile of products containing so-called active ingredients.

Abelmoschus moschatus (abelmosk, Malvaceae) is used in traditional medicine treatments and was selected for the intended bioprofiling as a plant-derived drug. Pharmacological effects are reported especially for its kidney-shaped seeds in a green-brownish capsule [9] and its lobed leaves [10]. It grows annually as a shrub or small tree and grows in tropical Asia, Africa and South America. Antiaging, antidiabetic, anti-oxidative, anticonvulsant, antidepressant, antimicrobial,

* Corresponding author.
E-mail address: Gertrud.Morlock@uni-giessen.de (G.E. Morlock).

https://doi.org/10.1016/j.talanta.2020.121701
Received 9 April 2020; Received in revised form 17 September 2020; Accepted 19 September 2020
Available online 25 September 2020

antiproliferative, anxiolytic, antilithiatic, diuretic, hepatoprotective, hemagglutinating, hypnotic, memory strengthening and muscle relaxant activities have been reported for it [11].

Seven effect-directed assays were selected for the bioprofiling. The detection of new plant-derived antibiotics against Gram-positive/-negative bacteria is demanded due to the worldwide antibiotic resistance caused by improper use and misuse of antibiotics [12,13]. The detection of antidiabetic effects is also important, as the diabetes mellitus type 2 patients are predicted to be 592 million by 2035 [14]. Most synthetic drugs target one pathway to control hyperglycemia [15], whereas plant-derived glucosidase inhibitors result in a reduced postprandial blood glucose level by its influence on carbohydrate digestion [16] with only few or less side effects compared to synthetic drugs [17–19]. On another enzymatic pathway, tyrosinase is responsible for melanogenesis in the skin of mammals [20], and plant-derived tyrosinase inhibitors are treasured ingredients in natural cosmetics [21]. In the same way, polyphenol oxidases are responsible for browning reactions of fungi, fruits, vegetables *etc*. [22]. The Alzheimer disease is a lethal neurodegenerative disorder predicted to be 150 million by 2050 [23]. Its current pharmacotherapy is most dependent on *N*-methyl D-aspartate antagonists and cholinesterase inhibitors [24,25]. For the latter, there is interest in inhibitors from natural sources with only minor side effects [26]. For an appropriate physiological function, a balance between free radicals or reactive oxygen/nitrogen species (generated as by-products in metabolic processes) and antioxidants is essential to limit degenerative diseases [27]. In particular, the detection and use of plant-derived radical scavengers or antioxidants is attractive [28].

Hence, multi-imaging bioanalytical screening methods are demanded to discover new bioactive compounds in natural sources. Hyphenated high-performance thin-layer chromatography (HPTLC) stands for minimalistic sample preparation but maximalistic detection performance to collect comprehensive information [29–31]. All in all, 18 different detection modes were used, *i.e.* ultraviolet (UV), white light (Vis), fluorescence detection (FLD), eight microchemical derivatizations and seven effect-directed assays (EDA). As samples, bark, leaf and seed of Sri Lankan abelmosk were screened to point to the most pronounced antibacterial, antidiabetic, anti-tyrosinase, anti-acetylcholinesterase and radical scavenging compounds, of which the most effective zone was characterized by heated electrospray ionization high-resolution mass spectrometry (HESI-HRMS).

2. Experimental

2.1. Chemicals and materials

HPTLC plates silica gel 60 with and without F_{254}, also respective HPTLC plates MS-grade, all 20 × 10 cm, *Bacillus subtilis* spores (BGA, DSM 618 strain) and ascorbic acid (99%) were obtained from Merck, Darmstadt, Germany. *Aliivibrio fischeri* bacteria (NRRI-B11177, strain 7151) were purchased from Leibniz Institute, DSMZ, German Collection of Microorganisms and Cells Cultures, Berlin, Germany. Acetic acid (100%), 2-aminoethoxydiphenyl borate (98%), hydrochloric acid (≥37%), kojic acid (98%), 3-(4,5-dimethylthiazol-2-yl)-2,5-diphenyltetrazolium bromide (MTT, 98%), polyethylene glycol (PEG) 8000, tris (hydroxymethyl) aminomethane (Tris, 99.8%), sulphuric acid (≥96%) and vanillin (≥99%) were purchased from Carl Roth, Karlsruhe, Germany. Acetone (100%), ethyl acetate (≥99.8%), *n*-hexane (≥95%) and orthophosphoric acid (≥85%) were bought from Th. Geyer, Renningen, Germany. Acarbose, AChE lyophylisate (6.66 U/mL, from *Electrophorus electricus* with ≥245 U/mg, 10 kU/vial), *p*-aminobenzoic acid (≥99%), *p*-anisaldehyde (98%), aniline (99.5%), 3-cyclohexyl amino-propane sulfonic acid (CAPS, ≥98%), 2,2-diphenyl-1-picrylhydrazyl ($DPPH^{\bullet}$, 95%), α-glucosidase (10 U/mL, from *Saccharomyces cervisiae* with 1000 U/vial), imidazole (≥99.5%), ninhydrin, primuline, physostigmine, sodium acetate (≥99%), tyrosinase (400 U/mL, from mushroom with ≥1000 U/mg), oleic, linoleic and palmitic acids (all ≥99%) were purchased from Sigma-Aldrich, Steinheim, Germany. 2-Naphthyl-β-D-glucopyranoside (95%) and β-glucosidase (1000 U/mL, from almond with 3040 U/mg) were purchased from abcr, Karlsruhe, Germany. α–Naphthyl acetate (≥99%) was bought from AppliChem, Darmstadt, Germany. Ethanol (≥99.8%) was purchased from Fisher Scientific, Loughborough, UK. 2-Naphthyl-α-D-glucopyranoside was bought from Flurochem, Hadfield, UK. Toluene (≥99.7%) was purchased from LGC standard, Wesel, Germany. Fast Blue B salt (~95%) was purchased from MP Biomedical, Illkrich, France. (2S)-2-Amino-3-(3,4-dihydroxy phenyl)propanoic acid (levodopa) was obtained from Santa Cruz Biotechnology, Dallas, TX, USA. Methanol (ca. 100%) was purchased from VWR International, Darmstadt, Germany. Bidistilled water was prepared by a Destamat Bi 18E (Heraeus, Hanau, Germany). The polypropylene box (26.5 cm × 16 cm x 10 cm) was from KIS, ABM, Wolframs-Eschenbach, Germany.

2.2. Sample origin, preparation and standard solutions

Sri Lankan *Abelmoschus moschatus* IDs 1–6 were from Karapitiya and IDs 7–18 from Wanduramba, both suburbs of Galle. The collected bark pieces, leaves and seeds were cleaned and shade-dried (4–5 days, 30 °C, 65% RH). Each sample was ground at 15,000 rpm for 6 min (Tube Mill, IKA, Staufen, Germany), 500-μm sieved (stainless steel test sieve, VWR International) and stored protected in the dark at ca. 18 °C. Seed and leaf powder (200 mg each) were extracted with 2 mL ethanol – water 4:1 (100 mg/mL) in a conical Eppendorf tube (15 mL, polypropylene), whereas 3 mL was used for extraction of 200 mg bark powder (67 mg/mL). For quantification, seed extract was 1:4 diluted with ethanol – water 4:1 (25 mg/mL). All suspensions were placed in an ultrasonic bath (480 W, frequency 35 kHz, Sonorex Digi plus DL 255H, Bandelin, Berlin, Germany) at 25 °C for 30 min and centrifuged (Heraeus Labofuge 400, Thermo Scientific, Dreieich, Germany) at 2400×*g* for 10 min. Each supernatant was transferred to a sampler vial, stored at ca. 8 °C in the dark. Methanolic solutions of oleic acid (1.35, 0.675 and 0.25 mg/mL), palmitic acid and linolic acid (each 0.25 mg/mL) were used.

2.3. HPTLC method

The extracts were applied as 8-mm band on the HPTLC plate silica gel F_{254} at a 150-nL/s dosage speed (Automatic TLC Sampler ATS 4, CAMAG, Muttenz, Switzerland) and dried in a stream of cold air for 2 min. The distance from the left plate edge or bottom edge was 10 mm and the track distance ≥9.4 mm. If required the plate was cut (TLC SmartCut, CAMAG). The plate was developed with toluene – ethyl acetate – methanol 6:5:2 or toluene – ethyl acetate 7:3 up to 65 mm in the twin trough chamber (20 × 10 cm, biostep or CAMAG) and dried (2 min). Each chromatogram was documented at UV 254 nm, FLD 366 nm and white light illumination (TLC Visualizer, CAMAG). Operation was controlled by visionCATS software version 2.5.18262.1 (CAMAG).

2.4. Chemical profiling

Eight identical chromatograms with representative extracts were detected via the following detection modes: (A) UV 254 nm, (B) Vis, (C) FLD 366 nm as well as after derivatization (immersion speed 3 cm/s, immersion time 2 s, TLC Immersion Device III, CAMAG) with (D) primuline reagent (250 mg primuline, 50 mL water, 200 mL acetone) at UV 366 nm after 1- min drying, (E) *p*-anisaldehyde sulphuric acid reagent (1.5 mL methoxybenzaldehyde, 210 mL methanol, 25 mL acetic acid, 13 mL sulphuric acid), (F) vanillin sulphuric acid reagent (3 g vanillin, 247 mL ethanol, 3 mL sulphuric acid), (G) *p*-aminobenzoic acid reagent (2 g 4-aminobenzoic acid, 50 mL glacial acetic acid, 50 mL water, 2 mL orthophosphoric acid), (H) the latter at FLD 366 nm, (I) diphenylamine aniline orthophosphoric acid reagent (100 mL diphenylamine and aniline, each 2% in isopropanol, 20 mL orthophosphoric acid), (J) ninhydrin reagent (500 mg ninhydrin, 230 mL ethanol, 20 mL glacial acetic

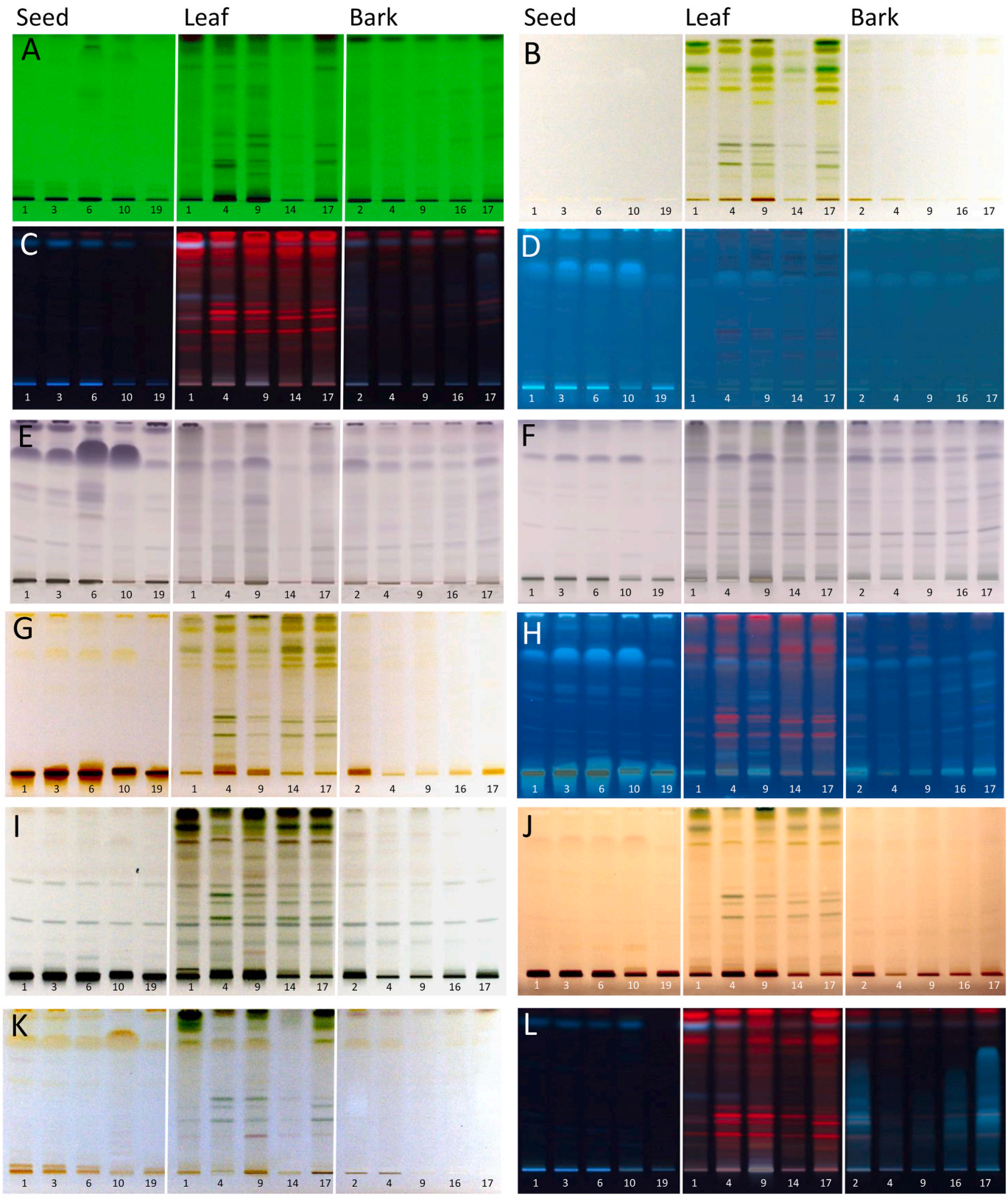

Fig. 1. Chemical profiling: HPTLC chromatograms of selected bark (1340 µg/band each), leaf and seed extracts (1000 µg/band each) of abelmosk (respective IDs per track) on HPTLC plates silica gel 60 F_{254} with toluene – ethyl acetate – methanol 6:5:2, detected at (A) UV 254 nm, (B) white light illumination, (C) FLD 366 nm, and by (D) primuline reagent at FLD 366 nm, (E) *p*-anisaldehyde sulphuric acid reagent, (F) vanillin sulphuric acid reagent, (G) *p*-aminobenzoic acid reagent, (H) same at FLD 366 nm, (I) diphenylamine aniline orthophosphoric acid reagent, (J) ninhydrin reagent, (K) Fast Blue B salt reagent and (L) natural product reagent at FLD 366 nm; E-G and I–K documented at white light illumination. (For interpretation of the references to color in this figure legend, the reader is referred to the Web version of this article.)

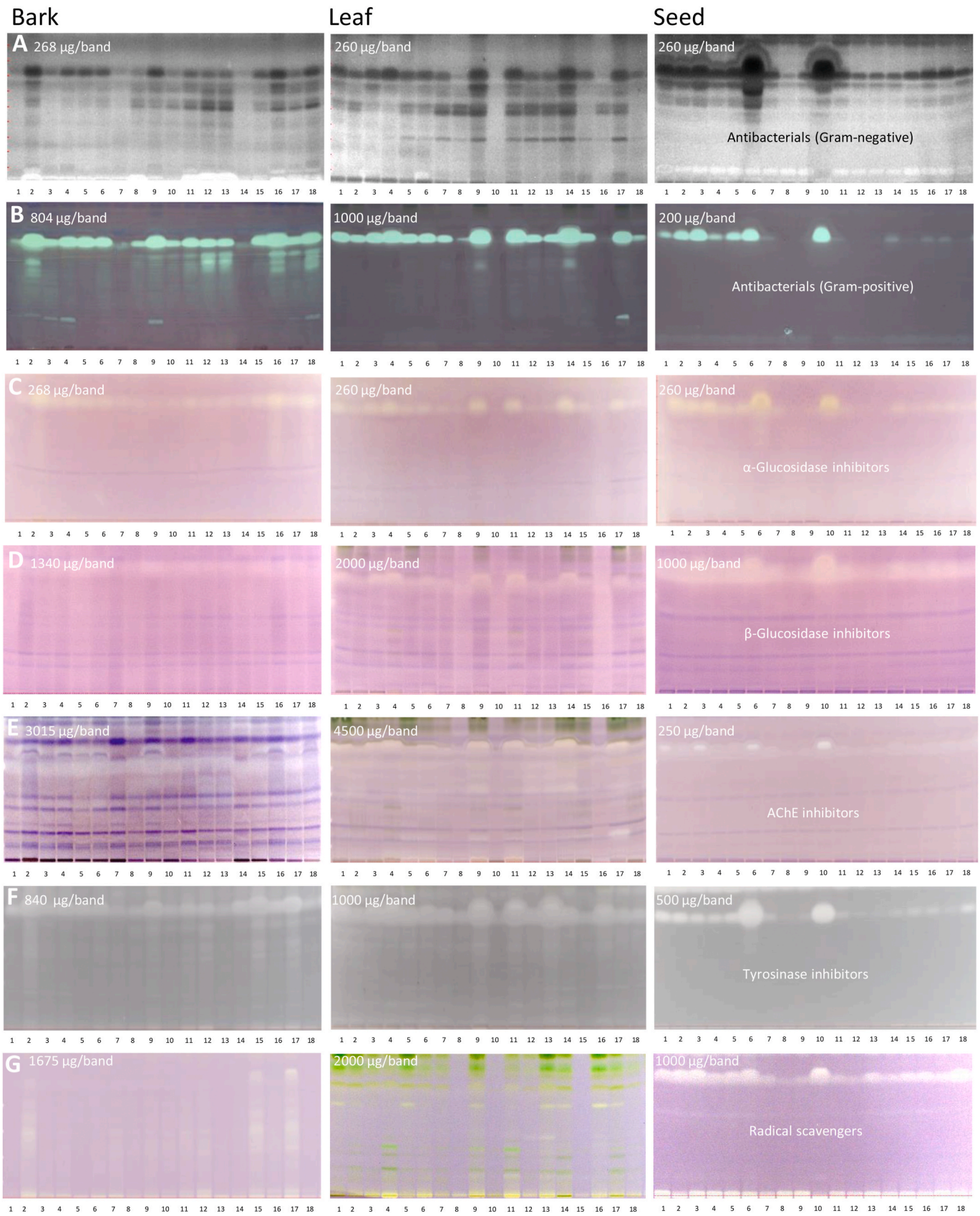

Fig. 2. Effect-directed profiling: HPTLC (bio)autograms of bark, leaf and seed extracts of abelmosk (IDs 1–18 applied depending on assay response and separated as in Fig. 1) detected by (A) Gram-negative *Aliivibrio fischeri* (grey-scale image of bioluminescence) and (B) Gram-positive *Bacillus subtilis* bioassays as well as (C) α-glucosidase, (D) β-glucosidase, (E) AChE and (F) tyrosinase inhibition assays, and (G) DPPH$^{\bullet}$ assay; (B–G) detected at white light illumination.

acid), (K) Fast Blue B salt reagent (250 mg Fast Blue B salt, 250 mL ethanol 70%), (E-K) Vis detection after heating at 140 °C for max. 5 min (TLC Plate Heater, CAMAG), and (L) natural product reagent (1.5 g 2-aminoethoxydiphenyl borate, 250 mL ethanol) at FLD 366 nm after air-drying.

2.5. Effect-directed profiling

HPTLC plates were pre-washed using methanol – water 3:1, *V/V,* dried at 110 °C for 30 min and stored protected until use. Extract volumes were applied depending on the assay response (see Fig. 2). After development, respective positive controls (PC) were applied as edge track pattern or above the solvent front. HPTLC chromatograms were further dried for 15 min (Automatic Developing Chamber ADC 2, CAMAG) to remove all residual mobile phase traces and then immersed in the respective assay solution/suspension (TLC Immersion Device III) or piezoelectrically sprayed with these (Derivatizer, both CAMAG). The plate was horizontally incubated in a moistened polypropylene box, afterward dried and documented at Vis (reflectance mode, TLC Visualizer, CAMAG), if not stated otherwise.

2.5.1. Gram-negative Aliivibrio fischeri bioassay

According to Ref. [32], the bacterial culture (prepared as in DIN EN ISO 11348-1) was piezoelectrically sprayed onto the chromatogram (4 mL, blue nozzle, level 6). The instant bioluminescence was recorded over a 30 min period (time interval 3 min, exposure time 60 s, Bioluminizer, CAMAG). The PC was caffeine (1–7 μL/band, 0.5 mg/mL in methanol).

2.5.2. Gram-positive Bacillus subtilis bioassay

According to Ref. [33], the chromatogram was dipped in the bacterial suspension (immersion speed 3.5 cm/s, immersion time 5 s) and incubated at 37 °C for 2 h. The plate was dipped into a 0.2% PBS-buffered MTT solution (immersion speed 3.5 cm/s, immersion time 1 s) and heated at 50 °C for 5 min. The PC was tetracycline (1–7 μL/band, 0.004 mg/mL in ethanol).

2.5.3. α-Glucosidase inhibition assay

According to Ref. [33], the chromatogram was piezoelectrically sprayed (2 mL, yellow nozzle, level 6) with substrate solution (12 mg 2-naphthyl-α-D-glucopyranoside in a mixture of 9 mL ethanol and 1 mL 10 mM sodium chloride) and dried (2 min). For pre-wetting, 1 mL sodium acetate buffer (10.25 g sodium acetate in 250 mL water adjusted to pH 7.5 with acetic acid 0.1 M) was piezoelectrically sprayed using the same nozzle, followed by 2 mL α-glucosidase (10 U/mL in sodium acetate buffer, pH 7.5). After plate incubation at 37 °C for 15 min, 0.75 mL Fast Blue B salt solution (4 mg/mL in water) was piezoelectrically sprayed and the plate was dried (2 min). The PC was acarbose (1–18 μL/band, 3 mg/mL in ethanol). Absorbance measurement at 546 nm was performed using the mercury lamp and an inverse scan, as zones were brighter than the background. Quantification was performed via peak area.

2.5.4. β-Glucosidase inhibition assay

The β-glucosidase inhibition assay was performed analogously to the α-glucosidase inhibition assay, but β-glucosidase (3040 U/mL) and 2-naphthyl-β-D-glucopyranoside were used. Incubation took longer (30 min). The PC was imidazole (1–7 μL/band, 1 mg/mL in ethanol).

2.5.5. AChE inhibition assay

According to Ref. [32], the chromatogram was piezoelectrically sprayed (green nozzle, level 6) with 1 mL Tris-HCl buffer (pH 7.8), then 3 mL AChE solution (6.66 U/mL in Tris-HCl buffer plus 1 mg BSA) and incubated at 37 °C for 25 min. The substrate solution (0.75 mL, ethanolic α-naphthyl acetate solution and aqueous Fast Blue B salt solution, 1:2) was piezoelectrically sprayed (red nozzle, level 6) and the plate was dried (2 min). The PC was physostigmine (2–8 μL/band, 2 μg/mL in ethanol).

2.5.6. Tyrosinase inhibition assay

According to Ref. [34], the chromatogram was piezoelectrically sprayed (blue nozzle, level 6) with 2 mL substrate solution (45 mg levodopa, 25 mg CAPS and 75 mg PEG 8000 dissolved in 10 mL 0.02 M phosphate buffer, pH 6.8), after drying (2 min) with 2 mL tyrosinase solution (400 U/mL phosphate buffer), incubated at ca. 20 °C for 15 min and dried (8 min). The PC was kojic acid (1–6 μL/band, 0.1 mg/mL in ethanol). Absorbance measurement at 579 nm was performed as mentioned in 2.5.3.

2.5.7. Radical-scavenging assay

According to Ref. [35], the chromatogram was immersed into 0.02% methanolic DPPH$^{\bullet}$ solution (immersion speed 2 cm/s, immersion time 2 s), followed by air-drying for 90 s and at 60 °C for 30 s (TLC Plate Heater). The PC was ascorbic acid (2–7 μL/band, 0.1 mg/mL in water).

2.6. HESI-HRMS

Samples were applied in duplicate on MS-grade HPTLC plates and cut into two halves after development. One plate half was subjected to the tyrosinase inhibition assay to transfer the coordinates/positions of the bioactive zones in the autogram to the other plate half (marked by a soft pencil). The marked zones were eluted with methanol (60 s, flow rate 0.1 mL/min) using an elution head-based interface (Plate Express, Advion, Ithaca, NY, USA) coupled to HESI-Q Exactive Plus mass spectrometer (Thermo Fisher Scientific, Dreieich, Germany). Full scan HPTLC-HESI-HRMS spectra (*m/z* 50–750) were recorded in the positive and negative ionization mode with a spray voltage of ±3.5 kV, the capillary temperature of 270 °C, sheath gas of 20 (arbitrary units), aux gas of 10 (arbitrary units) and S-Lens RF level of 50. The obtained spectra were processed with Xcalibur 3.0.63 software (Thermo Fisher Scientific). The plate background was subtracted from each analyte spectrum.

3. Results and discussion

3.1. Development of the HPTLC method

Bark pieces, leaves and seeds of *Abelmoschus moschatus* samples (Figure S1, IDs 1–6 collected from Karapitiya and IDs 7–18 from Wanduramba, both suburbs of Galle, Sri Lanka) were collected from 18 scrubs, cleaned, shade-dried, ground and sieved to obtain a homogenous powder. For the fiber-rich bark, a higher extraction volume was used. Three extraction solvent mixtures of different polarity (methanol – water, ethanol – water and *n*-hexane – ethyl acetate, all 4:1, *V/V*) were investigated for their extraction efficiency of the bioactive compounds from the different abelmosk parts (Figure S2). Among these, the mixture of ethanol and water 4:1 (medium polarity) extracted all bioactive compounds, including those found in the more polar/apolar extracts, as proven by the *Aliivibrio fischeri* bioassay. This bioassay is recommended as a start assay, since it detects the highest number of bioactive compounds based on our experience. For separation on normal phase HPTLC silica gel plates, four different solvent combinations were studied as mobile phase. Toluene – ethyl acetate – methanol 6:5:2 (*V/V/V*) or the more apolar toluene – ethyl acetate 7:3 (*V/V*) were suited for subsequent analyses, as the bioactive compound zones were sufficiently sharp and spread along the migration distance after the *Aliivibrio fischeri* bioassay (Figures S3 and S4). Both developments up to 65 mm took about 20 min.

3.2. Chemical profiling

Five representative extracts (each of bark, leaf and seed) were analyzed by the new method. Their UV/Vis/FLD images (Fig. 1 A-C)

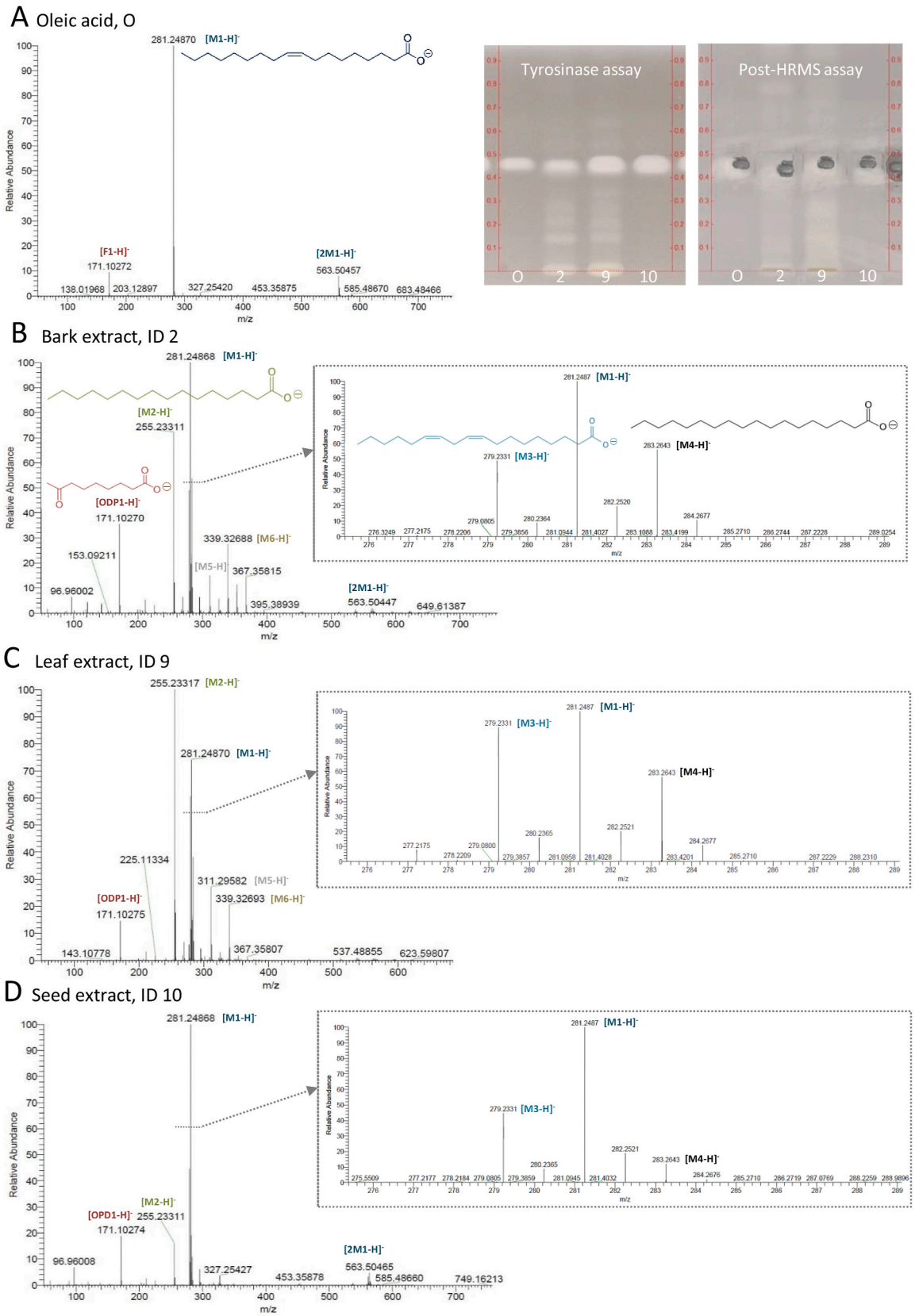

Fig. 3. HPTLC-HESI⁻-HRMS spectra of the multi-potent compound zone in abelmosk bark (ID 2; 800 ng/band), leaf (ID 9; 1000 ng/band) and seed extracts (ID 10; 500 ng/band) as well as oleic acid (1.3 μg/band, hR_F 45) applied in duplicate on respective MS-grade HPTLC plates, developed with toluene – ethyl acetate 7:3, for zone marking, one plate part detected at Vis after the tyrosinase inhibition assay and the other after HRMS recording (post-HRMS assay), showing oleic acid at *m/z* 281.2487 and palmitic acid at *m/z* 255.2331 as most intense mass signals, but also linolic acid at *m/z* 279.2331 and stearic acid at *m/z* 283.2643 (all assignments in Table 1).

revealed most detectable compounds to be present in the leaf extracts. These contained greenish chlorophylls in the Vis chromatogram, prominent as red fluorescent and UV-absorbing bands in the FLD and UV chromatograms, respectively. Since not all components in an extract are detectable by UV/Vis/FLD or MS, eight derivatization reagents were exploited to widen the detectable compound range. The information on functional groups is also helpful for later characterization of selected bioactive compounds and identification of their chemical nature. Eight identical chromatograms were detected via twelve different detection modes (Fig. 1). A lipophilic compound zone was detected at hR_F 75 by the primuline reagent at FLD in all extracts, but in particular in the seed extracts (Fig. 1 D). Using the *p*-anisaldehyde sulphuric acid reagent, additional organic compounds were detected at Vis. The previously detected lipophilic compound zone at hR_F 75 was also detected by this reagent, although the horizontal pattern across all tracks was differently pronounced (detecting another coeluting compound for IDs 6 and 10). However, many other compounds were observed by this more universal derivatization reagent, which have not been detected before (as not UV/Vis/FLD active or lipophilic, Fig. 1 E). The similarly detecting vanillin sulphuric acid reagent showed comparatively less and differently intense compounds in the profile (Fig. 1 F). Saccharides were selectively detected at Vis by the *p*-aminobenzoic acid reagent (Fig. 1 G/H, also detects acids and the lipophilic compound at hR_F 75) and diphenylamine aniline orthophosphoric acid reagent (Fig. 1 I). For the given mobile phase system, all saccharides remained at the start zone. In all extracts, two greenish glycosides at hR_F 30 and hR_F 57 were newly detected at Vis after the diphenylamine aniline orthophosphoric acid reagent, also weakly blue fluorescent at FLD after the *p*-aminobenzoic acid reagent (Fig. 1 H). The respective yellow zones were not or hardly detectable via the comparatively less sensitive Vis detection (Fig. 1 G). Via the ninhydrin reagent, primary (or secondary) amino group-containing compounds were detected at Vis in the start zones, whereas no additional compound zone was observed along the developing distance (Fig. 1 J). As for the saccharides, the amino acids remained at the start for the given mobile phase. Via the Fast Blue B salt reagent only the previous compound zone at hR_F 75 was detected at Vis in the seed extracts, and two further at the start zone (Fig. 1 K *versus* 1 B). Using the natural product reagent at FLD, blue fluorescent flavonoid-like compounds were revealed in bark extract IDs 2, 16 and 17 (Fig. 1 L; an acid addition to the mobile phase would be needed to sharpen the tailing zones).

3.3. Effect-directed profiling

In order to obtain information on bioactive compounds, all extracts were subjected to effect-directed assays, including two antibacterial assays (against Gram-negative *Aliivibrio fischeri* and Gram-positive *Bacillus subtilis*), four enzymatic assays (against α- and β-glucosidase, AChE and tyrosinase) and a chemical radical scavenging assay (DPPH$^•$). *Aliivibrio fischeri* is a marine bacterium that emits brilliant greenish-blue light above a certain cell density (>10^9/mL) for quorum sensing. In the *Aliivibrio fischeri* bioassay, antibacterial compounds were detected as dark or bright zones due to their impact on the energetic metabolism related to the bioluminescence of the *Aliivibrio fischeri* bacteria. In the bioautograms of the three plant parts, several antibacterial compounds were detected as dark zones reducing the bioluminescence on the otherwise bioluminescent plate background (depicted as greyscale image, Fig. 2 A). Among these, the previously detected zone at hR_F 75 revealed an antibacterial effect in almost all extracts. In particular, in seed extract IDs 1–6 and 10, this compound zone showed a strong antibacterial response against the Gram-negative bacteria (evident at a glance, as almost the same amount was applied for the different plant parts). Also, the opposite probiotic effect was detected in the bark and seed extracts, *i.e.* compounds at the start zone (bark) and at hR_F 10 (seed) which enhanced the bacterial bioluminescence. All bioactive zones increased in intensity in the bioautograms monitored over 30 min, which proved the pronounced antibacterial effect. For the Gram-positive *Bacillus subtilis* bioassay, the bark and leaf volumes were increased by a factor of 3–4. Colorless bright zones indicated antibacterials on an MTT-violet plate background (colored by living bacteria). Again, an intense antibacterial zone was discovered at hR_F 75 in all three extract types (Fig. 2 B). Similar to the previous antibacterial pattern (not evident at a glance, as higher volumes applied for bark/leaf), again seed extract IDs 1–6 and 10 displayed a strong antibacterial effect. The strong similar responses in both orthogonal bacterial assays suggest that antibacterial compounds are tentatively produced at a higher amount in the seeds of Karapitiya (IDs 1–6) than Wanduramba (IDs 7–18). Our results are in accordance to a previous study, in which a moderate antimicrobial activity was reported against two Gram-positive (*Staphylococcus aureus* and *Bacillus cereus*) and three Gram-negative bacteria (*Escherichia coli*, *Shigella dysenteriae* and *Shigella sonnei*) for ethanolic extracts of leaf, bark, seed and fruit pulp [36].

In the following enzyme inhibiting assays, inhibitors were detected as colorless bright zones on a violet or grey plate background. The horizontal α-/β-glucosidase inhibition patterns across all samples were in accordance with the previous antibacterial patterns. Thus, the previous antibacterial zone at hR_F 75 showed also α-/β-glucosidase inhibitory effects (Fig. 2 C/D), and it was concluded to be the same bioactive (multi-potent) compound. However, its inhibition was much stronger against α-glucosidase than β-glucosidase (4–5 times higher volumes applied). The same multi-potent compound zone at hR_F 75 showed AChE and tyrosinase inhibition, especially in the mentioned seed extract IDs 1–6 and 10 (Fig. 2 E/F). Diverse much weaker AChE/tyrosinase inhibitors appeared for highly increased volumes applied for bark and leaf extracts (11/3 and 17/4 fold for AChE/tyrosinase, respectively *versus* Fig. 2 A). Another weaker tyrosinase inhibitor in the seed extracts was observed near the solvent front. Radical (DPPH$^•$) scavengers appeared as bright zones at the start zone (indicating polar compounds) on a violet plate background. In particular in the seed extracts, the multi-potent zone at hR_F 75 was proven to be also a radical scavenger (Fig. 2 G).

A cross-check over the 54 abelmosk extracts and seven assays (Fig. 2) showed that the bioactivity profiles of the three different plant parts had comparatively more activity patterns in common than different. The seed extract IDs 1–6 and 10 were more potent than other seeds, bark and leaf. The multi-potent compound at hR_F 75 was most prominently detected in the seven assays, highlighting especially antibacterial, anti-α-glucosidase and anti-tyrosinase activities. The anti-β-glucosidase, anti-AChE and radical scavenging activities were comparatively weaker. Effective compounds also remained at the start zone, and further studies with acidic polar mobile phases are of interest.

3.4. HPTLC-HESI-HRMS of the multi-potent compound zone

The liphophilic multi-potent compound zone at hR_F 75 (Figs. 1 and 2) was assumed to be a fatty acid, and oleic acid was chosen as representative. The latter and selected samples were applied twice on a plate and developed with a mobile phase reduced in elution power (now hR_F 45, Figure S4 D?). One cut plate section was subjected to the tyrosinase assay to mark the bioactive zones on the other section, on which the assay was performed as proof of proper positioning after the HRMS recording of the eluted zones (post-HRMS assay, Fig. 3). In the positive ionization mode, the recorded HPTLC-HESI-HRMS spectra of the respective bioactive zone in the bark, leaf and seed extracts showed two oxidized degradation products (ODPs) of fatty acids. These mass signals were tentatively assigned to be the sodium adducts of 8-oxo-nonanoic acid at *m/z* 195.0991 $[ODP1+Na]^+$ (base peak) and of dihydroxydecanoic acid at *m/z* 227.1252 $[ODP2+Na]^+$(Figure S5). In the negative ionization mode, the recorded mass spectra showed several distinct mass signals, and even further ones when zooming in the base peak range (Fig. 3). The spectra proved that the mass signals obtained from each multi-potent zone of the three extract types matched to the deprotonated molecules of oleic acid C18:1 at *m/z* 281.2487 $[M1-H]^-$,

Table 1
Assignment of the HPTLC-HESI-HRMS signals obtained from oleic acid used as reference and the respective multi-potent compound zone at hR_F 45 in three *Abelmoschus moschatus* extracts.

ID	Observed *m/z*	Theoretical *m/z*	Formula	Mass error (ppm)	Tentative assignment	
HPTLC-HESI$^-$-HRMS						
Reference	281.24870	281.24860	$C_{18}H_{33}O_2^-$	−0.60	Oleic acid	[M1-H]$^-$
Bark ID 2	339.32687	339.32685	$C_{22}H_{43}O_2^-$	−0.06	Behenic acid	[M6-H]$^-$
	311.29568	311.29555	$C_{20}H_{39}O_2^-$	−0.42	Arachidic acid	[M5-H]$^-$
	283.26430	283.26425	$C_{18}H_{35}O_2^-$	−0.18	Stearic acid	[M4-H]$^-$
	281.24868	281.24860	$C_{18}H_{33}O_2^-$	−0.28	Oleic acid	[M1-H]$^-$
	279.23309	279.23295	$C_{18}H_{31}O_2^-$	−0.63	Linoleic acid	[M3-H]$^-$
	255.23311	255.23295	$C_{16}H_{32}O_2^-$	−0.63	Palmitic acid	[M2-H]$^-$
Leaf ID 9	339.32705	339.32685	$C_{22}H_{43}O_2^-$	−0.59	Behenic acid	[M6-H]$^-$
	311.29568	311.29555	$C_{20}H_{39}O_2^-$	−0.42	Arachidic acid	[M5-H]$^-$
	283.26436	283.26425	$C_{18}H_{35}O_2^-$	−0.39	Stearic acid	[M4-H]$^-$
	281.24870	281.24860	$C_{18}H_{33}O_2^-$	−0.75	Oleic acid	[M1-H]$^-$
	279.23312	279.23295	$C_{18}H_{31}O_2^-$	−0.75	Linoleic acid	[M3-H]$^-$
	255.23317	255.23295	$C_{16}H_{32}O_2^-$	−0.98	Palmitic acid	[M2-H]$^-$
Seed ID 10	283.26427	283.26425	$C_{18}H_{35}O_2^-$	−0.07	Stearic acid	[M4-H]$^-$
	281.24868	281.24860	$C_{18}H_{33}O_2^-$	−0.28	Oleic acid	[M1-H]$^-$
	279.23312	279.23295	$C_{18}H_{31}O_2^-$	−0.61	Linoleic acid	[M3-H]$^-$
	255.23317	255.23295	$C_{16}H_{32}O_2^-$	−0.86	Palmitic acid	[M2-H]$^-$
Oxidized degradation product (ODP)	171.10271	171.10266	$C_9H_{15}O_3^-$	−0.29	8-Oxo-nonanoic acid	[ODP1-H]$^-$
	HPTLC-HESI$^+$-HRMS					
	195.09918	195.09917	$C_9H_{16}O_3Na^+$	−0.05	8-Oxo-nonanoic acid	[ODP1+Na]$^+$
	227.12523	227.12538	$C_{10}H_{20}O_4Na^+$	0.66	Dihydroxydecanoic acid	[ODP2+Na]$^+$

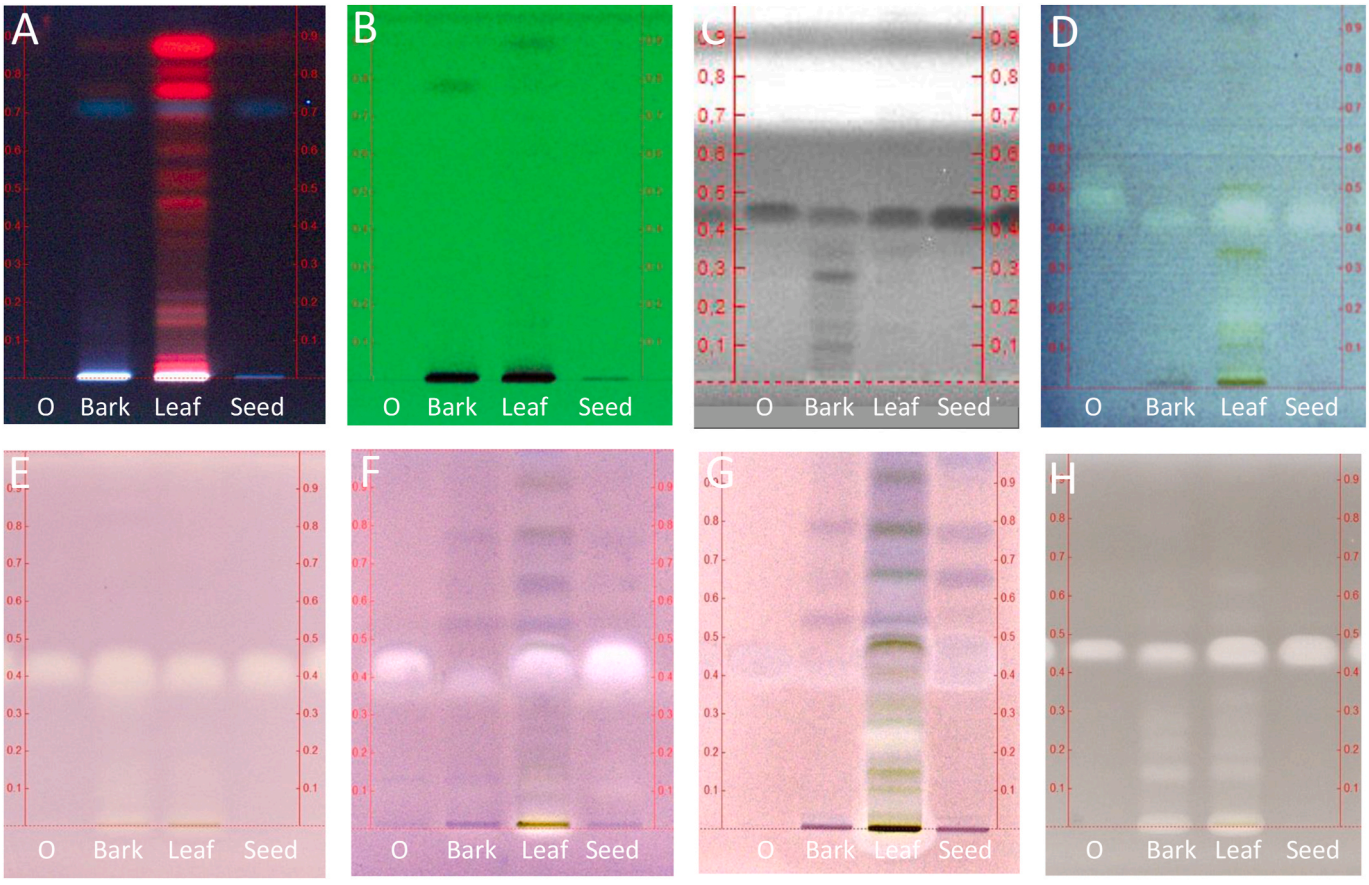

Fig. 4. Confirmation of the multi-potent compound assignment by co-development with exemplarily oleic acid (O, 1.3 µg/band), detected at (A) FLD 366 nm, (B) UV 254 nm, after (C) Gram-negative *Aliivibrio fischeri* bioassay (grey-scale image of bioluminescence), as well as at Vis after (D) Gram-positive *Bacillus subtilis* bioassay and (E) α-glucosidase, (F) β-glucosidase, (G) AChE and (H) tyrosinase inhibition assays; chromatographic system as in Fig. 3.

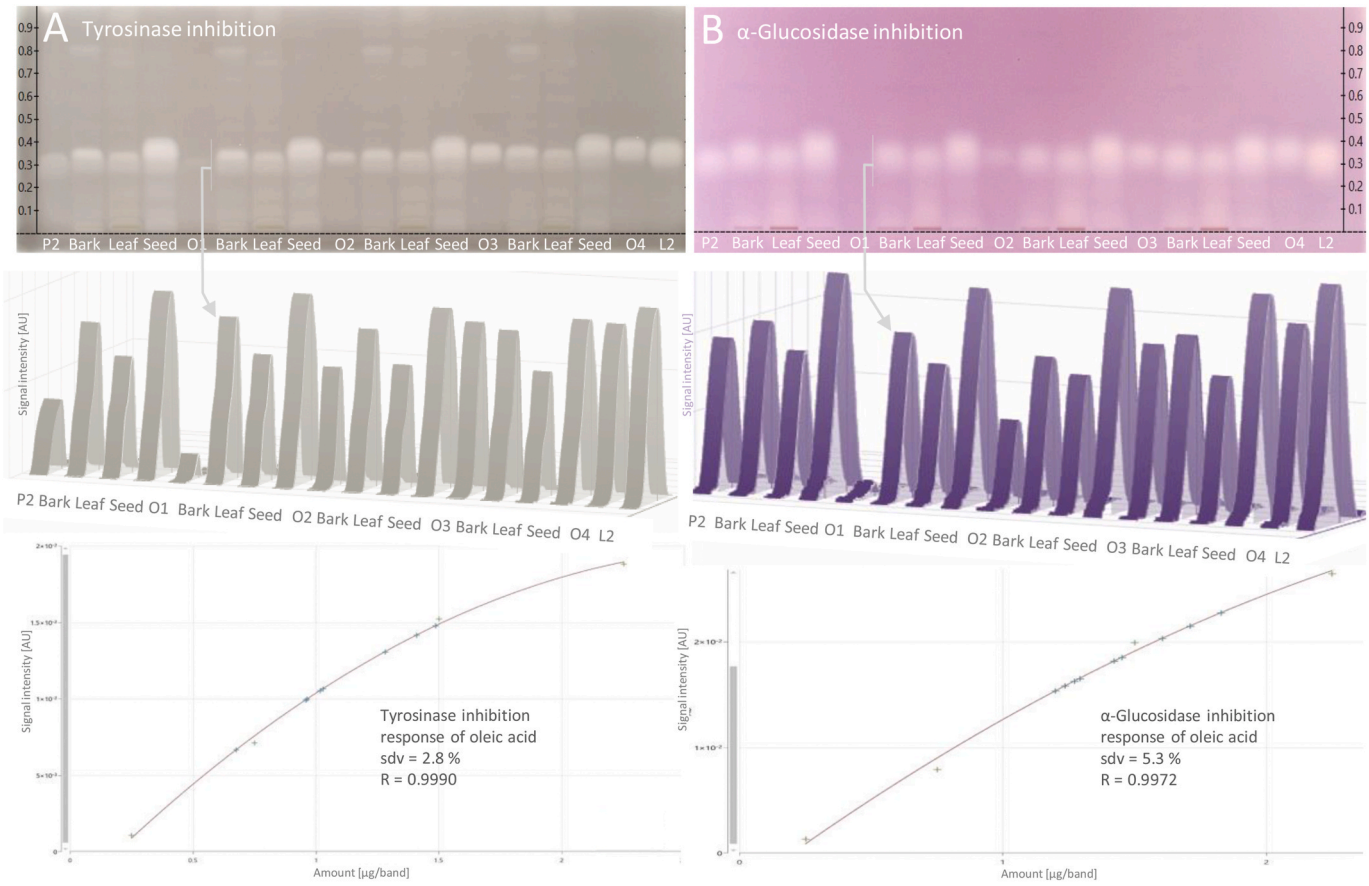

Fig. 5. Enzymatic quantification for equivalency calculation of the detected (A) tyrosinase and (B) α-glucosidase inhibiting compound zone: Autograms of abelmosk ID 6 extracts of bark (8 µL, 540 µg/band), leaf (2 µL, 200 µg/band) and seed (diluted 1:4, 1 µL, 25 µg/band) applied 4-fold along with palmitic acid (P2), linoleic acid (L2) as well as oleic acid calibration levels (O1–O4; 0.25 mg/mL, 1, 3, 6 and 9 µL, 0.25–2.25 µg/band); chromatographic system as in Fig. 3; respective densitograms at 546 nm and 579 nm (inverse absorbance measurement) as well as calibration curve plots.

palmitic acid C16:0 at *m/z* 255.2329 $[M2\text{-}H]^-$, linoleic acid C18:2 at *m/z* 279.2329 $[M3\text{-}H]^-$ and stearic acid C18:0 at *m/z* 283.2642 $[M4\text{-}H]^-$ (Table 1). Further, arachidic acid C20:0 at *m/z* 311.2955 $[M5\text{-}H]^-$ and behenic acid C22:0 at *m/z* 339.3268 $[M6\text{-}H]^-$ were detected in leaf and bark extracts. The oxidized fatty acid degradation product 8-oxo-nonanoic acid [37] was confirmed as deprotonated molecule at *m/z* 171.1027 $[ODP1\text{-}H]^-$. In agreement with our results, abelmosk seed was reported to be rich in unsaturated fatty acids and to contain about 40% linoleic acid, 30% oleic acid, 20% palmitic acid and 4% stearic acid as main fatty acid composition [38]. For bark and leaf, fatty acid values were not available. It is known that unsaturated linoleic acid and also oleic acid can easily be oxidized and that the fatty acid profile can vary naturally (*e.g.*, less polyunsaturated fatty acids are formed at a warmer location than colder). This and also the different extraction methods explain why the fatty acid distribution including degradation products may differ to our results.

3.5. Confirmation of the assignment

The tentatively assigned multi-potent compound zone to be coeluting fatty acids was confirmed by overlapped application with oleic acid as reference. Thus, the oleic acid migrated partly also within the abelmosk matrix (Figure S6). As a result, the oleic acid and the multi-potent compound were detected as common band, which confirmed the assignment by HPTLC-HESI-HRMS and multi-imaging. A sample comparison confirmed that fatty acids were more abundant in abelmosk seed than leaf and bark (Figure S7). Further the multi-potent activity of oleic acid was successfully proven in all assays (Fig. 4).

Table 2
Enzymatic quantification for equivalency calculation of the multi-potent compound zone in three different abelmosk extracts as well as response ratios for palmitic acid (P2) and linoleic acid (L2), all in reference to oleic acid (O2, all standard level 2) via the HPTLC-tyrosinase assay-Vis and HPTLC-α-glucosidase assay-Vis (as in Fig. 5).

Abelmosk extract ID 6	HPTLC-tyrosinase assay		HPTLC-α-glucosidase assay	
	Content of oleic acid (%)	Precision (%*RSD*, $n = 4$)	Content of oleic acid (%)	Precision (%*RSD*, $n = 4$)
Bark, 540 µg/band	0.3	5.7	0.3	8.8
Leaf, 200 µg/band	0.6	3.7	0.6	3.0
Seed, 25 µg/band	10.2	2.9	10.8	2.7
	Mean	**4.1**	**Mean**	**4.8**
Factor seed/bark	34		36	
Factor seed/leaf	17		18	
Peak area O2	0.0071	**Response ratio to O2**	0.0079	**Response ratio to O2**
Peak area P2	0.0066	1	0.0185	2
Peak area L2	0.0249	4	0.0384	5

3.6. Enzymatic quantifications for equivalency calculation

The comparison of results obtained by different methods is important for method verification. Hence, two different assays were evaluated concerning their calibration performance and quantitative results (Fig. 5). For this comparison, factors of influence and systematic errors were limited using the same extracts, standard dilution, application volumes, working range, automated application and piezoelectric spraying device. The coefficient of correlation of the polynomial calibration curve of oleic acid was 0.9990 (sdv 2.8%) and 0.9972 (sdv 5.3%) for the tyrosinase and α-glucosidase inhibition response, respectively. The respective mean precision ($n = 4$) of the oleic acid analysis in three different abelmosk extract types was 4.1% and 4.8% for the tyrosinase and α-glucosidase inhibition (Table 2). The bioactivity response of each abelmosk extract was calculated equivalently to the bioactivity response of oleic acid. It was 0.3%, 0.6% and 10.2% for bark, leaf and seed extracts, respectively, for the tyrosinase inhibition and almost the same (0.3%, 0.6% and 10.8%) for the α-glucosidase inhibition. The high activity of exemplarily seed extract ID 6 (Fig. 2) was confirmed. The seed had a 34 or 36-fold higher inhibiting activity (against tyrosinase or α-glucosidase, respectively) than the respective bark, and was 17 or 18-fold higher than the leaf. The comparison of the bioactivity responses of the three fatty acids (at the same amount) revealed that individual fatty acids contribute differently in its activity to the overall effect (Table 2). This has to be studied in detail in the future and highlights that individually active fatty acid responses and its meaning are still not explored to the full.

4. Conclusions

Comprehensive information was obtained by HPTLC-UV/Vis/FLD-EDA-HESI-HRMS on bioactive compounds present in 54 bark, leaf and seed extracts of abelmosk. In particular, antibacterial as well as α-glucosidase and tyrosinase inhibition effects were evident. In most extracts, a multi-potent compound zone was prominently detected by seven assays. It was identified to be coeluting fatty acids by HPTLC-HESI-HRMS, multi-imaging and co-chromatography (even in the matrix by overlapped application). All assay responses were successfully proven for oleic acid as reference, and this bioanalytical screening highlighted the bioactivity potential of unsaturated fatty acids. The multi-imaging (via all in all 19 detection modes) provided comprehensive information about multi-potent compounds and sample diversity. Such information is considered elementary for the assurance of the product quality in the field of botanicals, foods and medicinal plants, which are the backbone of traditional medicine.

CRediT author statement

N.G.A.S. Sumudu Chandana: Investigation, Writing - original draft preparation Gertrud E. Morlock: Supervision, Writing - original draft preparation, Writing- Reviewing and Editing

Declaration of competing interest

The authors declare that they have no known competing financial interests or personal relationships that could have appeared to influence the work reported in this paper.

Acknowledgment

Thank is owed to the Food Science group for their technical guidance during this project and Merck, Darmstadt, Germany, for the supply of plates. Instrumentation was partially funded by the Deutsche Forschungsgemeinschaft (DFG, German Research Foundation) – INST 162/471-1 FUGG; INST 162/536-1 FUGG.

Appendix A. Supplementary data

Supplementary data to this article can be found online at https://doi.org/10.1016/j.talanta.2020.121701.

Supplementary data

Supplementary data can be found at …

References

[1] S. Gayibova, E. Ivanišová, J. Árvay, M. Hŕstková, M. Slávik, J. Petrová, L Hleba, T Tóth, M. Kačániová, T. Aripov, In vitro screening of antioxidant and antimicrobial activities of medicinal plants growing in Slovakia, J. Microbiol. Biotechnol. Food Sci. 8 (2019) 1281–1289.
[2] A.G. Atanasov, B. Waltenberger, E.-M. Pferschy-Wenzig, T. Linder, C. Wawrosch, P. Uhrin, V. Temml, L. Wang, S. Schwaiger, E.H. Heiss, J.M. Rollinger, D. Schuster, J.M. Breuss, V. Bochkov, M.D. Mihovilovic, B. Kopp, R. Bauer, V.M. Dirsch, H. Stuppner, Discovery and resupply of pharmacologically active plant-derived natural products: a review, Biotechnol. Adv. 33 (2015) 1582–1614.
[3] B.N. Tefera, Y.-D. Kim, Ethnobotanical study of medicinal plants in the Hawassa Zuria district, Sidama zone, Southern Ethiopia, J. Ethnobiol. Ethnomed. 15 (2019) 25.
[4] X. Liu, S. Ahlgren, H.A.A.J. Korthout, L.F. Salomé-Abarca, L.M. Bayona, R. Verpoorte, Y.H. Choi, Broad range chemical profiling of natural deep eutectic solvent extracts using a high performance thin layer chromatography-based method, J. Chromatogr. A 1532 (2018) 198–207.
[5] V. Bardot, A. Escalon, I. Ripoche, S. Denis, M. Alric, S. Chalancon, P. Chalard, C. Cotte, L. Berthomier, M. Leremboure, M. Dubourdeaux, Benefits of the ipowder® extraction process applied to *Melissa officinalis* L.: improvement of antioxidant activity and in vitro gastro-intestinal release profile of rosmarinic acid, Food & Function 11 (2020) 722–729.
[6] Morlock, G.E., Heil, J., Bardot, V., Lenoir, L., Cotte, C., Dubourdeaux, M., Assessment of botanicals fortified by the addition of concentrated plant infusions via planar chromatography hyphenated to effect directed assays and high-resolution mass spectrometry, Food Chem., (in submission).
[7] M.J. Cheesman, A. Ilanko, B. Blonk, I.E. Cock, Developing new antimicrobial therapies: are synergistic combinations of plant extracts/compounds with conventional antibiotics the solution? Pharmacogn. Rev. 11 (2017) 57–72.
[8] M. Jamshidi-Aidji, G.E. Morlock, From bioprofiling and characterization to bioquantification of natural antibiotics by direct bioautography linked to high-resolution mass spectrometry: exemplarily shown for *Salvia miltiorrhiza* root, Anal. Chem. 88 (2016) 10979–10986.
[9] H.S. Sheik, N. Vedhaiyan, S. Singaravel, Evaluation of *Abelmoschus moschatus* seed extract in psychiatric and neurological disorders, Int. J. Basic Clin. Pharmacol. 3 (2014) 845–853.
[10] S. Babitha, H.G.A. Deepu, T. Nageena, Antimotility and antisecretory related antidiarrhoeal activity of the *Abelmoschus moschatus* medik in experimental animal models, International Journal of Pharmacy and Pharmceutical Sciences 10 (2018) 108–111.
[11] A.T. Pawar, N.S. Vyawahare, Antiurolithiatic activity of *Abelmoschus moschatus* seed extracts against zinc disc implantation-induced urolithiasis in rats, J. Basic Clin. Pharm. 7 (2016) 32–38.
[12] P.D. Gupta, T.J. Birdi, Development of botanicals to combat antibiotic resistance, J. Ayurveda Integr. Med. 8 (2017) 266–275.
[13] M.U. Anyanwu, R.C. Okoye, Antimicrobial activity of Nigerian medicinal plants, Journal of Intercultural Ethnopharmacology 6 (2017) 240–259.
[14] L. Guariguata, D.R. Whiting, I. Hambleton, J. Beagley, U. Linnenkamp, J.E. Shaw, Global estimates of diabetes prevalence for 2013 and projections for 2035, Diabetes Res. Clin. Pract. 103 (2014) 137–149.
[15] H.S. El-Abhar, M.F. Schaalan, Phytotherapy in diabetes: review on potential mechanistic perspectives, World J. Diabetes 5 (2014) 176–197.
[16] Y. Sivasothy, K.Y. Loo, K.H. Leong, M. Litaudon, K. Awang, A potent alpha-glucosidase inhibitor from *Myristica cinnamomea* King, Phytochemistry 122 (2016) 265–269.
[17] L. Flores-Bocanegra, M. González-Andrade, R. Bye, E. Linares, R. Mata, α-Glucosidase inhibitors from *Salvia circinata*, J. Nat. Prod. 80 (2017) 1584–1593.
[18] S.M. Fayaz, V.S. Suvanish Kumar, K.G. Rajanikant, Finding needles in a haystack: application of network analysis and target enrichment studies for the identification of potential anti-diabetic phytochemicals, PloS One 9 (2014), e112911.
[19] J. William, P. John, M.W. Mumtaz, A.R. Ch, A. Adnan, H. Mukhtar, S. Sharif, S. A. Raza, M.T. Akhtar, Antioxidant activity, α-glucosidase inhibition and phytochemical profiling of *Hyophorbe lagenicaulis* leaf extracts, PeerJ 7 (2019), e7022.
[20] S. Zolghadri, A. Bahrami, M.T. Hassan Khan, J. Munoz-Munoz, F. Garcia-Molina, F. Garcia-Canovas, A.A. Saboury, A comprehensive review on tyrosinase inhibitors, J. Enzyme Inhib. Med. Chem. 34 (2019) 279–309.
[21] S.Y. Lee, N. Baek, T.-G. Nam, Natural, semisynthetic and synthetic tyrosinase inhibitors, J. Enzyme Inhib. Med. Chem. 31 (2016) 1–13.
[22] P. García, I.A. Ramallo, R.L.E. Furlan, Reverse phase compatible TLC-bioautography for detection of tyrosinase inhibitors, Phytochem. Anal. 28 (2017) 101–105.

[23] J. Korabecny, M. Andrs, E. Nepovimova, R. Dolezal, K. Babkova, A. Horova, D. Malinak, E. Mezeiova, L. Gorecki, V. Sepsova, M. Hrabinova, O. Soukup, D. Jun, K. Kuca, 7-Methoxytacrine-*p*-Anisidine hybrids as novel dual binding site acetylcholinesterase inhibitors for Alzheimer's disease treatment, Molecules 20 (2015) 22084–22101.
[24] H. Kim, Detection of severity in Alzheimer's disease (AD) using computational modeling, Bioinformation 14 (2018) 259–264.
[25] M. Kozurkova, S. Hamulakova, Z. Gazova, H. Paulikova, P. Kristian, Neuroactive multifunctional tacrine congeners with cholinesterase, anti-amyloid aggregation and neuroprotective properties, Pharmaceuticals 4 (2011) 382–418.
[26] A. Gholamhoseinian, M.N. Moradi, F. Sharifi-far, Screening the methanol extracts of some Iranian plants for acetylcholinesterase inhibitory activity, Research in Pharmaceutical Sciences 4 (2009) 105–112.
[27] V. Lobo, A. Patil, A. Phatak, N. Chandra, Free radicals, antioxidants and functional foods: impact on human health, Pharmacogn. Rev. 4 (2010) 118–126.
[28] B. Mahdi-Pour, S.L. Jothy, L.Y. Latha, Y. Chen, S. Sasidharan, Antioxidant activity of methanol extracts of different parts of *Lantana camara*, Asian Pacific Journal of Tropical Biomedicine 2 (2012) 960–965.
[29] C.V. Jayachandran Nair, S. Ahamad, W. Khan, V. Anjum, R. Mathur, Development and validation of high-performance thin-layer chromatography method for simultaneous determination of polyphenolic compounds in medicinal plants, Pharmacogn. Res. 9 (2017) S67–S73.
[30] M. Attimarad, K.K.M. Ahmed, B.E. Aldhubaib, S. Harsha, High-performance thin layer chromatography: a powerful analytical technique in pharmaceutical drug discovery, Pharmaceutical Methods 2 (2011) 71–75.
[31] C.A. Simões-Pires, B. Hmicha, A. Marston, K. Hostettmann, A TLC bioautographic method for the detection of alpha- and beta-glucosidase inhibitors in plant extracts, Phytochem. Anal. 20 (2009) 511–515.
[32] E. Azadniya, G.E. Morlock, Automated piezoelectric spraying of biological and enzymatic assays for effect-directed analysis of planar chromatograms, J. Chromatogr. A 1602 (2019) 458–466.
[33] M. Jamshidi-Aidji, J. Macho, M.B. Mueller, G.E. Morlock, Effect-directed profiling of aqueous, fermented plant preparations via high-performance thin-layer chromatography combined with in situ assays and high-resolution mass spectrometry, J. Liq. Chromatogr. Relat. Technol. 42 (2019) 266–273.
[34] M. Jamshidi-Aidji, G.E. Morlock, Fast equivalency estimation of unknown enzyme inhibitors in situ the effect-directed fingerprint, shown for *Bacillus* lipopeptide extracts, Anal. Chem. 90 (2018) 14260–14268.
[35] S. Krüger, L. Hüsken, R. Fornasari, I. Scainelli, G.E. Morlock, Effect-directed fingerprints of 77 botanical extracts via a generic high-performance thin-layer chromatography method combined with assays and mass spectrometry, J. Chromatogr. A 1529 (2017) 93–106.
[36] M.M. Rahman, M.N. Haque, S. Hosen, J. Akhter, U.S.B. Kamal, E.N. Jahan, A.S.M. S. Hossain, M.N. Uddin, M.B. Islam, M.R. Islam, A.H.M.K. Alam, A. Mosaddik, Comparative evaluation of antimicrobial activity of different parts of *Abelmoschus moschatus* against multi-resistant pathogens, Int. J. Pharmaceut. Sci. Res. 8 (2017) 1874–1880.
[37] https://case.edu/artsci/chem/faculty/salomon/Mechanisms.htm; last access April 1st, 2020.
[38] R.L. Jarret, M.L. Wang, I.J. Levy, Seed oil and fatty acid content in okra (*Abelmoschus esculentus*) and related species, J. Agric. Food Chem. 59 (2011) 4019–4024.

Supplementary information

Comprehensive bioanalytical multi-imaging by planar chromatography *in situ* combined with biological and biochemical assays highlights bioactive fatty acids in abelmosk

N.G.A.S. Sumudu Chandana[a], Gertrud E. Morlock[a]

[a]Justus Liebig University Giessen, Institute of Nutritional Science, Chair of Food Science, and TransMIT Center for Effect-Directed Analysis, Heinrich-Buff-Ring 26-32, 35392 Giessen, Germany

*Corresponding author. Tel.: +49 641 9939141; fax: +49 641 9939149.

E-mail address: Gertrud.Morlock@uni-giessen.de (G.E. Morlock).

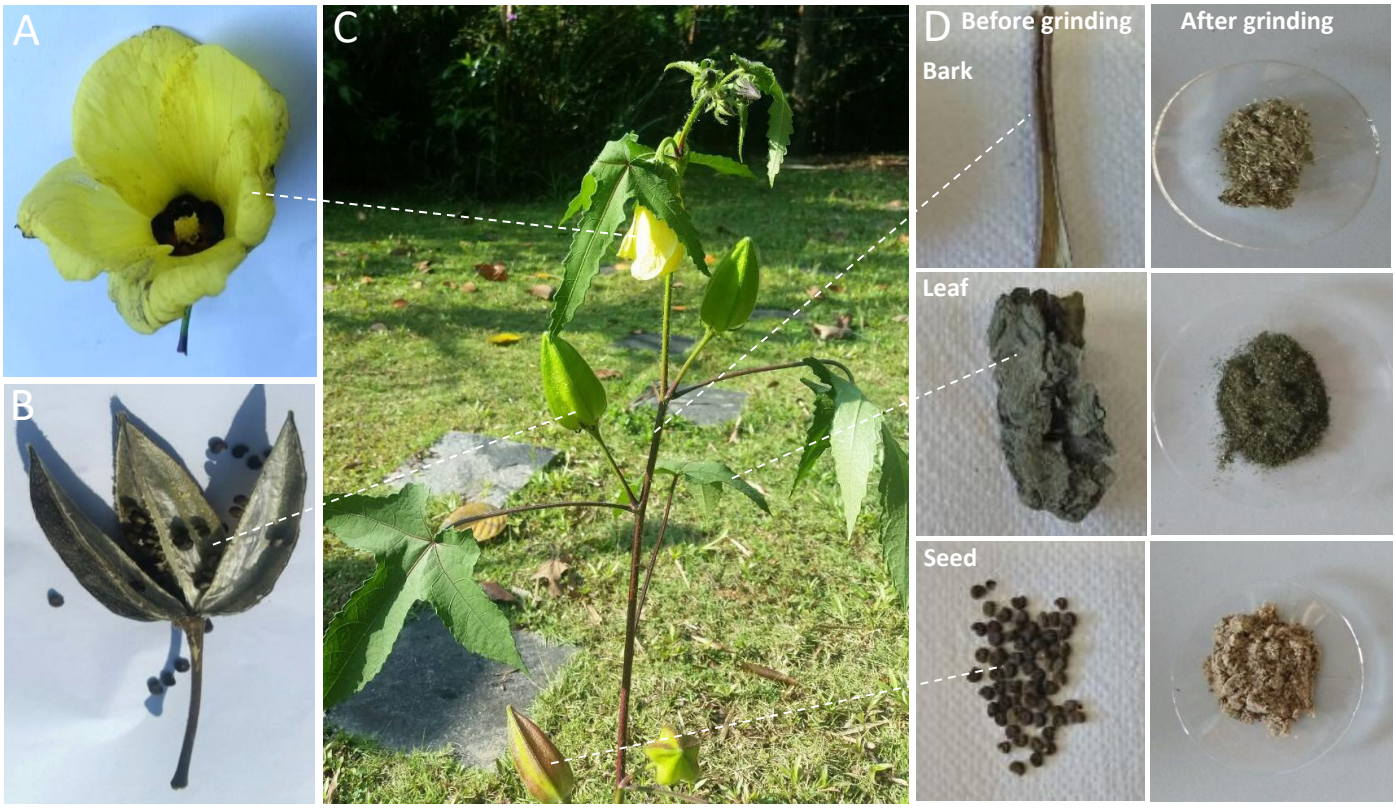

Figure S1 Parts of *Abelmoschus moschatus* plant and its specimens: (**A**) flower, (**B**) opened dried capsule with seeds, (**C**) aerial part of the tree, (**D**) dried specimens before and after grinding of bark, leaf and seed

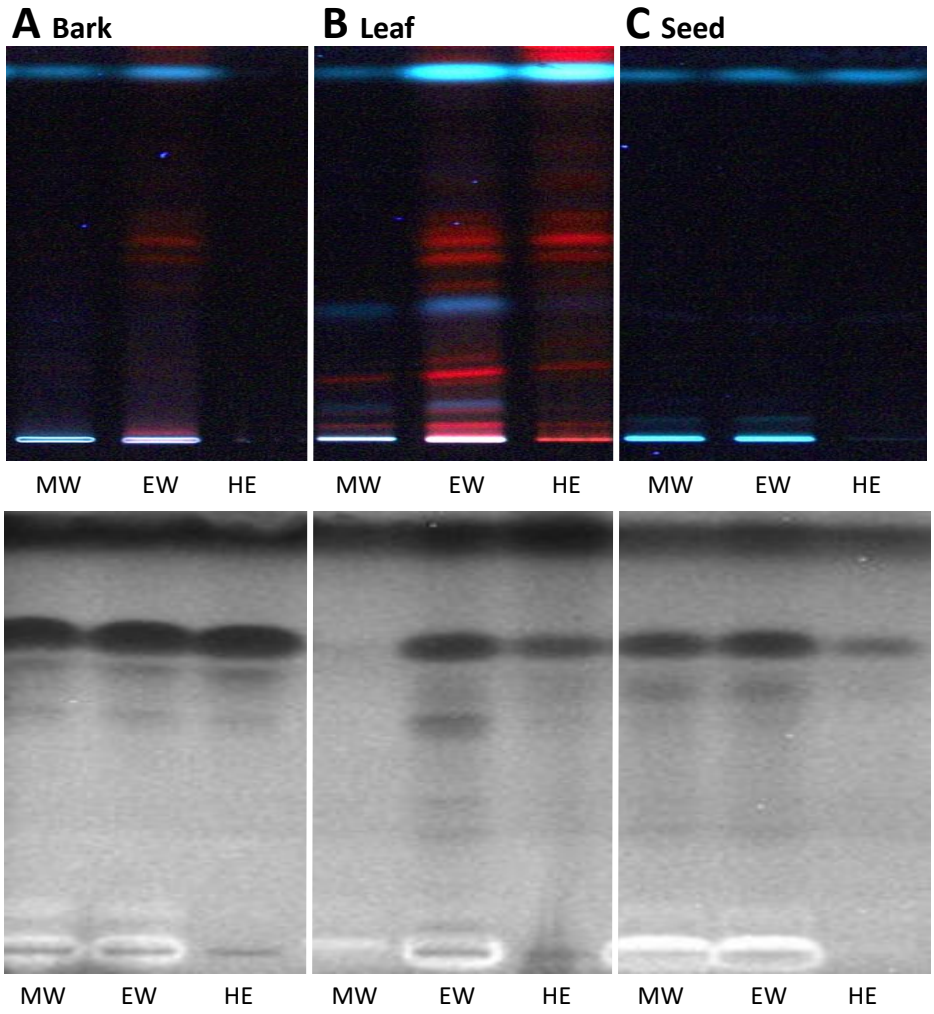

Figure S2 Extraction solvent selection: HPTLC chromatograms of *Abelmoschus moschatus* ID 1 (**A**) bark (80 µg/band), (**B**) leaf and (**C**) seed (250 µg/band) extracted with methanol – water (MW), ethanol – water (EW) and *n*-hexane – ethyl acetate (HE), all 4:1 *V/V,* separated on HPTLC plate silica gel 60 F_{254} with toluene – ethyl acetate – methanol 6:5:2 (V/V/V) and documented at FLD 366 nm and after the *Aliivibrio fischeri* bioassay (greyscale image of bioluminescence)

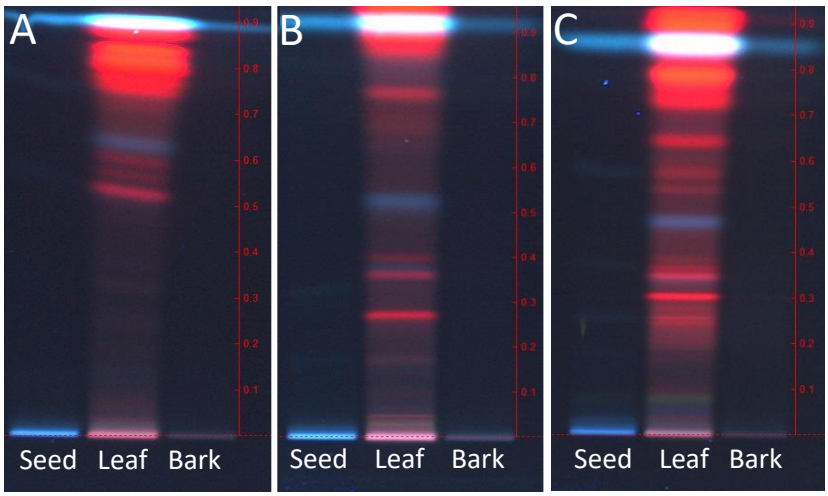

Figure S3 Mobile phase optimization study (all *V*/*V*): HPTLC chromatograms of *Abelmoschus moschatus* ID 1 seed, leaf (each 250 µg/band) and bark (80 µg/band), applied on HPTLC silica gel 60 F_{254} plates and developed with (**A**) *n*-hexane – acetone - water 7:7:0.2, (**B**) toluene - ethyl acetate - methanol 6:5:2 and (**C**) *n*-hexane - toluene - ethyl acetate - methanol - water 2:5:5:2:0.2, all up to 65 mm and documented at FLD 366 nm

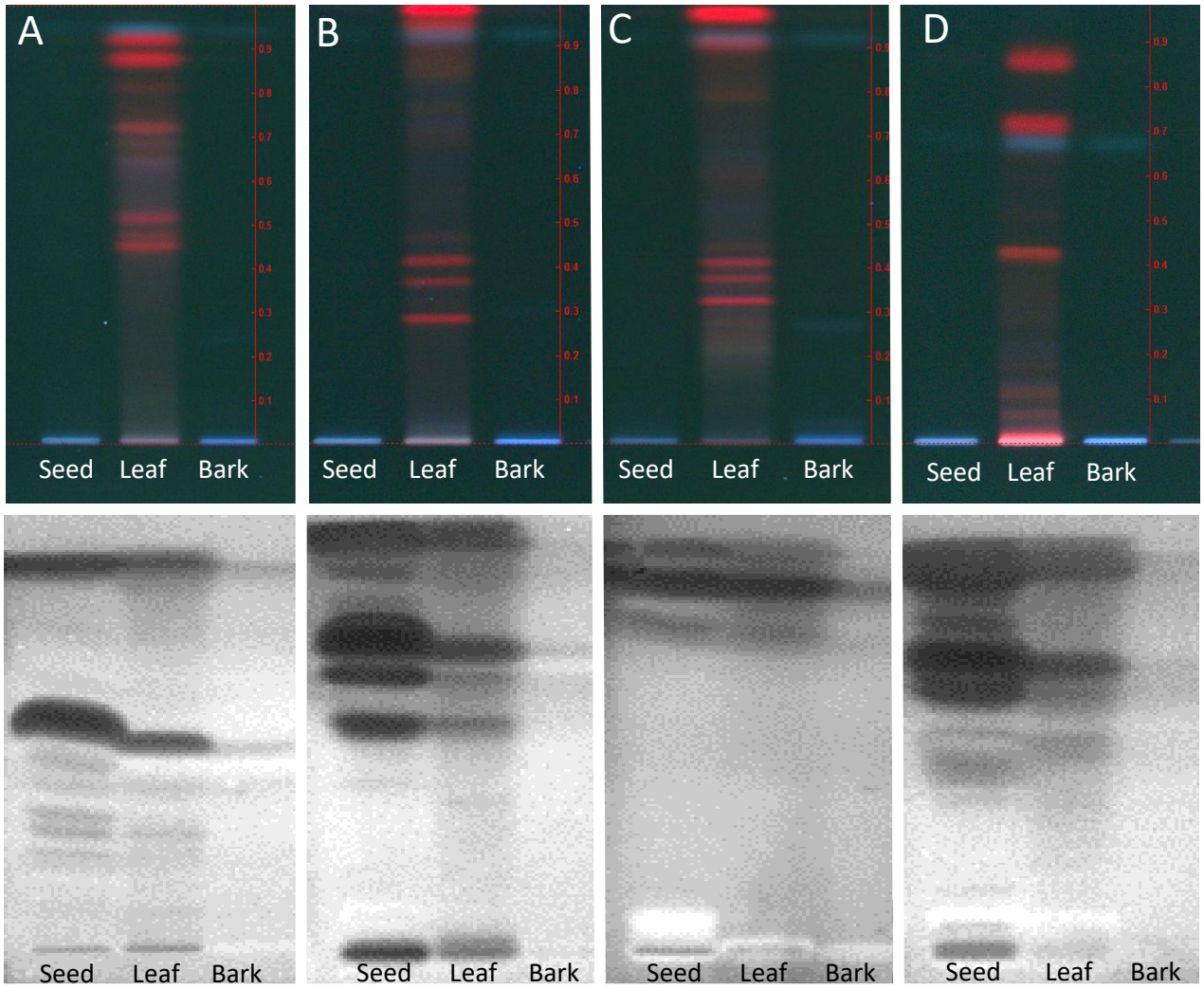

Figure S4 Mobile phase optimization study (all *V*/*V*) evaluated with regard to antibiotics detected: *Abelmoschus moschatus* ID 7 seed, leaf (each 250 µg/band) and bark (80 µg/band) applied on HPTLC plates silica gel 60 F_{254} and developed with (**A**) *n*-hexane – acetone - water 7:7:0.2, (**B**) toluene - ethyl acetate - methanol 6:5:2 and (**C**) *n*-hexane - toluene - ethyl acetate - methanol - water 2:5:5:2:0.2 and (**D**) toluene - ethyl acetate 7:3, developed up to 65 mm and documented at FLD 366 nm and after the *Aliivibrio fischeri* bioassay (greyscale image of bioluminescence)

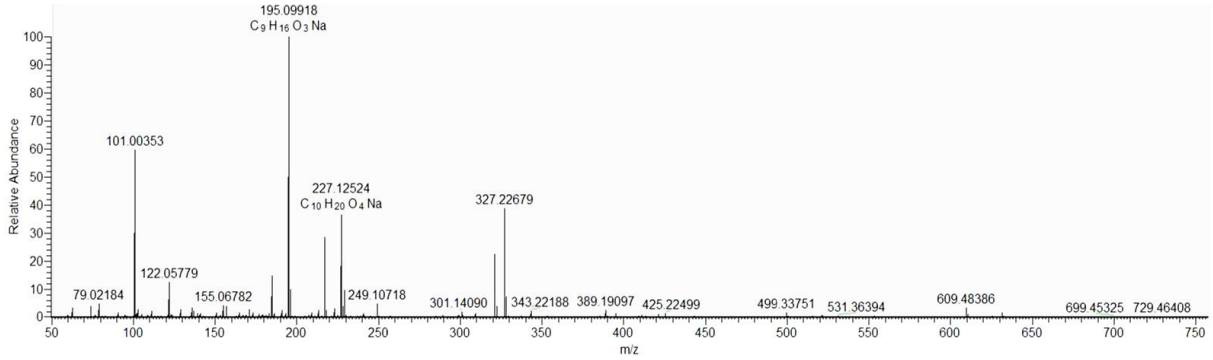

Figure S5 HPTLC-HESI$^+$-HRMS spectra recorded of the bioactive multi-potent zone in the seed extract ID 10 in the positive ionization mode showing the respective sodium adduct of the oxidized degradation products 8-oxo-decanoic acid at *m*/*z* 195.0991 $[ODP1+Na]^+$ (base peak) and dihydroxydecanoic acid at *m*/*z* 227.1252 $[ODP2+Na]^+$

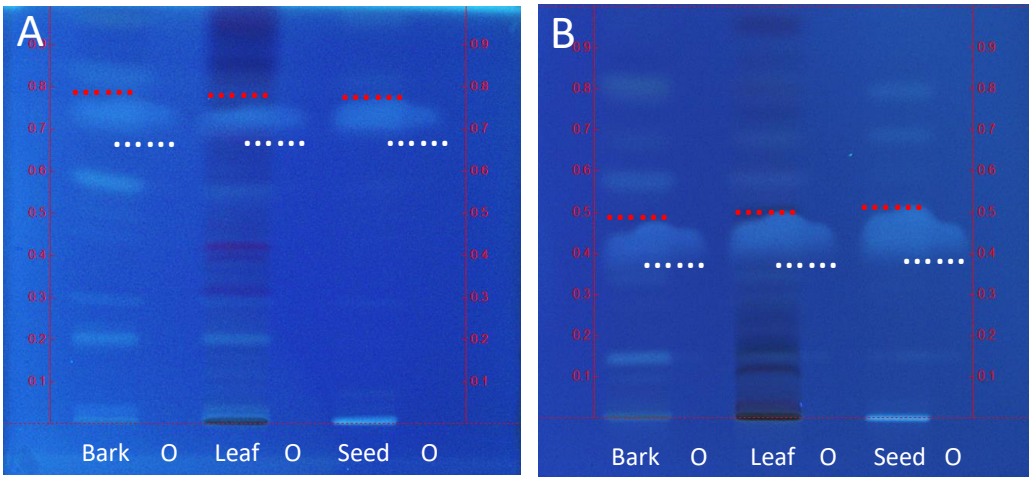

Figure S6 Confirmation and assignment of oleic acid assumed to be in the multipotent zone of *Abelmoschus moschatus*: HPTLC chromatograms with overlapped application of bark (ID 2; 800 µg/band), leaf (ID 9; 1000 µg/band) or seed (ID 10; 500 µg/band) extracts (red dotted line) with oleic acid (O, 1.3 µg/band, white dotted line), each applied as 8-mm bands in a 4-mm overlapped mode on HPTLC plate silica gel 60 F_{254} developed up to 65 mm with (**A**) toluene - ethyl acetate - methanol 6:5:2 (*V*/*V*/*V*) and (**B**) toluene - ethyl acetate 7:3 (*V*/*V*), detected by the primuline reagent followed by drying (4 min) and documented at FLD 366 nm

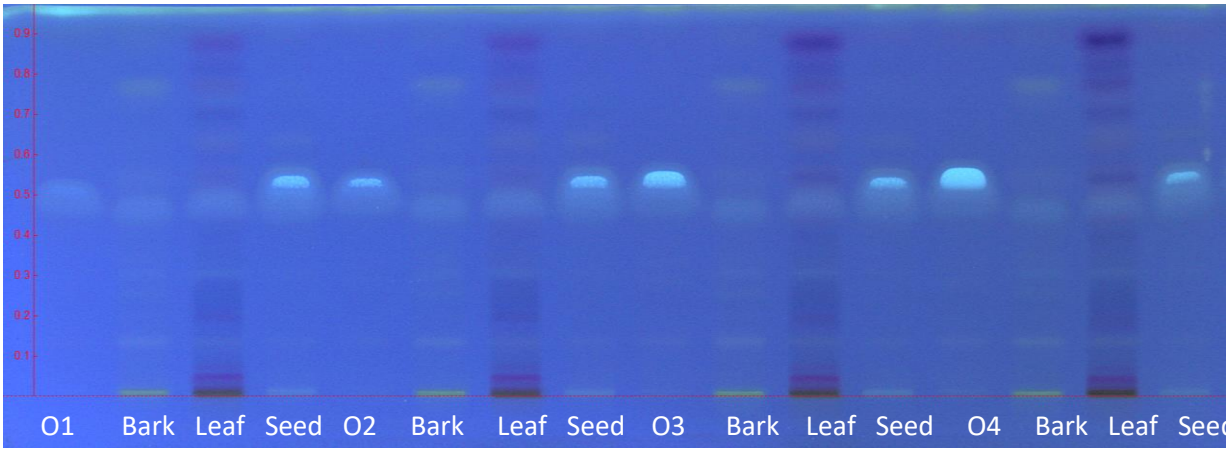

Figure S7 Comparison of oleic acid content of *Abelmoschus moschatus* in the different plant parts: HPTLC chromatogram with oleic acid standard levels (O1-O4; 3, 6, 9 and 12 µL/band; 1.35 mg/mL) and bark (ID 2, 20 µL, 1340 µg/band), leaf (ID 9, 12 µL, 1200 µg/band) and seed (ID 10, 2 µL, 200 µg/band) extracts applied four-fold on HPTLC plate silica gel 60 F_{254} developed with toluene - ethyl acetate 7:3 (*V/V*) up to 65 mm, detected and documented as before

3.2 Paper 2

Spices contain plenty of bioactive compounds, used to valorize foods. However, product quality may be affected by contaminations and adulterations along the global production chain. In the second study, an HPTLC based method was developed for the separation and identification of the single compounds effects in cinnamon, whereby the results of original samples were compared with those of market products. Four homemade cinnamon samples from Sri Lanka (*Cinnamomum zeylanicum*), considered to be authentic, 24 market products in Sri Lanka and 12 products from German discounters were investigated. HPTLC-UV/Vis/FLD-EDA–HRMS analytical platform was developed to study the single compounds effects in cinnamon samples and the results were compared with the authentic samples and market products. The following outcomes were achieved.

1. A newly developed multi-imaging in combination with bioactivity screening directly pointed to individual multi-potent compounds. This information on individual compounds cannot be obtained from other *in vitro* assays.
2. According to the results of EDA, higher activity was observed for tyrosinase, α-glucosidase, and β-glucosidase, moderate activity for antimicrobial bioassays and less activity for AChE and BChE.
3. According to HRMS findings, highlighted the bioactive potential of cinnamaldehyde, cinnamic acid, benzoic acid, coumarin, linoleic acid, oleic acid, stearic acid, palmitic acid, caproic acid, and linalool oxide.
4. This HPTLC-UV/Vis/FLD-EDA–HRMS profiling provided comprehensive information on product quality and safety.
5. Sri Lankan cinnamon (*Cinnamomum zeylanicum*) showed more intense bioactivity in the different assays (multi-potent compounds) and also proved to contain less coumarin compared to the other investigated samples.
6. To show the potential of the bioanalytical tool, exemplarily the cinnamic acid content was quantified via its enzymatic response by scanning densitometry of the respective bioactive zones and its quantification.

In Summary, via the newly developed HPTLC-UV/Vis/FLD-EDA–HRMS analytical platform, the individual bioactive compound was detected in the cinnamon samples, *i. e.* cinnamaldehyde, cinnamic acid, benzoic acid, coumarin, linoleic acid, oleic acid, stearic acid, palmitic acid, caproic acid, and linalool oxide. This HPTLC-UV/Vis/FLD-EDA–HRMS profiling using original samples parallel to the market product provided comprehensive information on product quality and safety.

Food Chemistry 357 (2021) 129135

Contents lists available at ScienceDirect

Food Chemistry

journal homepage: www.elsevier.com/locate/foodchem

Eight different bioactivity profiles of 40 cinnamons by multi-imaging planar chromatography hyphenated with effect–directed assays and high-resolution mass spectrometry

N.G.A.S. Sumudu Chandana, Gertrud E. Morlock *

Justus Liebig University Giessen, Institute of Nutritional Science, Chair of Food Science, and TransMIT Center for Effect–Directed Analysis, Heinrich–Buff–Ring 26–32, 35392 Giessen, Germany

ARTICLE INFO

Dedicated to the 75th birthday of Professor Dr. Teresa Kowalska, University of Silesia, Poland

Keywords:
Cinnamomum
Antibacterial
Enzyme inhibitor
Antioxidant
HPTLC–EDA–HRMS
Bioassay

ABSTRACT

Spices contain plenty of bioactive compounds, used to valorize foods. However, product quality may be affected by contaminations and adulterations along the global production chain. A newly developed multi–imaging in combination with bioactivity screening directly pointed to individual multi–potent compounds. For cinnamon as prominent example, the multi–imaging results provided a wealth of new information on their effects and clearly visualized the valorizing potential of cinnamon to foods. The separation focus was in the mid–polar to apolar range. Eight effect–directed assays (EDA, *i.e.* one radical scavenging, two biological and five biochemical assays) were performed *in situ* the high–performance thin–layer chromatography (HPTLC) adsorbent. Several multi–potent compound zones were revealed and further characterized by high–resolution mass spectrometry (HRMS), highlighting the bioactive potential of cinnamaldehyde, cinnamic acid, benzoic acid, coumarin, linoleic acid, oleic acid, stearic acid, palmitic acid, caproic acid, and linalool oxide. This HPTLC–UV/Vis/FLD–EDA–HRMS profiling provided comprehensive information on product quality and safety.

1. Introduction

The field of functional foods, health foods, nutraceuticals and personalized nutrition is steadily growing (Estevinho, 2018; Cetin Cakmak & Gülçin, 2019). Herbs and spices have great potential as flavoring agents, antioxidants and antibacterials for food preservation (Nabavi et al., 2015). One of the most popular and oldest spice in the world is cinnamon (Shan et al., 2007). Both *Cinnamomum cassia* Blume (Cassia cinnamon) and *Cinnamomum zeylanicum* Nees (*Cinnamomum verum* or true cinnamon) belong to the Lauraceae family. The broadly available and less expensive *Cinnamomum cassia* comes from a different region, is stronger in its taste and has a higher coumarin content than true cinnamon (Ranasinghe et al., 2017; Krüger et al., 2018). *Cinnamomum zeylanicum* is an evergreen tree native to Sri Lanka and the Malabar Coast of India (Hameed et al., 2016). Manufactured from its bark, cinnamon is available on the market as sticks or ground powder (Medagama, 2015). The bark contains 65–85% cinnamaldehyde and 5–10% eugenol as major constituents, but also catechins, procyanidins, cinnamic acid, cinnamate and essential oils, most with antioxidant and antibacterial properties (Rao & Gan, 2014). Such natural products became popular as substitutes for synthetic preservatives (Saber, 2019; Liang et al., 2019), and still many need to be studied for industrial application to mitigate food deterioration.

Cinnamon extracts or oil have shown inhibitory effects for a wide range of pathogenic microorganisms (Liu et al., 2017). For example, the antibacterial cinnamaldehyde inhibits the synthesis and function of cell walls, nucleic acids and proteins (Güneş Bayir & Bilgin, 2019). Among others, cinnamon is discussed as substitute for modern medications (Muhammad & Dewettinck, 2017). Ethanolic cinnamon bark extracts mixed with honey have shown antibacterial effects for acne–causing bacteria (Julianti et al., 2017). Further, cinnamon contains a lot of antioxidants such as polyphenols and is considered as a powerful anti–inflammatory and anti–cancer agent (Mousavi et al., 2020). For example, eugenol has antioxidative properties, *i.e.* is scavenging free radicals, inhibiting lipid peroxidation and influencing the enzyme activity of the glutathione system (Bastos et al., 2017). The world diabetes population is increasing and expect to rise 366 million (2011) to 552 million by 2030 (Whiting et al., 2011). Natural α–glucosidase inhibitors found in cinnamon attract interest in diabetes treatments (Kongstad et al., 2015). Cinnamon inhibited gastrointestinal enzymes, modulated

* Corresponding author.
E-mail address: gertrud.morlock@uni-giessen.de (G.E. Morlock).

https://doi.org/10.1016/j.foodchem.2021.129135
Received 22 August 2020; Received in revised form 2 January 2021; Accepted 13 January 2021
Available online 10 February 2021

insulin response and sensitivity, improved glucose uptake, inhibited glucogenesis and increased glycogen synthesis *in vitro* (Hayward et al., 2019). The effect of cinnamon on blood glucose can be characteristic of its active constituent cinnamaldehyde (Allen et al., 2013). Acetylcholinesterase (AChE) and butyrylcholinesterase (BChE) inhibitors in cinnamon are considered as effective agents against Alzheimer's disease (Gulcin et al., 2019; Boğa et al., 2011), a neurogenerative disorder threatening the health care system (Otaegui-Arrazola et al., 2014). For example, cinnamon is used as nerve stimulant and refresher for nerve stress in traditional medicine (Malik et al., 2015). In the enzyme–mediated browning reaction of food, phenolic compounds are oxidized via respective *o*–quinones to brown products (Echegoyen, Y., & Nerín, C., 2015) and coumarin is a potential inhibitor for enzyme mediated browning (Thada et al., 2013). Analogously, tyrosinase inhibitors in cinnamon extracts, such as cinnamaldehyde derivatives, are considered as candidates for skin whitening cosmetics (Lee et al., 2016; Cui et al., 2015). In addition to the mentioned antimicrobial, antioxidant, antidiabetic, anticholinesterase and antityrosinase effects of cinnamon, further beneficial potential has been reported, *e.g.*, anticancer, anti–inflammatory, lipid–lowering, metabolic syndrome reversing, lean body mass increasing, gastric emptying, insulin sensitivity improving and polycystic ovary syndrome mitigating potential (Hariri & Ghiasvand, 2016).

Current research on the activity of cinnamon is based on sum parameter assays (whole extract response), followed by tedious compound isolation and its activity proof. In contrast, the present study aimed at the development of a fast effect–directed screening for direct visualization of individual bioactive compounds in cinnamon. Therefore, multi–imaging by high–performance thin–layer chromatography (HPTLC) via eight planar effect–directed assays (EDA) and six derivatization reagents was explored. The discovered multi–potent compound zones were further characterized by heated electrospray ionization high–resolution mass spectrometry (HESI–HRMS). Authentic cinnamon samples were self–harvested. Further samples were bought on the market in Sri Lanka or in discounters in Germany, summing up to 40 samples all in all.

2. Materials and methods

2.1. Chemicals and materials

Aliivibrio fischeri bacteria (NRRI–B11177, strain 7151) were purchased from Leibniz Institute, DSMZ, German Collection of Microorganisms and Cells Cultures, Berlin, Germany. Acetic acid (100%), 2–aminoethyl diphenyl borate (≥98%), hydrochloric acid (HCl, 37%), kojic acid (98%), 3–(4,5–dimethylthiazol–2–yl)–2,5–diphenyltetrazolium bromide (MTT, 98%), polyethylene glycol (PEG) 8000, tris (hydroxymethyl) aminomethane (Tris, 99.8%), sulphuric acid (≥96%), vanillin (≥99%), stearic acid (≥98%), oleic acid (≥99%), caproic acid (≥98%), benzoic acid (≥99.5%) and potassium hydroxide (≥85%) were purchased from Carl Roth, Karlsruhe, Germany. Acetone (100%), ethyl acetate (≥99.8%), *n*–hexane (≥95%) and *o*–phosphoric acid (≥85%) were bought from Th. Geyer, Renningen, Germany. Acarbose, AChE lyophilisate (6.66 U/mL, from *Electrophorus electricus*), *p*–aminobenzoic acid (≥99%), *p*–anisaldehyde (98%), aniline (99.5%), 3–cyclohexyl amino–propane sulfonic acid (CAPS, ≥98%), 2,2–diphenyl–1–picrylhydrazyl (DPPH$^{\bullet}$, 95%), α–glucosidase (10 U/mL, from *Saccharomyces cerevisiae*), imidazole (≥99.5%), primuline, rivastigmine (≥98%), sodium chloride, sodium acetate (≥99%), tyrosinase (400 U/mL; from mushroom with ≥1000 U/mg), butyrylcholinesterase (3.34 U/mL, from equine serum), palmitic acid (≥99%) linoleic acid (≥99%), myristic acid (≥99%), D(+)–glucose (99.5%), D(+)–galactose (99%), D(+)–lactose monohydrate, D(+)–sucrose (99.5%) cinnamaldehyde (≥99%) and coumarin (≥99%) were purchased from Sigma–Aldrich–Fluka, Steinheim, Germany. Fructose was from Fagron, Glinde, Germany. 2–Naphthyl–β–D–glucopyranoside (95%) and β–glucosidase (3.3 mg/10 mL; from almond with 3040 U/mg) were purchased from abcr, Karlsruhe, Germany. α–Naphthyl acetate (≥99%) was bought from AppliChem, Darmstadt, Germany. Ethanol (≥99.8%) and acetonitrile (≥99.9%) were purchased from Fisher Scientific, Loughborough, UK. 2–Naphthyl–α–D–glucopyranoside was bought from Flurochem, Hadfield, UK. Toluene (≥99.7%) was purchased from LGC standard, Wesel, Germany. Fast Blue B salt (~95%) was purchased from MP Biomedical, Illkrich, France. Levodopa was obtained from Santa Cruz Biotechnology, Santa Cruz, TX, USA. Methanol (100%) was purchased from VWR International, Darmstadt, Germany. Formic acid (98%) was bought from Avantor Performance Materials, Deventer, Netherlands. Bidistilled water was prepared by a Destamat Bi 18E (Heraeus, Hanau, Germany). A polypropylene box (26.5 cm × 16 cm × 10 cm) was obtained by KIS, ABM, Wolframs–Eschenbach, Germany. *Bacillus subtilis* spores (BGA, DSM 618 strain), ascorbic acid (99%), cinnamic acid (≥98%), HPTLC plates silica gel 60 with/without F_{254} or MS grade (all 20 × 10 cm) or RP–8 $F_{254\,s}$ (10 × 10 cm) were provided by Merck, Darmstadt, Germany. For bioassay and HRMS experiments, a set of HPTLC plates were prewashed by development with methanol – bidistilled water 3:1, *V/V*, up to 95 mm (Simultan Separating Chamber, biostep, Burkhardtsdorf, Germany), followed by drying (Drying Rack, biostep, in clean oven) at 110 °C for 20 min. After cooling down, the plates were stacked, covered by a clean glass plate, packed in aluminum foil and stored protected in a desiccator.

2.2. Stock and standard solutions

Methanolic stock solutions of cinnamic acid, caproic acid, myristic acid, palmitic acid, stearic acid, oleic acid, linoleic acid (all 1 mg/mL each) and coumarin (5 mg/mL), and aqueous stock solutions of saccharides (1 mg/mL each), as well as respectively diluted standard solutions (0.5 mg/mL each, 0.25 mg/mL for cinnamic acid and 0.05 mg/mL for coumarin, latter in amber sampler vial) were prepared, all stored at 4–8 °C in the dark.

2.3. Sample origin and preparation

In Sri Lanka, 4 cinnamon stick samples were self–harvested (Fig. S1), whereas 24 sticks were bought on the market in Sri Lanka (Table S1, voucher specimens deposited at the Food Science Department, Justus Liebig University Giessen, Germany). In German discounters, 10 powders and 2 sticks were purchased. Cinnamon barks were milled (8000 rpm, 5 min, Tube Mill, IKA, Staufen, Germany) and sieved (500–μm test sieve, VWR) to obtain a homogenous powder stored in air–tied containers at room temperature. Each cinnamon powder (200 mg) was extracted with 2 mL methanol – water, 4:1, *V/V* (*t*–butyl methyl ether, or ethyl acetate – *n*–hexane, 4:1, *V/V*) in a conical Eppendorf tube (15 mL, polypropylene), vortexed (1 min), ultrasonicated (25 °C, 30 min, 480 W, 35 kHz, Sonorex Digi plus DL 255H, Bandelin, Germany) and centrifuged (3000 × g, 10 min, Heraeus Labofuge 400, Thermo Scientific, Dreieich, Germany). Each supernatant (100 mg/mL) was transferred to an amber sampler vial stored at 4–8 °C in the dark.

2.4. HPTLC method development

Each cinnamon extract (100 mg/mL, 2–5 μL, 200–500 μg/band depending on detectability) was applied as a 7 mm band (dosage speed 150 nL/s, Automatic TLC Sampler 4, ATS 4, CAMAG, Muttenz, Switzerland). The distance from the lower plate edge was 8 mm and from the left side 14 mm. Automatic distance between bands was chosen to obtain up to 20 tracks on the 20 × 10 cm plate. After drying (2 min, hairdryer), development was performed on the HPTLC plate silica gel 60 with toluene – ethyl acetate – methanol 6:5:3, *V/V/V* (or further mobile phases as described) up to 70 mm in the Twin Trough Chamber (biostep or CAMAG). For method development, respective extracts were applied 5–fold on the same plate, which was cut into 5 identical sections (TLC Plate Cutter, CAMAG) for the different developments.

2.5. Physico–chemical profiling by UV/Vis/FLD and six different derivatizations

Six identical chromatograms were prepared for the cinnamon extracts (5 µL, 500 µg/band each) and subjected to 9 different detection modes, *i.e.* white light illumination (only brown start zones evident), (A) UV 366 nm, (B) UV 254 nm and six different derivatization reagents applied by immersion (immersion speed 3 cm/s for 2 s, TLC Immersion Device III, CAMAG): (C) primuline reagent (100 mg primuline, 20 mL water and 80 mL acetone), (D) *p*–anisaldehyde sulphuric acid reagent (1 mL methoxy benzaldehyde, 140 mL methanol, 16 mL acetic acid and 8 mL sulphuric acid), (E) vanillin sulphuric acid reagent (1 g vanillin, 80 mL ethanol and 0.8 mL sulphuric acid), (F) diphenylamine aniline *o*–phosphoric reagent (2% each of diphenylamine and aniline in 100 mL isopropanol plus 20 mL *o*–phosphoric acid), (G) Fast Blue B salt reagent (100 mg Fast Blue B salt in 100 mL ethanol, 70%) and (H) natural product reagent (1 g 2–aminoethyl diphenyl borate in 100 mL ethanol). After air–drying or heating for 3–5 min (D 110 °C, E 120 °C, F 140 °C; TLC Plate Heater, CAMAG), documentation followed at white light illumination (D–G) or FLD 366 nm (C and H, TLC Visualizer, CAMAG).

2.6. Effect–directed profiling by eight different assays

Eight identical chromatograms were prepared for the cinnamon extracts (5 µL, 500 µg/band each), except for the *B. subtilis* bioassay (2 µL, 200 µg/band each). After drying for 2 min (if not stated otherwise, in a cold stream of air using a hairdryer) and then 20 min (Automatic Developing Chamber 2, ADC 2, CAMAG), the respective positive control was applied as reported (Morlock & Heil, 2020). Each chromatogram was documented at 254 nm (UV), 366 nm (FLD), and white light illumination (Vis; TLC Visualizer, CAMAG). The respective assay solution/suspension was applied, if not stated otherwise, either by immersion (TLC Immersion Device, immersion speed 3.5 cm/s) or piezoelectric spraying (Derivatizer, blue nozzle, level 6, both CAMAG). The plate was horizontally incubated in a moistened polypropylene box as reported (Morlock & Heil, 2020). Documentation was performed at white light illumination in the reflectance mode (TLC Visualizer or DigiStore 2, CAMAG), if not stated otherwise.

2.6.1. HPTLC–Aliivibrio fischeri bioassay

According to Azadniya and Morlock (2019), 4 mL *A. fischeri* culture suspension (prepared according to DIN EN ISO 11348–1) were piezoelectrically sprayed onto the chromatogram. The instant bioluminescence of the sprayed–on bacteria was recorded over 30 min (10 images, 60 s exposure time, 3 min interval, Bioluminizer, CAMAG).

2.6.2. HPTLC–Bacillus subtilis bioassay

According to Jamshidi-Aidji and Morlock (2016), the chromatogram was dipped into the *B. subtilis* culture suspension for 6 s and incubated at 37 °C for 2 h. Then it was dipped into a 0.2% PBS–buffered MTT solution for 1 s and heated at 50 °C for 5 min.

2.6.3. HPTLC–tyrosinase inhibition assay and densitometric evaluation

According to Jamshidi-Aidji and Morlock (2018), the chromatogram was piezoelectrically sprayed with 2 mL substrate solution (45 mg levodopa, 25 mg CAPS and 75 mg PEG 8000 dissolved in 10 mL phosphate buffer of 0.02 M, pH 6.8). After drying for 2 min, it was sprayed with 2 mL tyrosinase (400 U/mL phosphate buffer), incubated at room temperature for 15 min and dried for 5 min. For biochemical quantification of cinnamic acid via its tyrosinase inhibition, selected cinnamon extracts (3 µL, 300 µg/band each) were applied 4–fold along with cinnamic acid (S1–S6; 0.25 mg/mL, 1–8 µL), separated, subjected to the tyrosinase assay, measured by inverse densitometry at 579 nm and evaluated per peak area. Limits of enzymatic detection and quantification were calculated according to DIN 32645 based on the calibration curve method.

2.6.4. HPTLC–α–glucosidase and β–glucosidase inhibition assays

According to Jamshidi-Aidji et al. (2019), the chromatogram was piezoelectrically sprayed (yellow nozzle) with 2 mL substrate solution (12 mg 2–naphthyl–α–D–glucopyranoside or 2–naphthyl–β–D–glucopyranoside in a mixture of 9 mL ethanol and 1 mL 10 mM sodium chloride) and dried for 2 min. For pre–wetting, 1 mL sodium acetate buffer (10.25 g sodium acetate in 250 mL water, with acetic acid 0.1 M to pH 7.5) was sprayed. Then, 2 mL enzyme (10 U/mL α–glucosidase or 1000 U/mL β–glucosidase, both in sodium acetate buffer, pH 7.5) were sprayed and incubated at 37 °C for 15 min (α–glucosidase) or 30 min (β–glucosidase), followed by spraying 0.75 mL aqueous Fast Blue B salt solution (4 mg/mL).

2.6.5. HPTLC–AChE and BChE inhibition assays

According to Azadniya and Morlock (2019), the chromatogram was pre–wetted by spraying 1 mL Tris HCl buffer (pH 7.8, green nozzle). Then, 3 mL enzyme solution (6.6 U/mL AChE or 3.3 U/mL BChE, both in Tris HCl buffer) were piezoelectrically sprayed and incubated at 37 °C for 25 min, followed by spraying 0.75 mL of a 1:2 mixture of ethanolic α–naphthyl acetate solution and aqueous Fast Blue B salt solution (each 3 mg/mL, red nozzle).

2.6.6. HPTLC–DPPH• assay

According to Krüger et al. (2017), the chromatogram was immersed in 0.02% methanolic DPPH• solution for 2 s, followed by drying in the ambient air for 90 s and at 60 °C for 30 s (TLC Plate Heater, CAMAG).

2.7. HPTLC–HESI–HRMS

Cinnamon extracts (3 µL, 300 µg/band each; IDs 8, 9 and 12 via *A. fischeri* bioassay and IDs 7, 10 and 38 via tyrosinase inhibition assay) were applied in duplicate on two MS grade HPTLC plates together with caproic acid (5 µL, 2.5 µg/band), cinnamic acid, palmitic acid, stearic acid (4 µL, 2.0 µg/band each), myristic acid and oleic acid (3 µL, 1.5 µg/band each). After development, each HPTLC plate was cut in two identical halves, one was subjected to the respective assay and the other was used for the HRMS recording. For latter, the positions were marked on the chromatogram (using a soft pencil) in reference to the active zones on the other plate half. The marked zones were eluted with methanol for 1 min at a flow rate of 0.1 mL/min using an elution head–based interface (Plate Express, Advion, Ithaca, NY, USA) coupled to a Q Exactive Plus mass spectrometer (Thermo Fisher Scientific). Full scan mass spectra (m/z 50 – 750) were recorded in the positive and negative ionization mode (spray voltage ± 3.5 kV, capillary temperature 270 °C, sheath gas 20 arbitrary units, aux gas 10 arbitrary units, S–Lens RF level 50). The obtained spectra were processed with Xcalibur 3.0.63 software (Thermo Fisher Scientific). From each analyte spectrum, a plate background spectrum was subtracted.

3. Results and discussion

3.1. Development of the bioanalytical screening

HPTLC attracts interest as a complementary and even orthogonal analytical tool to most mainstream methods with regard to separation and detection principles (Bairy, 2015). HPTLC is an excellent option for screening, which promotes minimal sample preparations, parallel separations, small sample volumes, multi–imaging and cost–efficiency. HPTLC hyphenated with assays facilitates a non–target screening for bioactive compounds. Combined with chemical derivatizations and HRMS, it helps to characterize the found bioactive compounds. A screening method was developed that combined chromatography, multi–imaging and bioassays to detect individual bioactive compounds present in cinnamon extracts. Altogether, 40 self–harvested or bought cinnamon samples (sticks and powders, Table S1, Fig. S1) were investigated. In literature, cinnamon was extracted with different solvents, *i.e.* methanol (Krüger et al., 2018), ethanol (Abeysekera et al., 2017),

water (Koppikar et al., 2010) and their combinations. For the intended bioactivity profiling, two extraction mixtures (methanol – water and ethyl acetate – n–hexane, both 4:1, *V/V*) were compared. The methanol – water mixture extracted comparatively more compounds (Fig. S2) and was selected for the bioprofiling. Analytes are not pre–defined in case of a non–target bioactivity profiling by HPTLC–UV/Vis/FLD–EDA. Thus, five different mobile phases were studied whether the extracted compounds are sufficiently distributed along the developing distance (Figs. S3 and S4). Acidic or alkaline solvent systems (Krüger et al., 2018) were avoided due to the following bioactivity screening by means of pH–sensitive microorganisms or enzymes. Out of the 5 mobile phases investigated, a mixture of toluene – ethyl acetate – methanol 6:5:3 (*V/V/V*) lead to a comparatively good distribution of compounds, as evident in the anisaldehyde sulfuric acid reagent chromatogram and *A. fischeri* bioautogram. The development up to 70 mm took 17 min and provided a fast profiling of 20 samples, separated in parallel on the same plate.

3.2. Physico–chemical profiling by UV/Vis/FLD and six different derivatizations

The physico–chemical profiling at UV/Vis/FLD, and in addition, with six different derivatization reagents was applied to widen the view on the multi–component cinnamon samples and potential differences to each other. This information was also helpful for the later characterization of the discovered bioactive compounds. Six identical chromatograms were prepared, each containing 20 cinnamon extracts (500 µg/band each). Thus for the altogether 40 samples, 12 plates were prepared. Variances of hR_F values were explained by different analysis days and thus humidity of the surrounding air. All chromatograms were documented at UV 254 nm for UV–active compounds (on plates with F_{254}), at FLD 366 nm for natively fluorescent compounds and at white light illumination for visible compounds (Vis). The UV/FLD/Vis chromatograms exhibited comparatively more UV–active and natively fluorescent compounds than visibly brown compounds, which all remained at the start zones (Fig. S5). In the UV 254 nm chromatogram (Fig. 1A), three prominent UV–active compounds were observed at hR_F 50, 74 and 90 in most samples. As for the rather middle polar separation, other UV–active compounds remained at the start zone. Four different UV–profile types of cinnamon samples were evident by the vertical profiling: (I) dominant UV–active zones at hR_F 74 and 90 in the self–harvested sample IDs 1–4, which were similar to most samples obtained at the market in Colombo (IDs 5–7), Galle (IDs 21–26 and 34) and Matara (ID 38). (II) Dominant UV–active zones at hR_F 50 and 90 in all discounter samples (IDs 9–19), which were similar to several cinnamons obtained at the market in Galle (IDs 27–32). However, the sample ID 20 (Galle market) was different to the other samples of the profile II, as it contained almost no UV–active compounds in the start zone, which could indicate a falsified/adulterated sample (also the FLD profile was different to other samples). (III) Dominant UV–active zone at hR_F 90 and only faint zones at hR_F 50 and 74 in samples obtained at the market in Galle (IDs 33–35) and Matara (IDs 37, 39 and 40), whereby ID 39 was less intense in the total UV profile (same for Vis and FLD profiles), which could indicate another falsified/adulterated sample. (IV) More pronounced in the two sample IDs 8 and 27 (Iranian and Galle market, respectively), another dominant UV–active compound was observed at hR_F 82 (marked*). In the FLD chromatogram (Fig. 1B), chlorophylls were observed as red fluorescent bands at 366 nm, especially for IDs 14–17 and 30–32. This finding is in contradiction to inner bark extracts, and was explained through contamination with outer bark chlorophylls by the harvesting process. In many samples, two natively blue fluorescent zones were evident at hR_F 78 (light blue) and 90 (mid–blue). At a first glance, the latter compound seemed to be also UV–active, however, the zone intensity did not correlate across all samples in the horizontal profiling, and thus was considered as a coeluting different compound. Altogether, a first impression was already obtained by this UV/Vis/FLD multi–imaging on the same plate.

The evaluation by derivatization reagents followed. For the primuline reagent detection at FLD 366 nm, sharply–bounded faint lipophilic zones were evident in the methanol – water 4:1 extracts (Fig. 1C, compounds still extractable with the polar solvent mixture). In Galle and Matara market samples (IDs 21–40, in particular ID 29) and some discounter samples (IDs 11–13), a lipophilic compound zone was detected at hR_F 74 (marked$^{\#}$). This lipophilic compound zone seemed also to be detected as a grey zone by the *p*–anisaldehyde sulphuric acid reagent (Fig. 1D) because the horizontal profiling confirmed the similar zone intensity pattern across all samples. The vanillin sulphuric acid reagent (Fig. 1E) detected it as lilac zone but less intense; as a comparatively weaker detecting reagent, fewer other compound zones were visible. By the diphenylamine aniline *o*–phosphoric acid reagent detection (Fig. 1F), saccharides in the cinnamon samples were detected at and above the start zone (slightly stronger eluted on the second plate for IDs 21–40 due to different plate activity). A further development with a mobile phase of increased solvent strength according to Morlock and Heil (2020) revealed fructose (red zone) and glucose (blue zone) as the main saccharides (Fig. S6). Especially in sample ID 27 also sucrose (brown zone) was evident. Further glycon moieties were not detected. However, two intense yellow zones were evident in all samples (Fig. 1F). By horizontal profiling, these two yellow zones fit to the two previously discussed natively blue fluorescent zones at hR_F 78 and 90 (Fig. 1B). The Fast Blue B salt reagent (Fig. 1G) is known to detect phenols, pyrones and tannins among others. Brownish tailing zones were observed in the lower hR_F range for the given neutral mobile phase. This gave a hint on polyphenolic compounds, which require an acidic mobile phase to avoid the pronounced tailing. By the natural product reagent detection at UV 366 nm (Fig. 1H), flavonoid–like compounds were revealed. A yellow fluorescent zone at hR_F 74 was most prominently detected across all cinnamon extracts, similar in the horizontal profile to the UV–active zone at hR_F 74 (Fig. 1A). Another yellow zone at the start zone was dominant for the sample IDs 14–17 and 30–32, which all contained also a comparatively higher amount of red–fluorescent chlorophylls (Fig. 1B).

In summary, a wealth of information was gathered by this comparative profiling of cinnamon extracts. It allowed the differentiation of the individual cinnamon samples by vertical profiling, useful as proof for authentication/falsification/adulteration. The four self–harvested Sri Lankan cinnamon barks, home–made from different trees in the suburb Hiyare in Galle, showed the most comparable pattern in all 8 detection modes, whereas discounter samples and samples even from the same Sri Lankan market place varied to a higher extent. In the horizontal profiling, several compounds–in–common were highlighted via the eight different detection modes. The higher chlorophyll content of some samples raised questions as well as the overall weaker band patterns of sample IDs 20 and 39. Cinnamon powder can lose its freshness by volatilization of the contained active substances into the air (Hariri & Ghiasvand, 2016). Although this can be a possible explanation for the reduced signal responses of the two cinnamon samples; both were found to be suspect.

3.3. Effect–directed profiling by eight different assays

The more you see/detect, the more you know. The physico–chemical profiling was followed by an effect–directed profiling. The orthogonal detection principles detected compounds in the multi–component cinnamon extract mixture according to different detection mechanisms. All 40 cinnamon extracts (500 µg/band each, if not stated otherwise) were screened for bioactive compounds by HPTLC–EDA. Two orthogonal antibacterial bioassays (Gram–negative *A. fischeri* and Gram–positive *B. subtilis*), five enzymatic assays (tyrosinase, AChE, BChE, α–glucosidase and β–glucosidase) and one radical–scavenging assay (DPPH$^{\bullet}$) were exploited. The proper performance of each planar assay was proven by a respective positive control (Morlock & Heil, 2020; well–known bioactive compound used in *in vitro* assays). The marine bacterium *A. fischeri* emits a greenish–blue light above a certain cell density (>10^9/mL) for quorum sensing. Antibacterial compounds that influence the energetic

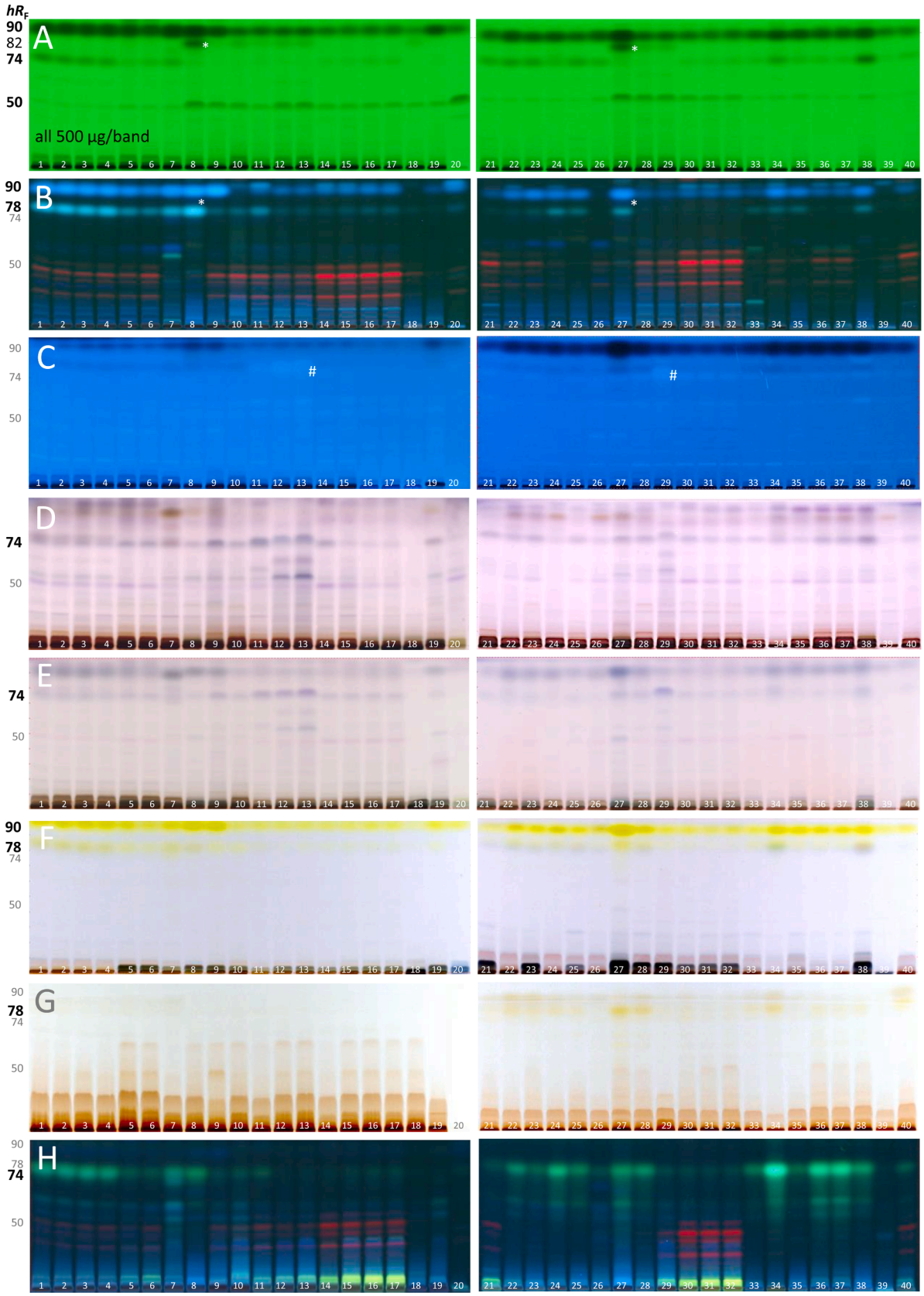

Fig. 1. Physico–chemical profiling: HPTLC chromatograms of cinnamon extract IDs 1–40 (5 µL, 500 µg/band) on HPTLC plates silica gel 60 F_{254} with toluene – ethyl acetate – methanol 6:5:3, detected at (A) 254 nm (UV), (B) 366 nm (FLD), and at 366 nm (C and H) and white light illumination (D–G) after the (C) primuline, (D) *p*–anisaldehyde sulphuric acid, (E) vanillin sulphuric acid, (F) diphenylamine aniline *o*–phosphoric acid, (G) Fast Blue B salt and (H) natural product reagents; hR_F values 90, 82, 78, 74 and 50 indicate prominent zones. (For interpretation of the references to colour in this figure legend, the reader is referred to the web version of this article.)

metabolism were directly detected as dark or bright zones (bioluminescence as greyscale image, Fig. 2A). In the two bioautograms of the 40 cinnamon extracts, several dark zones which reduced the bacterial bioluminescence were observed along the developing distance, especially for IDs 7–9 and 27–33, but also near the front. Exemplarily for IDs 7 and 8, the separations with mobile phases of a reduced solvent strength clearly revealed three zones (Fig. S4B), which were otherwise more or less close together near the solvent front. In contrast, only a faint bioactive zone remained at the application zone, whereas it was opposite for the Gram–positive *B. subtilis* bioassay. Most intense antibacterial effects were displayed as bright zones on a violet plate background at the start zone. The oxidoreductase or other metabolic processes in the viable ubiquitous soil bacteria reduced the MTT substrate to purple formazan. The assay is considered not only to be a measure of antibacterial activity but also cytotoxicity or cytostatic activity. In contrast to all other assays, only 2 μL (instead of 5 μL) of each cinnamon extract were applied (200 μg/band each). Apart from the intense start zone containing polar antibacterials, a more apolar Gram–positive antibacterial zone was discovered at hR_F 82, especially for IDs 9, 11–13 and 27–32 (Fig. 2B). The most antibacterial effect was evident at the start zones of all samples, except for sample IDs 20 and 39. Both samples were previously discussed to be suspect due to the overall weaker band patterns and higher chlorophyll content. Also in this antibacterial bioassay, both samples showed a clear difference to the other samples. In order to separate the antibacterials which remained at the start zone, the separation was repeated with a mobile phase of a higher elution power (Fig. S7, acetonitrile – water 9:1, *V/V*). Both antibacterial bioassays proved that cinnamon extracts contain abundant antibacterial compounds acting against Gram–negative and Gram–positive bacteria. In accordance to our results, cinnamon extracts have exhibited antibacterial activity against *Bacillus cereus* and antifungal activity against *Penicillium* species and synergistic effects as food preservatives (Liu et al., 2017).

In the five biochemical assays, respective enzyme inhibiting compounds present in the cinnamon extracts were detected as bright zones on a violet (grey for tyrosinase) plate background. In the tyrosinase inhibition autogram (Fig. 2C), two intense tyrosinase inhibiting compound zones were detected at hR_F 74 and 90 in almost all cinnamon extracts. The horizontal pattern at hR_F 74 was in accordance to the dark zone in the chromatogram detected by the primuline reagent (Fig. 1C). Some extracts showed more pronounced a further inhibition zone at hR_F 50, and another one at hR_F 65 in sample IDs 12, 13, 28 and 29 as well as at hR_F 82 in several samples. Tyrosinase inhibiting compounds were also observed at the start zone. Tyrosinase inhibiting effects of cinnamon have been reported, *i.e.* ethanolic extracts of *Cinnamomum osmophloeum* Kanehira decreased melanin formation in the B16–F10 melanoma cells and inhibited tyrosinase promoter activities (Lee et al., 2016). Coumarin and coumarin derivatives have also been reported as tyrosinase inhibitors (Zolghadri et al., 2019). In the α–glucosidase and β–glucosidase inhibition assays (Fig. 2D/E), the same prominent horizontal patterns of inhibition zones at hR_F 74 as well as hR_F 90 were displayed across all samples. In literature, methanol extracts of cinnamon bark showed α–glucosidase inhibitory activity (IC_{50} < 20 μg/mL), and therein, 2–hydroxy cinnamaldehyde, coumarin, cinnamyl alcohol, cinnamic acid and cinnamaldehyde were assigned as specific α–glucosidase inhibitors (Kongstad et al., 2015). In several samples in the AChE autogram (Fig. 2F), AChE inhibiting compounds zones were detected at hR_F 74 and hR_F 90 (whereby a sharp inhibition zone at hR_F 74 was observed for sample IDs 12, 13 and 29). Sample IDs 8 and 27 (also coelution in ID 38) showed an additional AChE inhibiting compound at hR_F 82. In almost all cinnamon extracts, a BChE inhibiting compound zone was evident at hR_F 74 (Fig. 2G). It had the same pattern across all samples as the previous tyrosinase inhibiting zone at the same position.

In the DPPH$^•$ assay, antioxidative compounds capable of scavenging DPPH$^•$ appear as bright zones on a violet plate background (Fig. 2H). Although intense zones were evident at hR_F 50, 82 and 90 for several samples, most of the antioxidative compounds remained at the start zone in all cinnamon extracts. Only, the previously discussed suspected sample ID 20 did not show an effect at all. The antioxidative compounds which remained at the start zone were applied at a 5–fold lower amount (100 μg/band instead of 500 μg/band) and separated with a mobile phase of a higher elution power (Fig. S8, ethyl acetate – toluene – formic acid – water 16:4:3:2, *V/V/V/V*).

3.4. Characterization of multi–potent compounds by HPTLC–HESI–HRMS

The multi–potent zones observed in the *A. fischeri* bioautogram and tyrosinase inhibition autogram were exemplarily characterized further by HPTLC–HESI–HRMS in both ionization modes (Fig. 3, Table S2). In the *A. fischeri* bioautogram, the obtained mass signal (base peak) at *m/z* 147.0451 $[M\text{-}H]^-$ for the bioactive zone 8a was tentatively assigned as deprotonated molecule of cinnamic acid in the negative ion mode. Cinnamic acid was reported to be one of the important substances in cinnamon (Dorri et al., 2018). For the bioactive zone 9c, the deprotonated molecules obtained as mass signals at *m/z* 279.2329, 281.2485 and 283.2643 [all M-H]$^-$ were tentatively assigned as linoleic acid, oleic acid and stearic acid, respectively. This finding is confirmed by Evdokimova et al. (2013), reporting that true cinnamon contains six fatty acids (palmitic, stearic, oleic, linoleic and linolenic acids), among which palmitic acid (48%) and stearic acid (23%) are the major ones. However, there is natural variance. Cassia cinnamon contains the same fatty acids, but only 8% stearic acid and instead 87% palmitic acid. For the bioactive zone 8b in the positive ion mode, the obtained mass signals at *m/z* 147.0440 $[M+H]^+$ and *m/z* 169.0260 $[M+Na]^+$ were tentatively assigned as protonated molecule and respective sodium adduct of coumarin. For the bioactive zone 12d, the protonated molecule and respective sodium adduct obtained at *m/z* 133.0649 $[M+H]^+$ and *m/z* 155.0468 $[M+Na]^+$ were tentatively assigned to cinnamaldehyde. These results were in accordance to literature (Chen et al., 2014). Cinnamaldehyde at hR_F 90 as a major chemical compound in cinnamon extracts (ranging from 62 to 90% depending on the extraction method according to Nabavi et al., 2015) acted prominently against *A. fischeri*. Spices such as cinnamon (cinnamaldehyde), clove (eugenol), cumin (cumin aldehyde) have antimicrobial and antioxidant properties due to their respective major chemical compound, which partially explains their use as preservatives in foods (La Jessica Elizabeth et al., 2017).

In the tyrosinase inhibiting autogram, in the negative ion mode, the deprotonated molecule at *m/z* 121.0295 $[M\text{-}H]^-$ was obtained for zone 38e (coeluting with cinnamic acid) and *m/z* 255.2330 $[M\text{-}H]^-$ for zone 10f, tentatively assigned to benzoic acid and palmitic acid, respectively. Further tyrosinase inhibiting compounds were assigned as cinnamaldehyde, coumarin and also α-methyl cinnamic (Table S3). This finding is confirmed by literature, reporting cinnamon to be rich in benzoic acid (335 mg/kg according to Del Olmo et al., 2017). In the positive ion mode, the sodium adduct of linalool oxide at *m/z* 193.1200 $[M+Na]^+$ was tentatively assigned to the bioactive zone 38e. In literature, the therapeutic potential of linalool in cinnamon was reported for glycemic control in diabetes (Lee et al., 2013). As this tyrosinase inhibiting compound zone was also evident in both glucosidase assays (based on the horizontal pattern intensity across all samples), we confirmed the bioactivity of the linalool, although in its oxidized form. In this study, cinnamic acid, benzoic acid and linalool oxide at hR_F 50, linoleic, oleic, stearic and palmitic acids at hR_F 74, coumarin at hR_F 82 and cinnamaldehyde at hR_F 90 were tentatively assigned as multi–potent compounds.

3.5. Confirmation of multi–potent compounds by co–chromatography with references

Tentatively assigned by HPTLC–HESI–HRMS, the bioactive compounds were proven and confirmed by co–chromatography of respective references along with selected cinnamon extracts (Fig. S9). Cinnamic acid and benzoic acid at hR_F 50, coumarin at hR_F 82 and

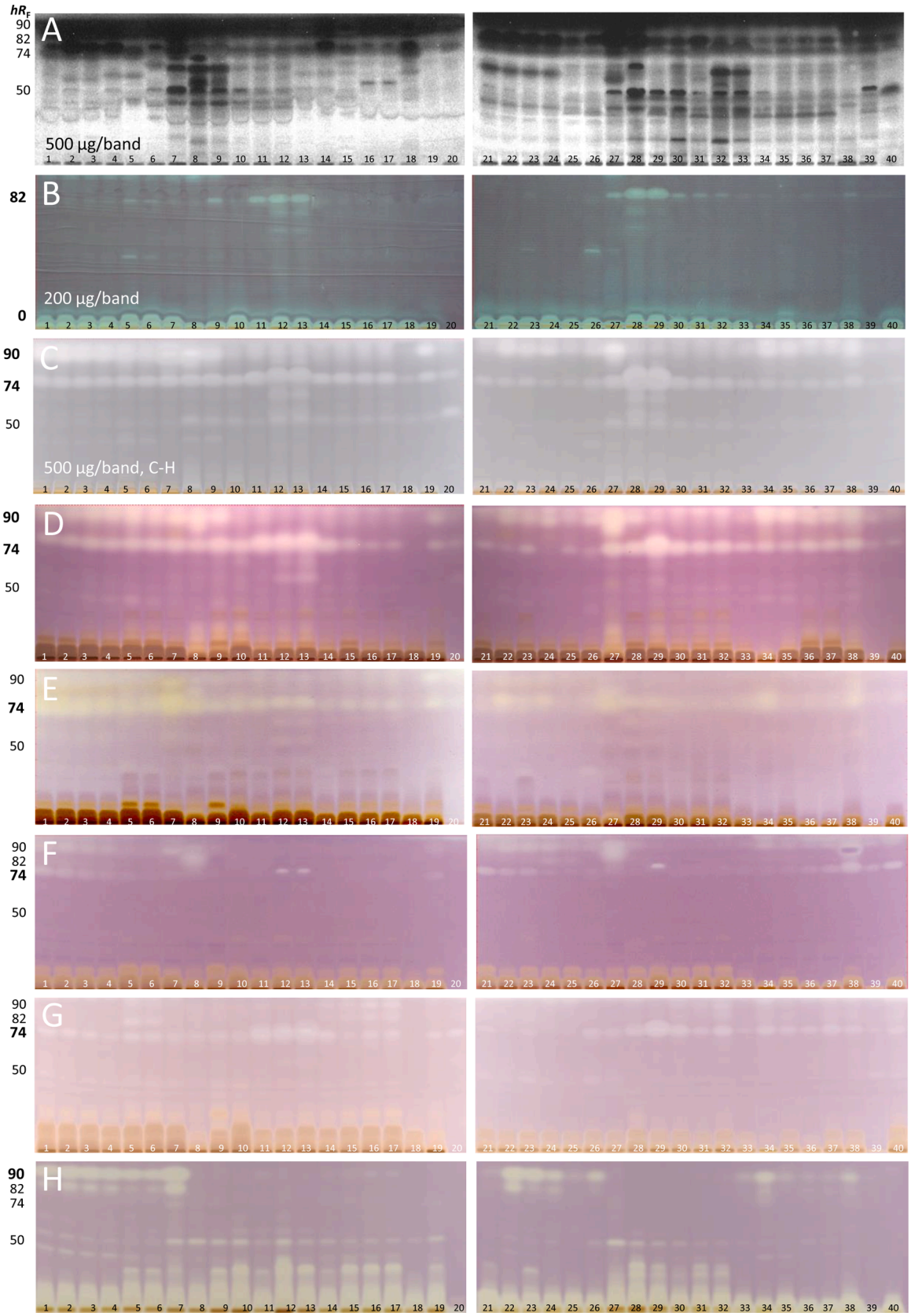

Fig. 2. Effect–directed profiling: HPTLC (bio)autograms of cinnamon extracts (as in Fig. 1, except 200 µg/band for B) after the (A) bioluminescent Gram–negative *A. fischeri* bioassay (grey–scale image), and at white light illumination, (B) Gram–positive *B. subtilis* bioassay, (C) tyrosinase, (D) α–glucosidase, (E) β–glucosidase, (F) AChE and (G) BChE inhibition assays and (H) DPPH$^{\bullet}$ assay; hR_F values 90, 82, 74 and 50 indicate prominent bioactive zones.

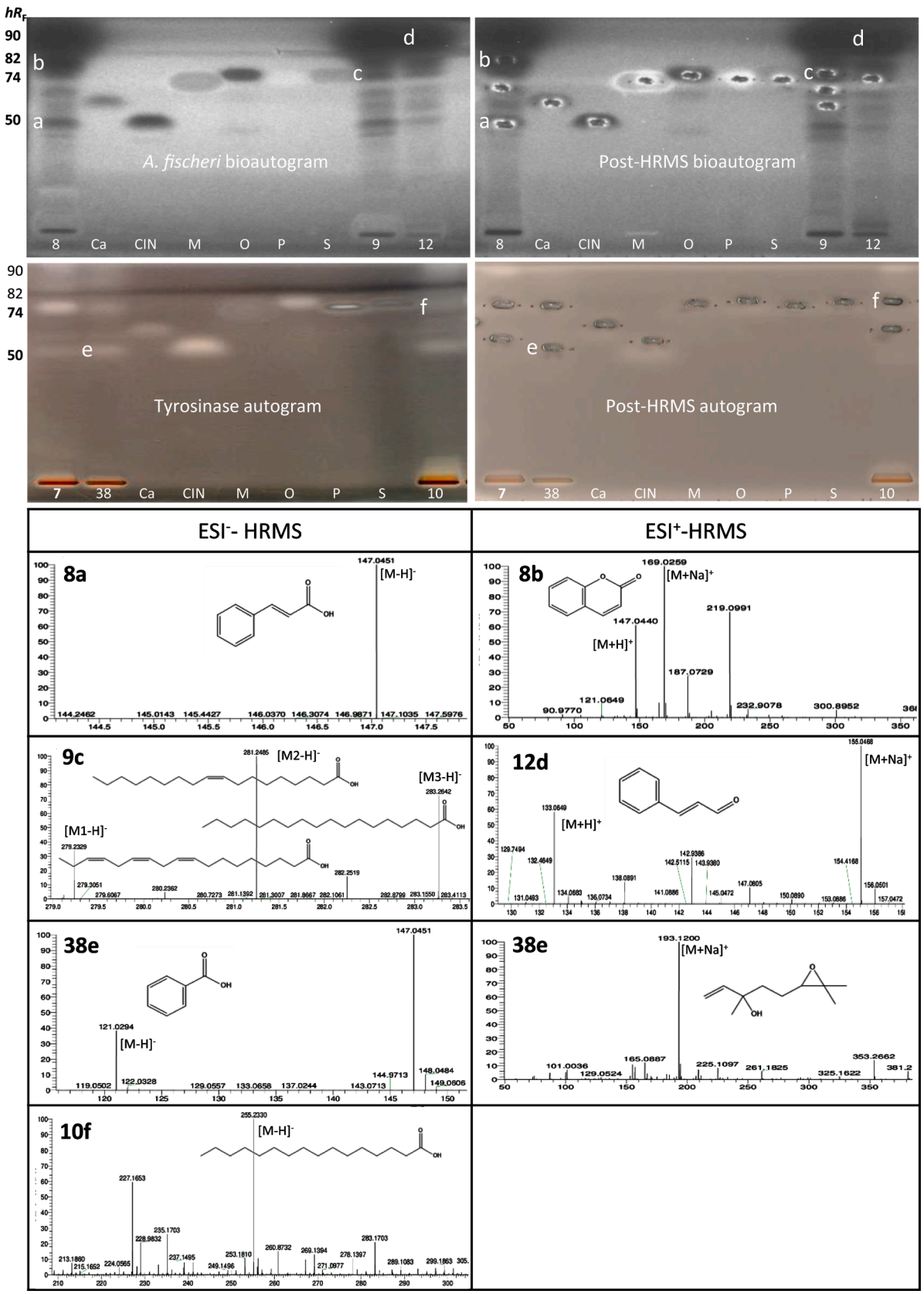

Fig. 3. HPTLC–HESI–HRMS in the positive and negative ionization mode for characterization of the multi–potent bioactive zones in selected cinnamon extracts (IDs 8, 9 and 12 for *A. fischeri*bioassay, and IDs 7, 10 and 38 for tyrosinase inhibition assay) in reference to caproic acid (Ca), cinnamic acid (CIN), myristic acid (M), oleic acid (O), palmitic acid (P) and stearic acid (S); a sample set on one plate part was used for the assay and the other for HRMS (depicted as post–HRMS bioautogram).

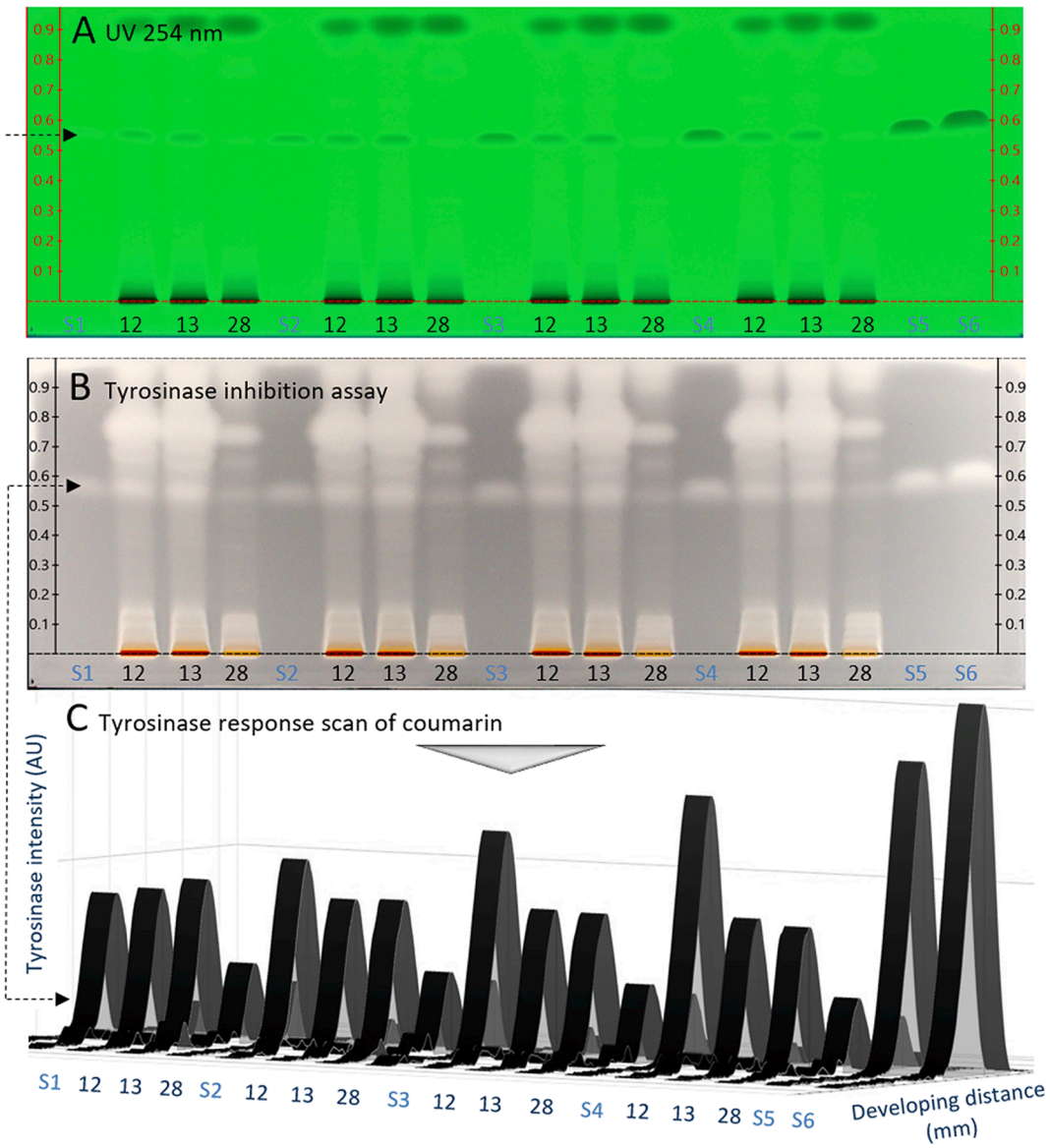

Fig. 4. Enzymatic quantification of the cinnamic acid via its tyrosinase inhibition response in cinnamon extract IDs 12, 13 and 28 (300 µg/band each) via cinnamic acid (S1–S6, 0.25–2.0 µg/band): (A) pre–assay UV 254 nm chromatogram, (B) tyrosinase inhibition autogram and (C) respective inverse scan densitograms at 579 nm.

cinnamaldehyde at hR_F 90 were detected at UV 254 nm, whereas coumarin was detected at FLD 366 nm. As expected, none of the fatty acids at hR_F 74 was detectable at UV/Vis/FLD. For all co–developed references, bioactivity was proven and confirmed via the tyrosinase inhibition and DPPH$^{\bullet}$ assays. For similar amounts applied, cinnamaldehyde, coumarin and stearic acid showed a lower response in comparison to the other bioactive references. Linoleic, oleic, stearic and palmitic acids were confirmed to be present in the cinnamon extracts by HRMS and co–chromatography. The bioactivity of fatty acids was studied in detail, integrating further acids (Figs. S10–S12). In the *A. fischeri* bioassay, myristic and palmitic acids showed bioluminescence enhancing effects for the Gram–negative bacteria, while caproic, cinnamic, oleic and stearic acids showed inhibitory effects. All selected acids were proven to be bioactive in the bioassays performed, although the intensity of caproic acid was comparatively lower for the *B. subtilis* bioassay and tyrosinase inhibition assay.

3.6. Detected multi–potent compounds in context with literature

In all cinnamon extracts antibacterial activity was observed (Fig. 2A). Cinnamaldehyde exhibited as diffuse zone a pronounced antibacterial activity against Gram–negative *A. fischeri* bacteria (hR_F 90 with toluene – ethyl acetate – methanol 6:5:3, Fig. 2A, and hR_F 80 with *n*–hexane – ethyl acetate – ammonia 3.8:1.3:0.05, Fig. S14). Coumarin (hR_F 82), cinnamic acid (hR_F 50) as well as palmitic, stearic and oleic acids (hR_F 74) also acted antibacterial (Fig. S10C). Inhibitory mechanisms of bacteria were described by antiquorum sensing effects, cell membrane damaging, lipid profile changes, ATPase inhibition, cell division, porin membranes, motility and biofilm formation (Vasconcelos et al., 2018). Apart from its use as food preservative, cinnamaldehyde and cinnamon essential oil showed antibacterial effects against *Escherichia coli* when used as an adjunctive treatment for patients with suspected colorectal cancers (Kosari et al., 2020). Moreover, a recent study has proved the therapeutic effect of cinnamaldehyde for canine otitis externa (Sim et al., 2019).

Latest literature reported *in vitro* antibacterial activity of ethanolic extracts of *C. zeylanicum* being more effective against Gram–positive *Staphylococcus aureus* than Gram–negative *Escherichia coli* (Salma et al., 2019). A similar outcome was obtained in our study, as the total antibacterial activity of each sample was stronger against Gram–positive than Gram–negative bacteria (200 versus 500 µg/band). In the Gram–positive *B. subtilis* bioautogram, antibacterial effects were observed for all methanol– water extracts and studied compounds (Figs. 2B and S10D). In

addition, several antibacterials remained at the start zone. The detected antibacterial response of several fatty acids (hR_F 74) is compatible with previous *in vitro* studies reported, although poor solubility, delivery and bioavailability are questionable (Jung & Lee, 2016).

In the tyrosinase inhibition assay, the cinnamon extracts displayed inhibition zones such as cinnamaldehyde (hR_F 90), coumarin (hR_F 82), fatty acids (hR_F 74) and cinnamic acid (hR_F 50, Figs. 2C and S10I). Cinnamaldehyde in cinnamon essential oil was reported as tyrosinase inhibitor (Echegoyen & Nerín, 2015). Cinnamic acid showed anti–diabetic, anti–inflammatory, anti–cancer, anti–obesity (Kang et al., 2019), antioxidant, antimalarial, hepatoprotective and anti–tyrosinase activities (Anlar et al., 2018).

All studied compounds and cinnamon extracts revealed α– and β–glucosidase inhibition (Figs. 2D/E and S10E/F). Cinnamaldehyde (hR_F 90) and fatty acids (hR_F 74) showed higher α– than β–glucosidase inhibition. According to Zhu et al. (2017), the use of cinnamaldehyde in supplements for diabetic animals improved glucose and lipid homeostasis. Out of 10 fatty acids tested (caproic, lauric, myristic, palmitic, stearic, palmitoleic, oleic, linoleic, linolenic and arachidonic acids), oleic acid and linoleic acid showed a stronger α–glucosidase inhibition than acarbose (Su et al., 2013).

Further, AChE and BChE inhibition compounds like cinnamaldehyde (hR_F 90) and fatty acids (hR_F 74) were detected (Figs. 2F/G and S10G/H), whereby a halo–effect (indicating a strong response; the halo–effect is reduced for lower amounts applied) was observed for palmitic acid and stearic acid. Cinnamon oil and its major compounds (cinnamaldehyde, cinnamyl acetate) were reported to have strong cholinesterase inhibition (78%) (Sihoglu Tepe & Ozaslan, 2020). Ethanolic cinnamon extracts were capable of inhibiting 63% of AChE and 85% of BChE at a 200–μg/mL concentration using the Ellmann method and showed high antioxidant activity using the cupric reducing antioxidant capacity assay (Boğa et al., 2011). The presence of the fatty acids (hR_F 74) was also confirmed by detection via the primuline reagent (Fig. S10J). The strong activity of linoleic acid against antibacterials was confirmed, and although much weaker, also against tyrosinase, α–glucosidase and AChE (Fig. S11). A better separation of fatty acids was obtained on reversed phases detected by the primuline reagent (Fig. S12). However, water–wettability is not given for this layer (not compatible to the assay application).

3.7. Analysis of coumarin in cinnamon extracts

The HRMS results pointed to the presence of coumarin. Hence, all cinnamon extracts were screened for coumarin according to Krüger et al. (2018), which exploited a specific detection of coumarin (Fig. S13). In sample IDs 8 (Iranian market product), 9–13 and 17–19 (all from German discounters) a higher coumarin content was evident. Such samples with a higher coumarin content were quantified. In all samples labelled as Ceylon cinnamon, coumarin was very low for the applied sample amount or not detected at all. This was according to literature, in which was reported that *C. zeylanicum* (true cinnamon from Ceylon) had the lowest coumarin content out of the further four major commercial cinnamon types, *i.e.* Chinese *C. cassia*, Indonesian *C. burmanii* and Vietnamese *C. loureirii* (Hayward et al., 2019). The bioactivity of coumarin was studied in detail to further confirm the coumarin in selected cinnamon extracts (Fig. S14, Table S3). Coumarin showed an antibiotic effect against Gram–negative *A. fischeri* bacteria and inhibited also the tyrosinase, however, it was not inhibiting α–glucosidase, β–glucosidase, AChE and BChE, even not or hardly at approximately 10–fold higher amounts applied.

3.8. Quantification of the tyrosinase inhibiting power of cinnamic acid

Exemplarily, the tyrosinase inhibiting power of cinnamic acid (hR_F 50) was quantified via its enzymatic response in some selected samples (Fig. 4). In the autogram, the tyrosinase inhibition of the samples was measured at 579 nm by an inverse scan and referred to the Michaelis–Menten calibration curve of cinnamic acid (ranged 0.25–2.0 μg/band, correlation coefficient of 0.9910, *%RSD* of 5%). The limits of enzymatic detection and quantification were 55 ng/band and 192 ng/band, respectively. Via the enzymatic response, the mean cinnamic acid content ($n = 4$) of cinnamon IDs 12, 13 (German market products) and 28 (Sri Lankan market product) was calculated to be 1.1 mg/g ± 3.2%, 1.2 mg/g ± 3.9% and 0.5 mg/g ± 3.8%, respectively.

4. Conclusions

For foods or spices or botanicals with assumed or claimed benefits for consumers' health, effect-directed profiling was found to be a valuable tool. The information–rich sample profiles are highly suited as indicator for the product quality. The bioprofiling of the popular cinnamon spice by HPTLC–UV/Vis/FLD–EDA–HESI–HRMS revealed diverse bioactivities, such as antibacterial activity against Gram–positive and Gram–negative bacteria, inhibiting activity of tyrosinase, AChE, BChE, α–glucosidase and β–glucosidase as well as radical scavenging (antioxidative) capacity. Additional information was easily obtained by multi–imaging, exploring altogether 17 different detection modes. The targeted characterization of selected multi–potent compounds by HPTLC–HESI–HRMS highlighted the bioactive potential of cinnamaldehyde, cinnamic acid, benzoic acid, coumarin, linoleic acid, oleic acid, stearic acid, palmitic acid and linalool oxide. As an example, cinnamic acid was quantified in selected samples via its tyrosinase inhibition response, which highlighted the potential for *in situ* enzymatic quantifications. If compared to other bioactive ingredients, the coumarin showed only a moderate antibacterial and tyrosinase inhibiting activity (no further response for the given amounts in the other assays). In accordance to literature, the coumarin content was very low in all Ceylon cinnamon samples. As this non–target bioprofiling laid the focus on the mid–polar to apolar range, active polar compounds which yet remained at the start zone still need to be explored in future.

CRediT authorship contribution statement

N.G.A.S. Sumudu Chandana: Conceptualization, Investigation, Writing - original draft. **Gertrud E. Morlock:** Conceptualization, Methodology, Resources, Supervision, Data curation, Writing - original draft.

Declaration of Competing Interest

The authors declare that they have no known competing financial interests or personal relationships that could have appeared to influence the work reported in this paper.

Acknowledgment

Thank is owed to the Food Science group for technical guidance, especially to Annabel Mehl for HRMS spectra recording and Julia Heil for assay assistance, and Merck, Darmstadt, Germany, for the supply of plates. Instrumentation was partially funded by the Deutsche Forschungsgemeinschaft (DFG, German Research Foundation) – INST 162/471–1 FUGG; INST 162/536–1 FUGG.

Appendix A. Supplementary data

Supplementary data to this article can be found online at https://doi.org/10.1016/j.foodchem.2021.129135.

References

Abeysekera, W. P. K. M., Arachchige, S. P. G., & Ratnasooriya, W. D. (2017). Bark Extracts of Ceylon Cinnamon Possess Antilipidemic Activities and Bind Bile Acids *In Vitro*. *Evidence-Based Complementary and Alternative Medicine, 2017*, 7347219.

Allen, R. W., Schwartzman, E., Baker, W. L., Coleman, C. I., & Phung, O. J. (2013). Cinnamon use in type 2 diabetes: an updated systematic review and meta–analysis. *Annals of Family Medicine, 11*(5), 452–459.

Anlar, H. G., Bacanlı, M., Çal, T., Aydın, S., Arı, N., Ündeğer Bucurgat, Ü., Başaran, A. A., & Başaran, A. N. (2018). Effects of cinnamic acid on complications of diabetes. *Turkish Journal of Medical Sciences, 48*(1), 168–177.

Azadniya, E., & Morlock, G. E. (2019). Automated piezoelectric spraying of biological and enzymatic assays for effect–directed analysis of planar chromatograms. *Journal of Chromatography A, 1602*, 458–466.

Bairy, P.S., (2015), A comparison study of HPLC and HPTLC: principles, instrumentations and applications, ASIO Journal of Analytical Chemistry, 1(1), 20–28.

Bastos, M. S., Del Vesco, A. P., Santana, T. P., Santos, T. S., de Oliveira Junior, G. M., Fernandes, R. P. M., … Gasparino, E. (2017). The role of cinnamon as a modulator of the expression of genes related to antioxidant activity and lipid metabolism of laying quails. *PLoS ONE, 12*(12), e0189619.

Boğa, M., Hacıbekiroğlu, I., & Kolak, U. (2011). Antioxidant and anticholinesterase activities of eleven edible plants. *Pharmaceutical Biology, 49*(3), 290–295.

Cetin Cakmak, K., & Gülçin, İ. (2019). Anticholinergic and antioxidant activities of usnic acid–an activity–structure insight. *Toxicology Reports, 6*, 1273–1280.

Chen, P., Sun, J., & Ford, P. (2014). Differentiation of the four major species of Cinnamons (*C. burmannii, C. verum, C. cassia,* and *C. loureiroi*) using a Flow Injection Mass Spectrometric (FIMS) fingerprinting method. *Journal of Agricultural and Food Chemistry, 62*(12), 2516–2521.

Cui, Y., Liang, G., Hu, Y.–H., Shi, Y., Cai, Y.–X., Gao, H.–J., Chen, Q.–X., & Wang, Q. (2015). Alpha–substituted derivatives of cinnamaldehyde as tyrosinase inhibitors: inhibitory mechanism and molecular analysis. Journal of Agricultural and Food Chemistry, 63(2), 716–722.

Del Olmo, A., Calzada, J., & Nuñez, M. (2017). Benzoic acid and its derivatives as naturally occurring compounds in foods and as additives: Uses, exposure, and controversy. *Critical Reviews in Food Science and Nutrition, 57*(14), 3084–3103.

Dorri, M., Hashemitabar, S., & Hosseinzadeh, H. (2018). Cinnamon (*Cinnamomum zeylanicum*) as an antidote or a protective agent against natural or chemical toxicities: a review. *Drug and Chemical Toxicology, 41*(3), 338–351.

Echegoyen, Y., & Nerín, C. (2015). Performance of an active paper based on cinnamon essential oil in mushrooms quality. *Food Chemistry, 170*, 30–36.

Estevinho, L. M. (2018). Editorial–Special Issue "Nutraceuticals in Human Health and Disease", International Journal of Molecular Sciences, 19, 1213.

Evdokimova, O. V., Neneleva, E. V., Tarrab, I., & Glazkova, I. Y. (2013). Comparison of Lipophilic Substances of the Bark of Chinese (*Cinnamomum cassia* (L.) C. Presl.) and Ceylon Cinnamon (*Cinnamomum zeylanicum* Blume). *World Applied Sciences Journal, 27*(1), 70–73.

Gulcin, I., Kaya, R., Goren, A. C., Akincioglu, H., Topal, M., Bingol, Z., … Alwasel, S. (2019). Anticholinergic, antidiabetic and antioxidant activities of cinnamon (*Cinnamomum verum*) bark extracts: polyphenol contents analysis by LC–MS/MS. *International Journal of Food Properties, 22*(1), 1511–1526.

Güneş, Bayır, A., & Bilgin, M. G. (2019). The Effect of Cinnamon on Microbiological, Chemical and Sensory Analyses of Probiotic Yogurt. *Bezmialem Science, 7*(4), 311–316.

Hameed, I. H., Altameme, H., & Mohammed, G. H. (2016). Evaluation of Antifungal and Antibacterial Activity and Analysis of Bioactive Phytochemical Compounds of *Cinnamomum zeylanicum* (Cinnamon Bark) using Gas Chromatography-Mass Spectrometry. *Oriental Journal of Chemistry, 32*(4), 1769–1788.

Hariri, M., & Ghiasvand, R. (2016). Cinnamon and Chronic Diseases. *Advances in Experimental Medicine and Biology, 929*, 1–24.

Hayward, N. J., McDougall, G. J., Farag, S., Allwood, J. W., Austin, C., Campbell, F., Horgan, G., & Ranawana, V. (2019). Cinnamon Shows Antidiabetic Properties that Are Species–Specific: Effects on Enzyme Activity Inhibition and Starch Digestion. *Plant Foods for Human Nutrition, 74*(4), 544–552.

Jamshidi-Aidji, M., Macho, J., Mueller, M. B., & Morlock, G. E. (2019). Effect–directed profiling of aqueous, fermented plant preparations via high–performance thin–layer chromatography combined with *in situ* assays and high–resolution mass spectrometry. *Journal of Liquid Chromatography & Related Technologies, 42*(9–10), 266–273.

Jamshidi-Aidji, M., & Morlock, G. E. (2016). From Bioprofiling and Characterization to Bioquantification of Natural Antibiotics by Direct Bioautography Linked to High-Resolution Mass Spectrometry: Exemplarily Shown for *Salvia miltiorrhiza* Root. *Analytical Chemistry, 88*(22), 10979–10986.

Jamshidi-Aidji, M., & Morlock, G. E. (2018). Fast Equivalency Estimation of Unknown Enzyme Inhibitors *in situ* the Effect-Directed Fingerprint, Shown for *Bacillus* Lipopeptide Extracts. *Analytical Chemistry, 90*(24), 14260–14268.

Julianti, E., Rajah, K. K., & Fidrianny, I. (2017). Antibacterial Activity of Ethanolic Extract of Cinnamon Bark, Honey, and Their Combination Effects against Acne-Causing Bacteria. *Scientia Pharmaceutica, 85*(2), 19.

Jung, S. W., & Lee, S. W. (2016). The antibacterial effect of fatty acids on *Helicobacter pylori* infection. *The Korean Journal of Internal Medicine, 31*, 30–35.

Kang, N. H., Mukherjee, S., & Yun, J. W. (2019). *Trans*-Cinnamic Acid Stimulates White Fat Browning and Activates Brown Adipocytes. *Nutrients, 11*(3), 577.

Kongstad, K. T., Özdemir, C., Barzak, A., Wubshet, S. G., & Staerk, D. (2015). Combined use of high–resolution α–glucosidase inhibition profiling and high–performance liquid chromatography–high–resolution mass spectrometry–solid–phase extraction–nuclear magnetic resonance spectroscopy for investigation of antidiabetic principles in crude plant extracts. *Journal of Agricultural and Food Chemistry, 63*(8), 2257–2263.

Koppikar, S. J., Choudhari, A. S., Suryavanshi, S. A., Kumari, S., Chattopadhyay, S., & Kaul-Ghanekar, R. (2010). Aqueous cinnamon extract (ACE–c) from the bark of *Cinnamomum cassia* causes apoptosis in human cervical cancer cell line (SiHa) through loss of mitochondrial membrane potential. *BMC Cancer, 10*, 210.

Kosari, F., Taheri, M., Moradi, A., Alni, R. H., & Alikhani, M. Y. (2020). Evaluation of cinnamon extract effects on clbB gene expression and biofilm formation in Escherichia coli strains isolated from colon cancer patients. *BMC Cancer, 20*, 267.

Krüger, S., Bergin, A., & Morlock, G. E. (2018). Effect–directed analysis of ginger (*Zingiber officinale*) and its food products, and quantification of bioactive compounds via high–performance thin–layer chromatography and mass spectrometry. *Food Chemistry, 243*, 258–268.

Krüger, S., Hüsken, L., Fornasari, R., Scainelli, I., & Morlock, G. E. (2017). Effect–directed fingerprints of 77 botanical extracts via a generic high–performance thin–layer chromatography method combined with assays and mass spectrometry. *Journal of Chromatography. A, 1529*, 93–106.

Krüger, S., Winheim, L., & Morlock, G. E. (2018). Planar chromatographic screening and quantification of coumarin in food, confirmed by mass spectrometry. *Food Chemistry, 239*, 1182–1191.

La Jessica Elizabeth, D. T., Gassara, F., Kouassi, A. P., Brar, S. K., & Belkacemi, K. (2017). Spice use in food: Properties and benefits. *Critical Reviews in Food Science and Nutrition, 57*(6), 1078–1088.

Lee, S. C., Chen, C. H., Yu, C. W., Chen, H. L., Huang, W. T., Chang, Y. S., … Lee, T. L. (2016). Inhibitory effect of *Cinnamomum osmophloeum* Kanehira ethanol extracts on melanin synthesis via repression of tyrosinase expression. *Journal of Bioscience and Bioengineering, 122*(3), 263–269.

Lee, S. C., Xu, W. X., Lin, L. Y., Yang, J. J., & Liu, C. T. (2013). Chemical composition and hypoglycemic and pancreas–protective effect of leaf essential oil from indigenous cinnamon (*Cinnamomum osmophloeum* Kanehira). *Journal of Agricultural and Food Chemistry, 61*(20), 4905–4913.

Liang, Y., Li, Y., Sun, A., & Liu, X. (2019). Chemical compound identification and antibacterial activity evaluation of cinnamon extracts obtained by subcritical n–butane and ethanol extraction. *Food Science & Nutrition, 7*(6), 2186–2193.

Liu, Q., Meng, X., Li, Y., Zhao, C.-N., Tang, G.-Y., & Li, H.–B. (2017). Antibacterial and Antifungal Activities of Spices. *International Journal of Molecular Sciences, 18*(6), 1283.

Malik, J., Munjal, K., & Deshmukh, R. (2015). Attenuating effect of standardized lyophilized *Cinnamomum zeylanicum* bark extract against streptozotocin–induced experimental dementia of Alzheimer's type. *Journal of Basic and Clinical Physiology and Pharmacology, 26*(3), 275–285.

Medagama, A. B. (2015). The glycaemic outcomes of Cinnamon, a review of the experimental evidence and clinical trials. *Nutrition Journal, 14*, 108.

Morlock, G. E., & Heil, J. (2020). HI–HPTLC–UV/Vis/FLD–HESI–HRMS and bioprofiling of steviol glycosides, steviol, and isosteviol in *Stevia* leaves and foods. *Analytical and Bioanalytical Chemistry, 412*, 6431–6448.

Mousavi, S. M., Rahmani, J., Kord-Varkaneh, H., Sheikhi, A., Larijani, B., & Esmaillzadeh, A. (2020). Cinnamon supplementation positively affects obesity: A systematic review and dose–response meta–analysis of randomized controlled trials. *Clinical Nutrition, 39*(1), 123–133.

Muhammad, D. R. A., & Dewettinck, K. (2017). Cinnamon and its derivatives as potential ingredient in functional food—A review. *International Journal of Food Properties, 20*(2), 2237–2263.

Nabavi, S. F., Di Lorenzo, A., Izadi, M., Sobarzo-Sánchez, E., Daglia, M., & Nabavi, S. M. (2015). Antibacterial Effects of Cinnamon: From Farm to Food. *Cosmetic and Pharmaceutical Industries. Nutrients, 7*(9), 7729–7748.

Otaegui-Arrazola, A., Amiano, P., Elbusto, A., Urdaneta, E., & Martínez-Lage, P. (2014). Diet, cognition, and Alzheimer's disease: food for thought. *European Journal of Nutrition, 53*(1), 1–23.

Ranasinghe, P., Galappaththy, P., Constantine, G. R., Jayawardena, R., Weeratunga, H. D., Premakumara, S., & Katulanda, P. (2017). *Cinnamomum zeylanicum* (Ceylon cinnamon) as a potential pharmaceutical agent for type–2 diabetes mellitus: study protocol for a randomized controlled trial. *Trials, 18*(1), 446.

Rao, P. V., & Gan, S. H. (2014). Cinnamon: a multifaceted Medicinal Plant. *Evidence-Based Complementary and Alternative Medicine, 2014*.

Saber, J. I. (2019). Utilization of Cinnamon in Preparation and Preservation of Food Products from Microbial Contamination. *Alexandria Science Exchange Journal, 40*, 82–89.

Salma, U., Saha, S. K., Sultana, S., Ahmed, S. M., Haque, S. D., & Mostaqim, S. (2019). The Antibacterial Activity of Ethanolic Extract of Cinnamon (*Cinnamomum zeylanicum*) against two Food Borne Pathogens: *Staphylococcus aureus* and *Escherichia coli*. *Mymensingh Medical Journal, 28*(4), 767–772.

Shan, B., Cai, Y. Z., Brooks, J. D., & Corke, H. (2007). Antibacterial properties and major bioactive components of cinnamon stick (*Cinnamomum burmannii*): activity against foodborne pathogenic bacteria. *Journal of Agricultural and Food Chemistry, 55*(14), 5484–5490.

Sihoglu Tepe, A., & Ozaslan, M. (2020). Anti-Alzheimer, anti–diabetic, skin–whitening, and antioxidant activities of the essential oil of *Cinnamomum zeylanicum*. *Industrial Crops and Products, 145*.

Sim, J. X. F., Khazandi, M., Pi, H., Venter, H., Trott, D. J., & Deo, P. (2019). Antimicrobial effects of cinnamon essential oil and cinnamaldehyde combined with EDTA against canine otitis externa pathogens. *Journal of Applied Microbiology, 127*(1), 99–108.

Su, C.–H., Hsu, C.–H., & Ng, L.–T. (2013). Inhibitory potential of fatty acids on key enzymes related to type 2 diabetes. BioFactors, 39(4), 415–421.

Thada, R., Chockalingam, S., Dhandapani, R. K., & Panchamoorthy, R. (2013). Extraction and quantitation of coumarin from cinnamon and its effect on enzymatic browning in fresh apple juice: a bioinformatics approach to illuminate its antibrowning activity. *Journal of Agricultural and Food Chemistry, 61*(22), 5385–5390.

Vasconcelos, N. G., Croda, J., & Simionatto, S. (2018). Antibacterial mechanisms of cinnamon and its constituents: A review. *Microbial Pathogenesis, 120*, 198–203.

Whiting, D. R., Guariguata, L., Weil, C., & Shaw, J. (2011). IDF diabetes atlas: global estimates of the prevalence of diabetes for 2011 and 2030. *Diabetes Research and Clinical Practice, 94*(3), 311–321.

Zhu, R., Liu, H., Liu, C., Wang, L., Ma, R., Chen, B., Li, L., Niu, J., Fu, M., Zhang, D., & Gao, S. (2017). Cinnamaldehyde in diabetes: A review of pharmacology, pharmacokinetics and safety. *Pharmacological Research, 122*, 78–89.

Zolghadri, S., Bahrami, A., Khan, M. T. H., Munoz-Munoz, J., Garcia-Molina, F., Garcia-Canovas, F., & Saboury, A. A. (2019). A comprehensive review on tyrosinase inhibitors. *Journal of Enzyme Inhibition and Medicinal Chemistry, 34*(1), 279–309.

Supplementary information

Eight different bioactivity profiles of 40 cinnamons by multi-imaging planar chromatography hyphenated with effect-directed analysis and high-resolution mass spectrometry

N.G.A.S. Sumudu Chandana[a], Gertrud E. Morlock[a]

[a]Justus Liebig University Giessen, Institute of Nutritional Science, Chair of Food Science, and TransMIT Center for Effect-Directed Analysis, Heinrich-Buff-Ring 26-32, 35392 Giessen, Germany

*Corresponding author. Tel. +49 641 9939141; fax +49 641 9939149.

E-mail address: gertrud.morlock@uni-giessen.de (G.E. Morlock).

Table S1 Investigated cinnamon samples originating from different countries, suppliers and manufacturers.

ID	Product name	Type	Origin labelled	Manufacturer
1 - 4	Home-made	bark	Sri Lanka	Self-harvested from 4 cinnamon trees at Hiyare, Galle, Sri Lanka
5-7	Cinnamon (Kurudu*)	bark	Sri Lanka	Market, Colombo, Sri Lanka
8	Cinnamon	powder	-	Dehghanzadeh medicinal plant store, Sari, Iran
9	Cinnamon	powder	China	TRS Wholesale, Southall, UK
10	Cinnamon	powder	India	TRS Wholesale, Southall, UK
11	Zimt gemahlen, Le Gusto	powder	-	Teuto Markenvertrieb, Dissen, Germany
12	Ceylon-Zimt gemahlen	powder	-	Ostmann, Schönbrunn, Germany
13	Zimt Ceylon gemahlen	powder	Madagaskar, Sri Lanka	Lebensbaum, Diepholz, Germany
14	Zimt gemahlen, Kania	powder	Afrika	Teuto Markenvertrieb, Dissen, Germany
15	Ceylon-Zimt gemahlen, Kania	powder	-	Teuto Markenvertrieb, Dissen, Germany
16	Zimt gemahlen, Kania	powder	Afrika	Teuto Markenvertrieb, Dissen, Germany
17	Zimt gemahlen, Kania	powder	Afrika	Teuto Markenvertrieb, Dissen, Germany
18	Zimtstangen	bark	-	Flora Gewürze, Dissen, Germany
19	Pau de canella	bark	-	Unimarketing CRL, Lisboa, Portugal
20-35	Cinnamon (Kurudu)	bark	Sri Lanka	Market, Galle, Sri Lanka
36-40	Cinnamon (Kurudu)	bark	Sri Lanka	Market, Matara, Sri Lanka

Bought in German discounter

*Kurudu is the word for cinnamon in Sinhala language.

Table S2. HPTLC-HESI-HRMS data of bioactive zones in cinnamon extract IDs 8, 9 and 12 in the *A. fischeri* bioautogram and IDs 10 and 38 in the tyrosinase autogram in reference to fatty/phenolic acids (Fig. 3).

Bioactive zone	*m/z* observed	*m/z* theoretical	Mass error	Formula	Assignment	Signal
8a	147.04512	147.04515	0.20	C9H7O2	Cinnamic acid	$[M-H]^-$
9c	279.23292	279.23295	0.12	C18H32O2	Linoleic acid	$[M1-H]^-$
	281.24854	281.24860	0.23	C18H34O2	Oleic acid	$[M2-H]^-$
	283.26425	283.26425	0.00	C18H36O2	Stearic acid	$[M3-H]^-$
38e	121.02945	121.02950	0.45	C7H6O2	Benzoic acid	$[M1-H]^-$
	147.04513	147.04515	0.16	C9H8O2	Cinnamic acid	$[M2-H]^-$
10f	255.23295	255.23295	0.00	C16H32O2	Palmitic acid	$[M-H]^-$
8b	147.04404	147.04406	0.14	C9H7O2	Coumarin	$[M+H]^+$
	169.02597	169.0260	0.18	C9H6O2		$[M+Na]^+$
12d	133.06488	133.06479	-0.68	C9H9O	Cinnamaldehyde	$[M+H]^+$
	155.04679	155.04674	-0.32	C9H8O		$[M+Na]^+$
38e	193.12004	193.11990	-0.72	C10H18O2	Linalool oxide	$[M+Na]^+$
References						
Caproic acid	115.07636	115.07645	0.82	C6H12O2		
Cinnamic acid	147.04514	147.04515	0.10	C9H8O2		
Myristic acid	227.20167	227.20165	-0.07	C14H28O2		
Oleic acid	281.24850	281.24860	0.37	C18H34O2		
Palmitic acid	255.23296	255.23295	0.02	C16H32O2		
Stearic acid	283.26417	283.26424	0.30	C18H36O2		

Table S3. HPTLC-HESI$^+$-HRMS data of bioactive zones in cinnamon extract IDs 9–11 in the tyrosinase inhibition autogram and reference coumarin (further coumarin activities in Fig. S14, quantification of the enzymatic response of coumarin in Fig. 4).

Bioactive zone	*m/z* observed	*m/z* theoretical	Mass error	Formula	Assignment	Signal
9a	133.06490	133.06479	-0.82	C9H8O	Cinnamaldehyde	$[M+H]^+$
11b	185.05741	185.05730	-0.59	C10H10O2	Alpha-methyl cinnamic acid	$[M+Na]^+$
10c, 11c	169.02608	169.02600	-0.47	C9H6O2	Coumarin	$[M+Na]^+$
Coumarin	169.02608	169.02600	-0.47	C9H6O2		

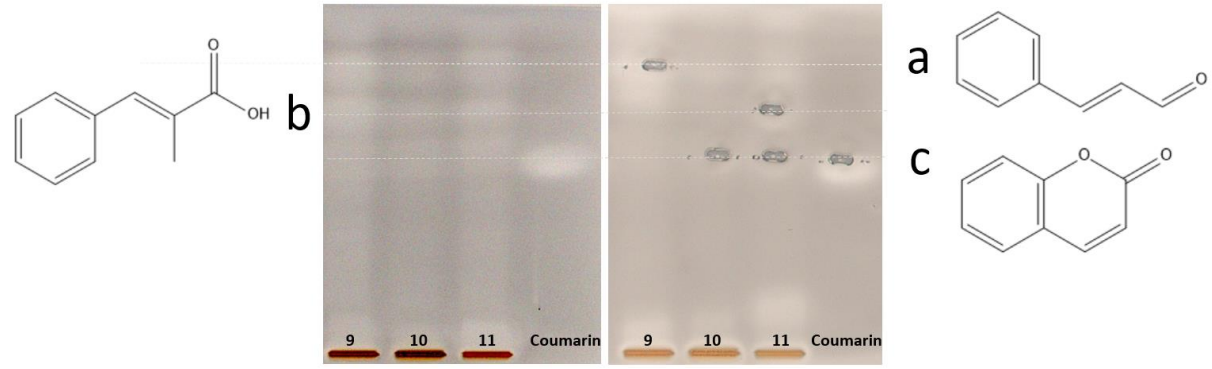

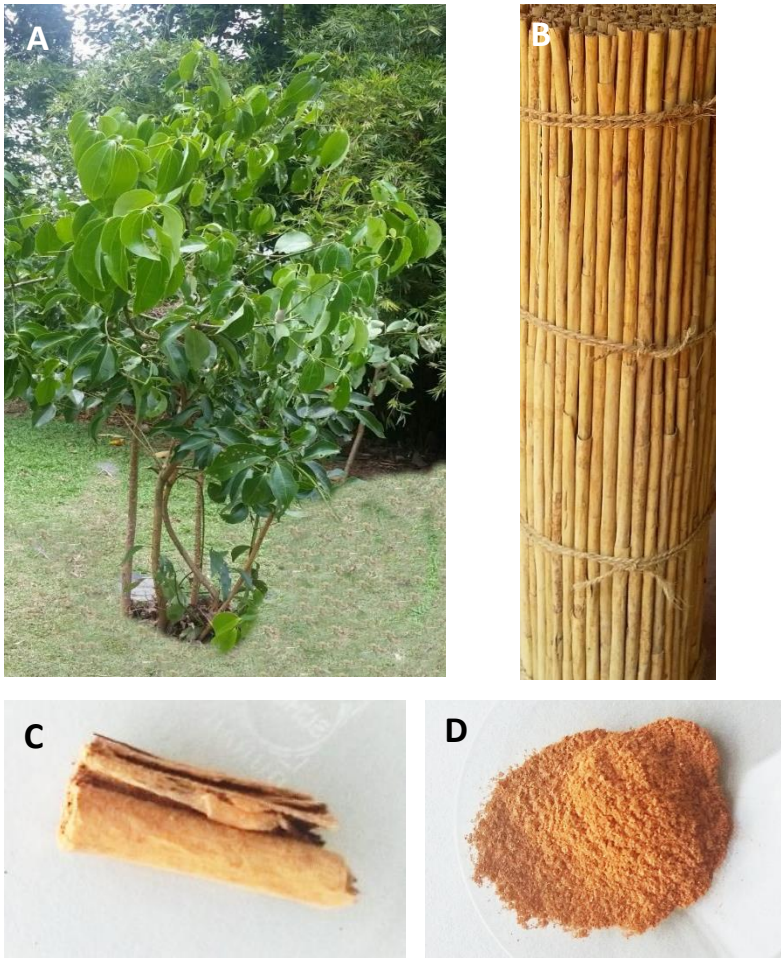

Figure S1 Representative *Cinnamomum zeylanicum* from Galle, Sri Lanka (**A**) tree, (**B**) bundle of sticks, (**C**) stick, and after grinding, (**D**) respective powder.

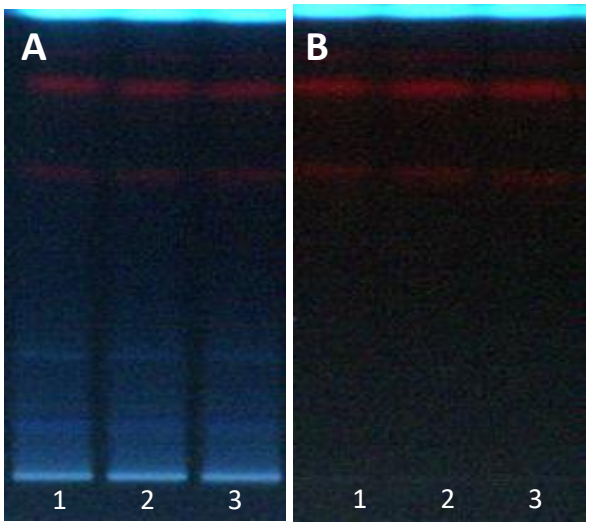

Figure S2 Extraction solvent selection: HPTLC chromatograms at FLD 366 nm of cinnamon IDs 1-3 (1 µL, 100 mg/mL, 100 µg/band) (**A**) extracted with methanol – water and (**B**) ethyl acetate – *n*-hexane, for both 4:1, *V*/*V*, on HPTLC plate silica gel 60 F_{254} with ethyl acetate – methanol – water 17:2:1 (*V*/*V*/*V*).

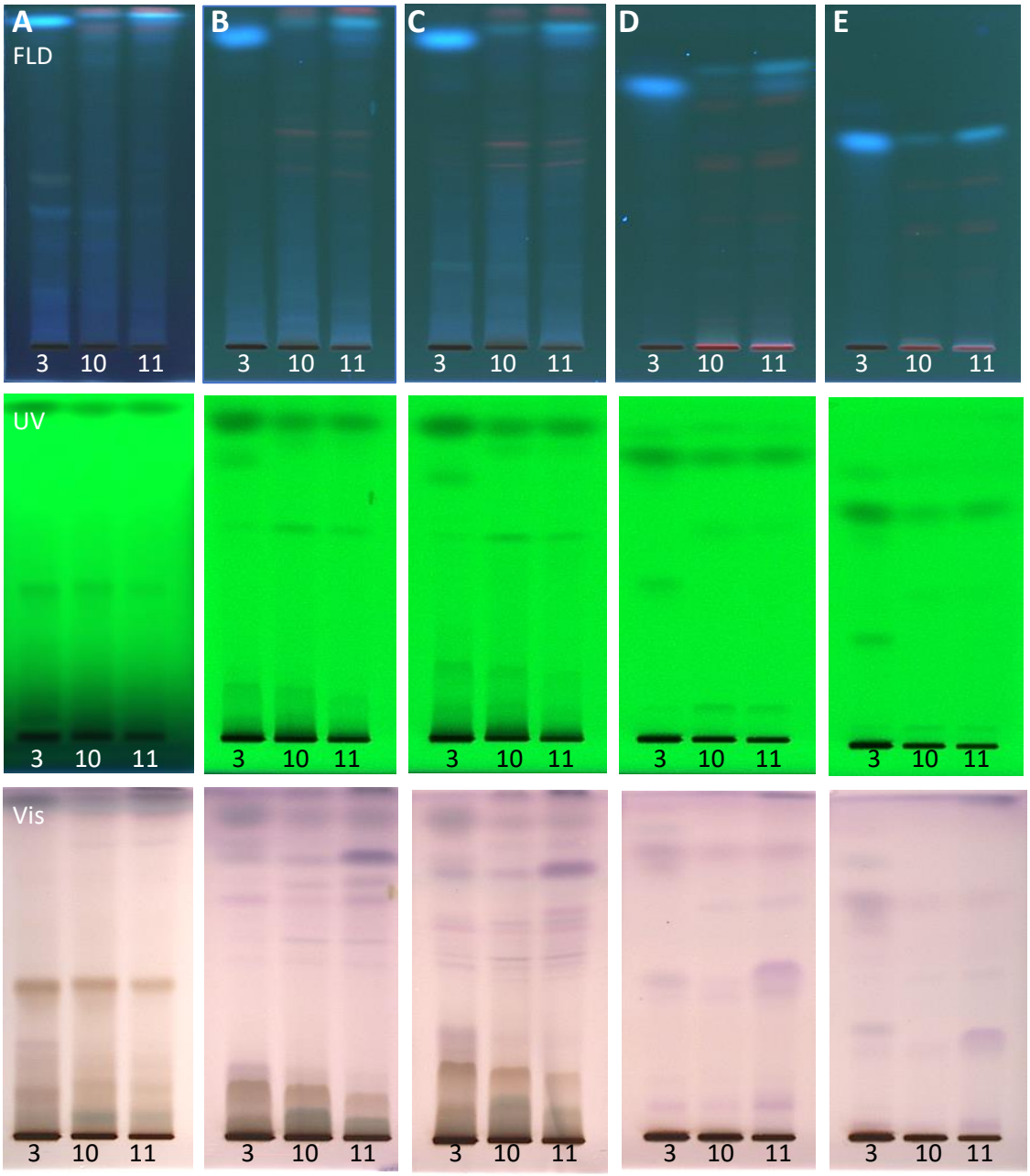

Figure S3 Mobile phase selection: HPTLC chromatograms of cinnamon extract IDs 3, 10 and 11 (each 2 µL, 100 mg/mL, 200 µg/band) on HPTLC plates silica gel 60 F_{254} with (**A**) ethyl acetate - toluene - formic acid - water 16:4:3:2, (**B**) toluene – ethyl acetate – methanol 6:5:3 (**C**) toluene - ethyl acetate - methanol 3:2:2, (**D**) petroleum ether – ethyl acetate – acetone 15:4:1 and (**E**) petroleum ether - ethyl acetate – cyclohexane 5:2:3, all *V*/*V* and up to 70 mm, documented at UV 366 nm (FLD), 254 nm (UV) and white light illumination (Vis) after the *p*-anisaldehyde sulphuric acid reagent.

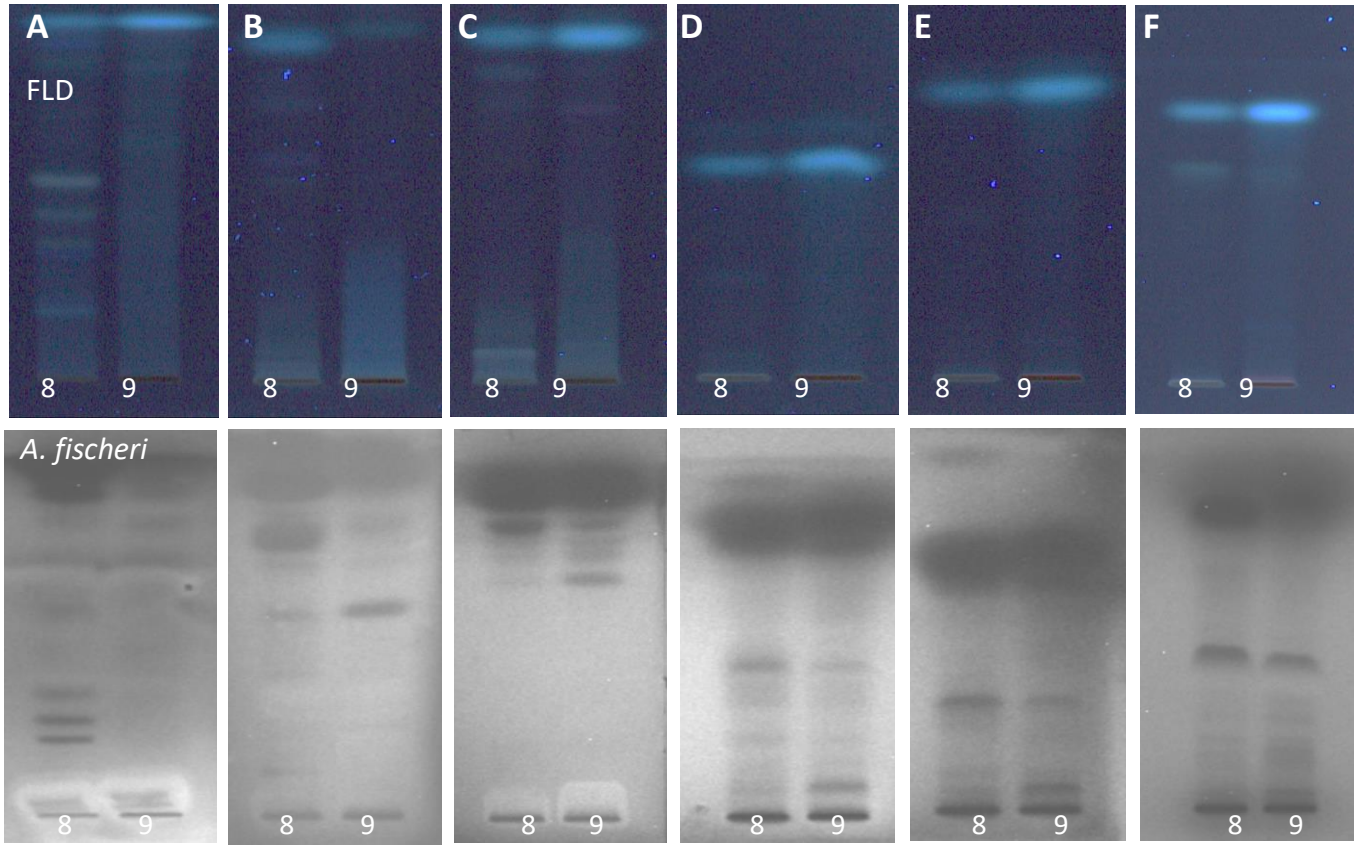

Figure S4 Extended mobile phase selection with regard to effects: HPTLC chromatograms of cinnamon extract IDs 8 and 9 (each 2 µL, 100 mg/mL, 200 µg/band) on HPTLC silica gel 60 plates with (**A–E**) mobile phases as in Figure S3 and (**F**) ethyl acetate – toluene 1:1, all up to 70 mm, documented at FLD 366 nm and after the bioluminescent *Aliivibrio fischeri* bioassay (greyscale image).

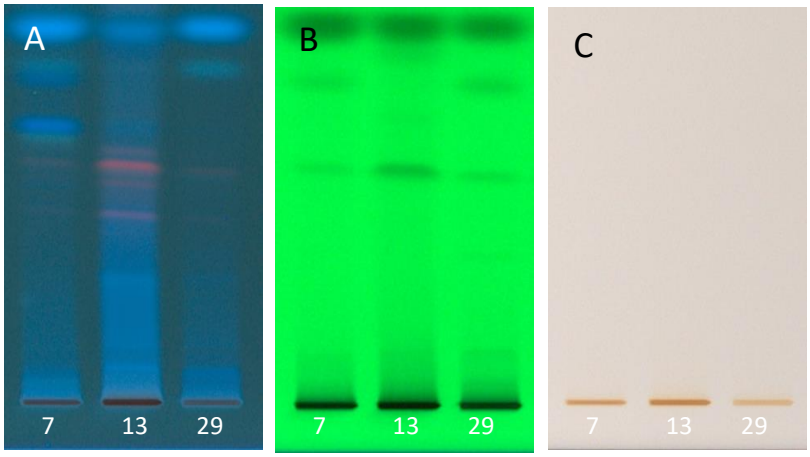

Figure S5 Selected mobile phase: HPTLC chromatograms of cinnamon extract IDs 7, 13 and 29 (each 2 µL, 100 mg/mL, 200 µg/band) on HPTLC plates silica gel 60 F_{254} with toluene – ethyl acetate – methanol 6:5:3 (*V/V/V;* as in Figure S3/4 B) up to 70 mm, documented at (**A**) FLD 366 nm, (**B**) UV 254 nm and (**C**) white light illumination.

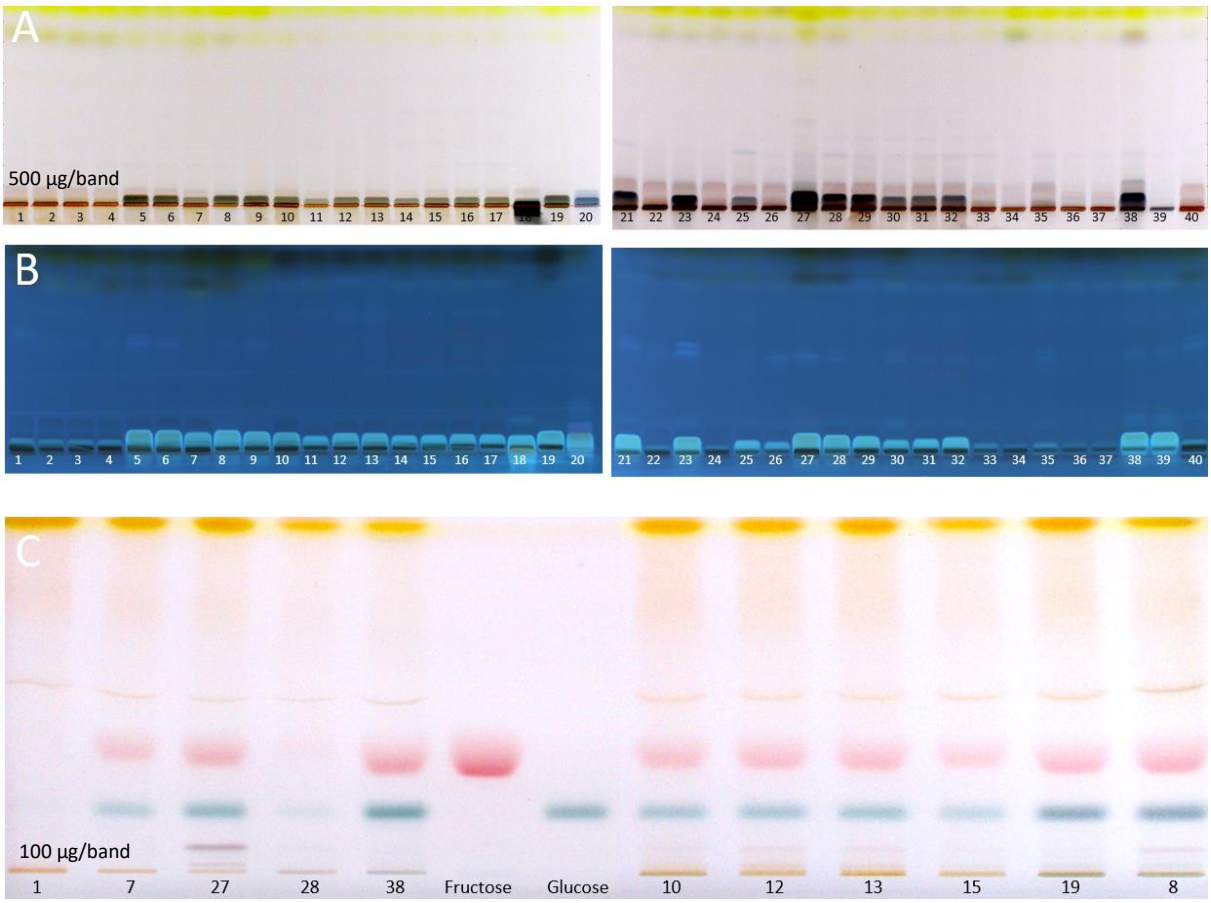

Figure S6 Saccharide screening of selected cinnamon extracts (assignment in Table S1, each 500 µg/band for A/B and 100 µg/band for C) on HPTLC plates silica gel 60 (**A**/**B**) with toluene – ethyl acetate – methanol 6:5:3 (*V*/*V*/*V*) detected at (**A** and **C**) white light illumination via the diphenylamine aniline *o*-phosphoric acid reagent and (**B**) FLD 366 nm via the *p*-aminobenzoic acid reagent (2 g *p*-aminobenzoic acid, 50 mL glacial acetic acid, 50 mL water and 2 mL orthophosphoric acid): all saccharides remained at the start position or slightly above; hence, (**B**) subsequent separation with an adjusted mobile phase of increased solvent strength (acetonitrile – water 9:1, *V/V,* plus 1 mg/mL 2-aminoethyl diphenyl borate according to Morlock & Heil, 2020), which revealed fructose (red zone, 1 µg/band) and glucose (blue zone, 1 µg/band) as main saccharides (for some samples such as IDs 8 and 27 sucrose as brown zone).

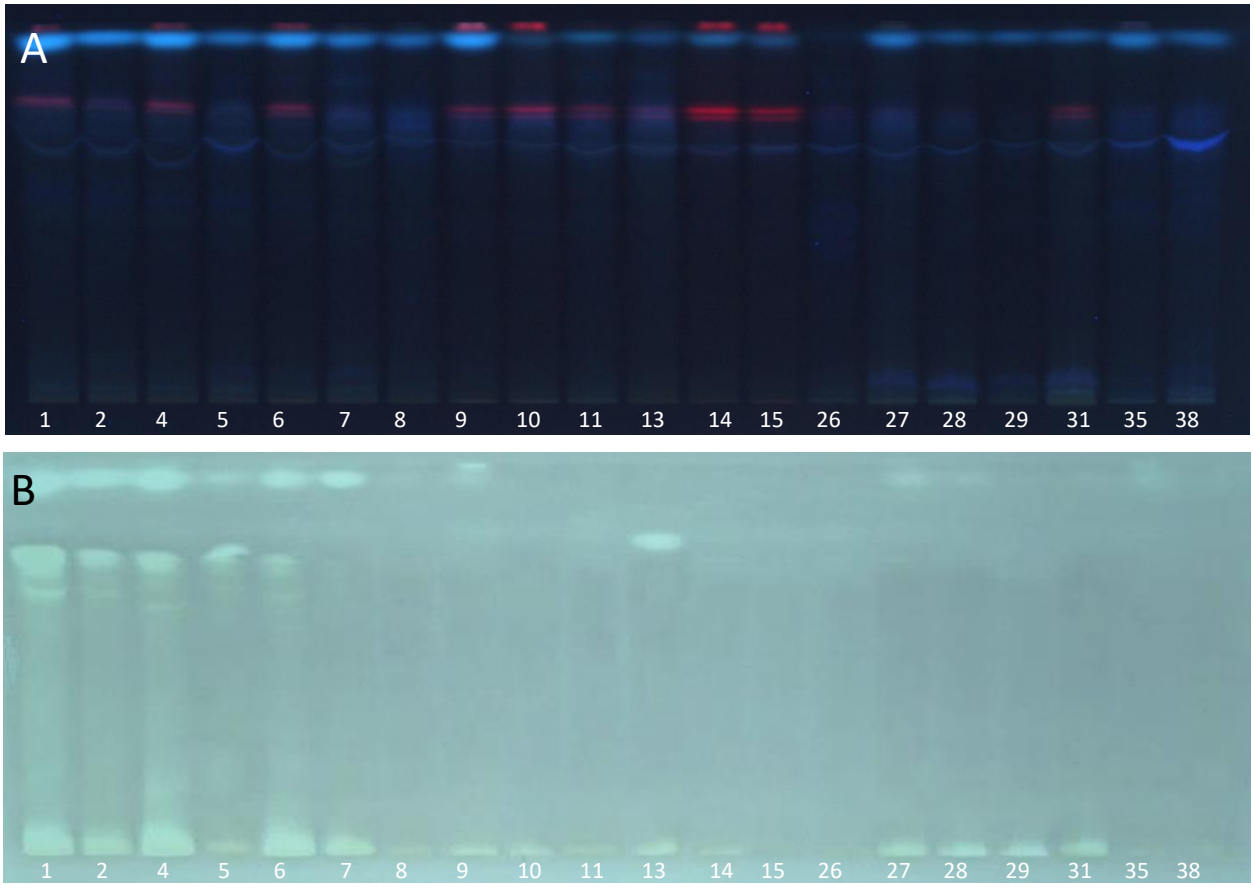

Figure S7 Antimicrobial screening against Gram-positive *Bacillus subtilis* bacteria of selected cinnamon extracts (200 µg/band) on HPTLC plate silica gel 60 with acetonitrile – water 9:1 (*V*/*V*) documented at (**A**) FLD 366 nm and (**B**) white light illumination after the bioassay.

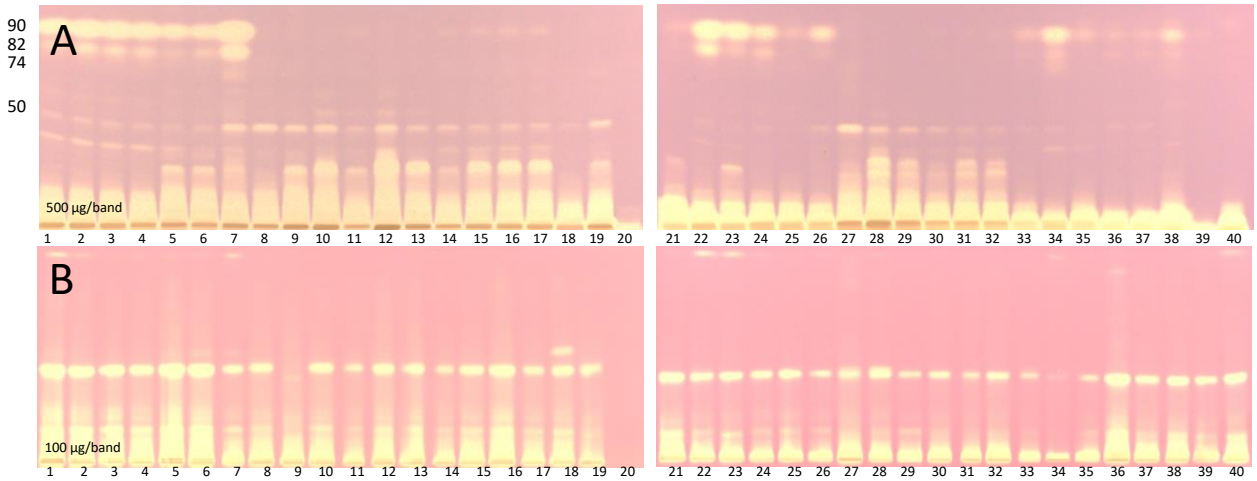

Figure S8 DPPH• radical scavenger screening of cinnamon extract IDs 1-40 (500 µg/band for A and 100 µg/band for B) on HPTLC plates silica gel 60 F_{254} with (**A**) toluene – ethyl acetate – methanol 6:5:3 *versus* a mobile phases of higher elution power with (**B**) ethyl acetate – toluene – formic acid – water 16:4:3:2, both *V/V/V.*

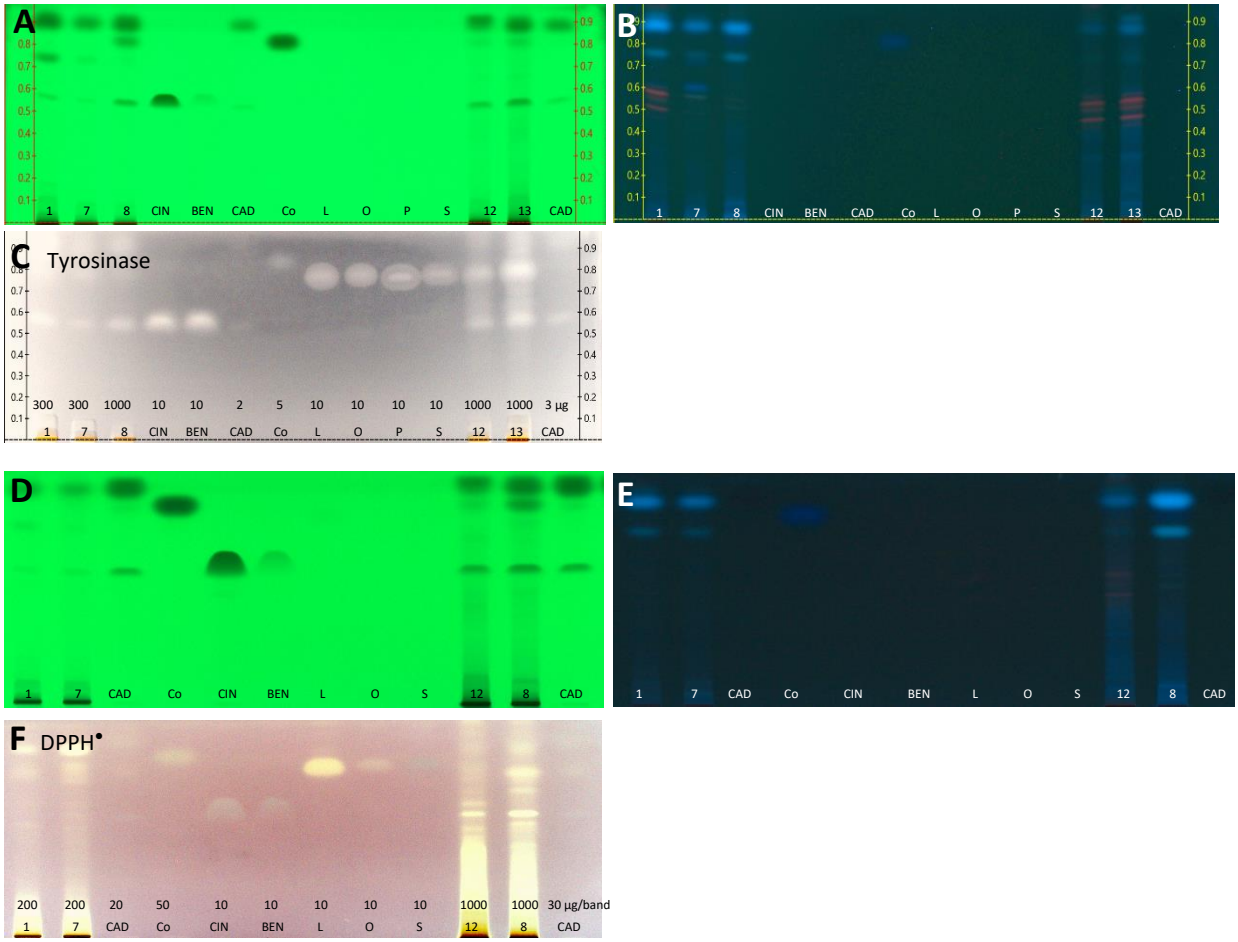

Figure S9 Co-chromatography of cinnamon extract IDs 1, 7, 8, 12 and 13 along with cinnamaldehyde (CAD), coumarin (Co), cinnamic acid (CIN), benzoic acid (BEN), linoleic acid (L), oleic acid (O), stearic acid (S) on HPTLC plates silica gel 60 F_{254} with toluene - ethyl acetate - methanol 6:5:3 (*V/V/V*), detected at (**A**/**D**) UV 254 nm, (**B**/**E**) FLD 366 nm and (**C**/**F**) white light illumination for tyrosinase inhibition and DPPH• assays.

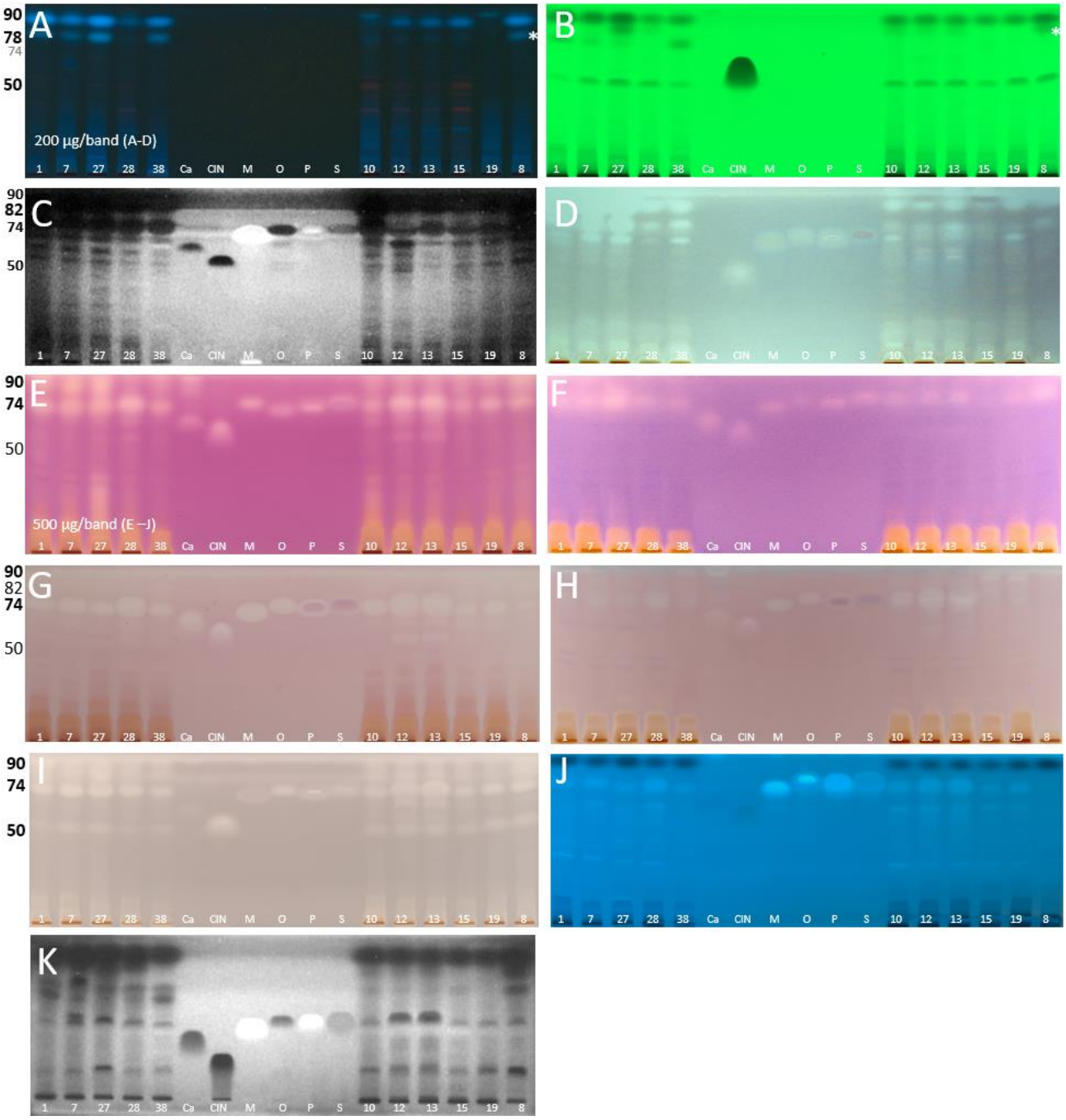

Figure S10 Selected cinnamon extracts (200 or 500 µg/band depending on the assay) along with fatty/phenolic acids (3–15 µL, 1.5–7.5 µg/band depending on the assay) on HPTLC plates silica gel 60 F_{254} with (**A**-**J**) toluene – ethyl acetate – methanol 6:5:3 (*V/V/V*) or (**K**) toluene – ethyl acetate 1:1 (*V*/*V*), detected at (**A**) FLD 366 nm, (**B**) UV 254 nm, (**C**/**K**) bioluminescent *A. fischeri* bioassay (grey-scale image) and at white light illumination after the (**D**) *B. subtilis* bioassay, (**E**) α-glucosidase, (**F**) β-glucosidase, (**G**) AChE, (**H**) BChE and (**I**) tyrosinase inhibition assays as well as (**J**) at 366 nm by the primuline reagent. Note that myristic acid (M) and caproic acid (Ca) were not detected in cinnamon, however, used to compare the bioactivities of the fatty acids.

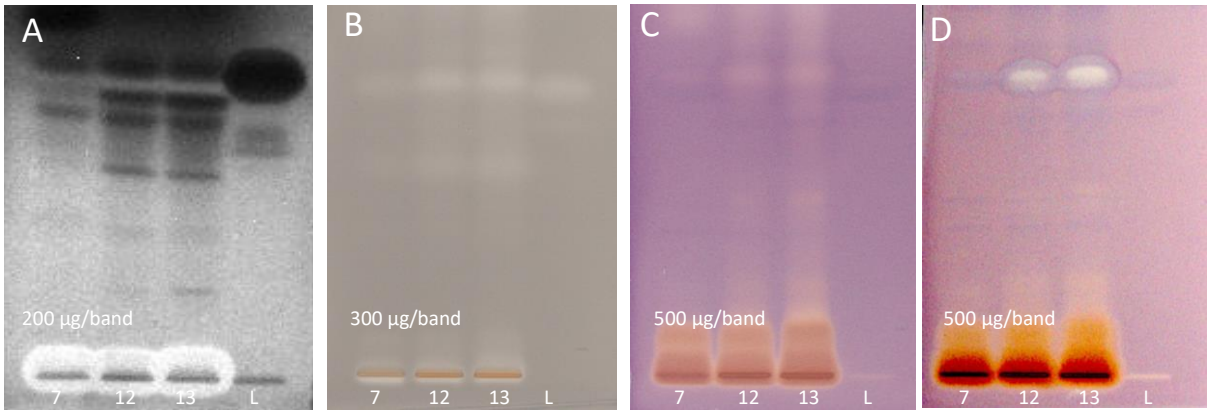

Figure S11 Co-chromatography of cinnamon extract IDs 7, 12 and 13 (200–500 µg/band depending on the assay) along with linoleic acid (L; 2.5 µg/band) on HPTLC plates silica gel 60 F_{254} with toluene – ethyl acetate – methanol 6:5:3 (*V/V/V*) detected via (**A**) the bioluminescent *Aliivibrio fischeri* bioassay, and at white light illumination, (**B**) the tyrosinase, (**C**) α-glucosidase and (**D**) AChE inhibition assays.

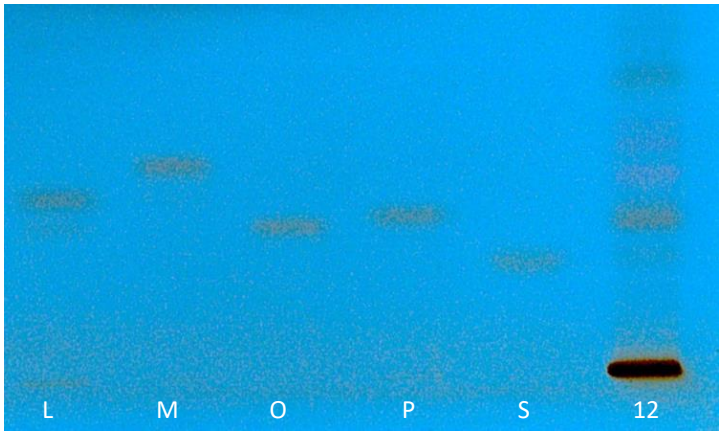

Figure S12 Co-chromatography of linoleic acid (L), myristic acid (M), oleic acid (O), palmitic acid (P), stearic acid (S; 25 µL, 0.5 mg/mL, 12.5 µg/band each) and cinnamon *t*-butyl methyl ether extract ID 12 (25 µL, 100 mg/mL, 2500 µg/band) on HPTLC plate silica gel RP 8 F_{254S} with methanol – water – formic acid 9:1:0.1 (*V/V/V*) up to 70 mm, detected at 366 nm using the primuline reagent.

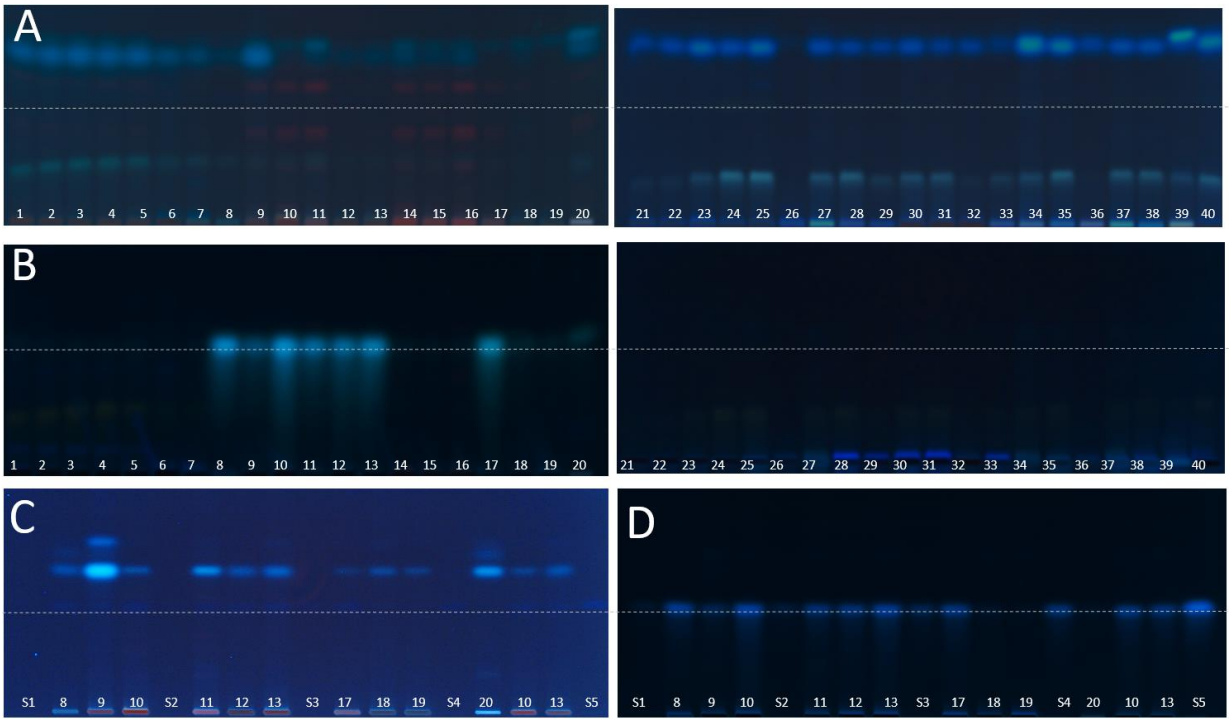

Figure S13 Analysis of coumarin in cinnamon extracts: (**A**/**B**) Screening of extract IDs 1–40 (each 2 µL, 200 µg/band) and (**C**/**D**) quantification of selected extract IDs (calibration range 25–500 ng/band, S1–S5) on HPTLC plates silica gel 60 with *n*-hexane – ethyl acetate – ammonia 3.8:1.3:0.05, *V/V/V*, detected at FLD 366 nm (**A**/**C**) before and (**B**/**D**) after derivatization with 10% ethanolic potassium hydroxide solution, followed by 10% methanolic PEG 400 solution for fluorescence stabilization.

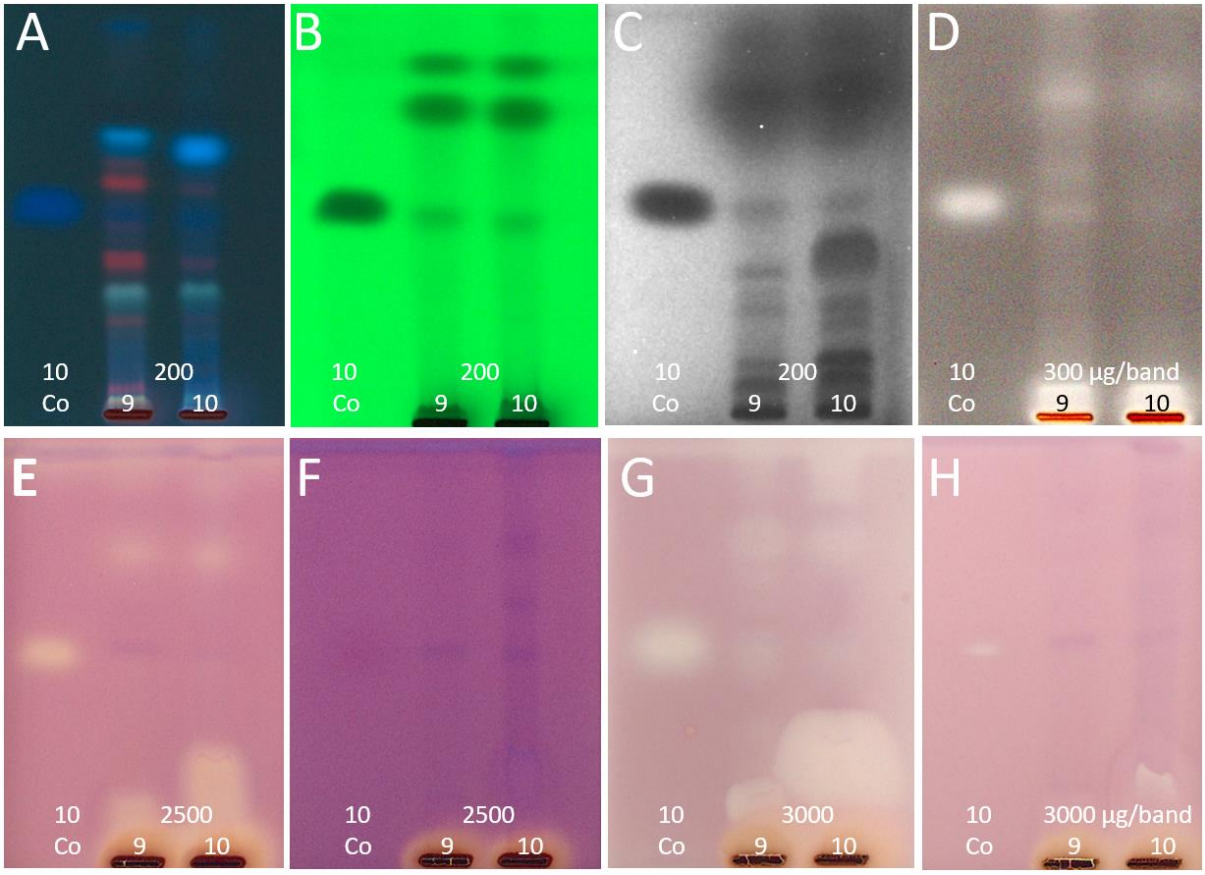

Figure S14 Bioactivity of coumarin (Co, 10 µg/band) and cinnamon extract IDs 9 and 10 (200–3000 µg/band depending on the assay) on HPTLC plates silica gel 60 with *n*-hexane – ethyl acetate – ammonia 3.8:1.3:0.05, *V/V/V*, detected at (**A**) FLD 366 nm, (**B**) UV 254 nm, (**C**) via bioluminescent *A. fischeri* bioassay, (**D**) tyrosinase, (**E**) α-glucosidase, (**F**) β-glucosidase, (**G**) AChE and (**H**) BChE inhibition assays.

4. Summary

Citizens in developing countries rely on indigenous knowledge and practices and use locally available medicinal plants for different treatments. Most of these plants have not been investigated for their chemical composition or physiological properties. Due to limited scientific instrumentation and facilities for chemical characterization and conducting bioassays, most studies investigating the bioactive properties of Sri Lankan medicinal plants rarely progress to the molecular level. While for some plants, the whole plant extracts have been tested for their bioactivity, most of the individual compounds and their effects have still not been identified. The separation of bioactive compounds from natural sources is a challenging task. Undoubtedly, hyphenated approaches like high-performance HPTLC combined with EDA and mass spectrometry, provide impressive opportunities for the identification of natural products without prior tedious compound isolation. Separating complex plant-based samples into individual compounds and studying their effects allows us to study the potential impact of medicinal plants on consumers. These findings can be used to substantiate current traditional medicinal knowledge and to evaluate their benefits, risks and limitations. The newly developed hyphenated HPTLC-UV/Vis/FLD-EDA-HESI-HRMS method for identification of single compound effects in Sri Lankan *Abelmoschus moschatus* and *Cinnamomum zeylanicum* included (1) non-target screening, (2) assignment of prominent individual bioactive compounds, and (3) comparison of product profiles to check the quality of commercial products. Both studies revealed not only the phytochemical but also the prominent bioactive constituents or fractions in the multi-compound mixtures. Diverse antimicrobials, antioxidants and inhibitors of glucosidase, tyrosinase and cholinesterase were detected. Running reference materials in parallel to identified compounds, confirmed the assignments and biological effects. The cost-efficient and environmentally friendly HPTLC-UV/Vis/FLD-EDA technique can be used in developing countries for profiling and valorization of plant-based foods, botanicals and medicinal herbal preparations.

5. Zusammenfassung

In Entwicklungsländern verlassen sich die Menschen auf einheimisches Wissen und traditionelle Praktiken. Sie verwenden lokal verfügbare Heilpflanzen für verschiedene Behandlungen. Die meisten dieser Pflanzen wurden bisher nicht auf ihre chemische Zusammensetzung oder physiologischen Eigenschaften hin untersucht. Aufgrund begrenzter wissenschaftlicher Geräte und Einrichtungen für die chemische Charakterisierung sowie die Durchführung von Bioassays gehen die meisten Studien zur Untersuchung der bioaktiven Eigenschaften srilankischer Heilpflanzen nur selten bis zur molekularen Ebene. Während bei einigen Pflanzen die gesamten Pflanzenextrakte auf ihre Bioaktivität getestet wurden, sind die meisten einzelnen Verbindungen und ihre Wirkungen noch nicht identifiziert worden. Die Trennung bioaktiver Verbindungen aus natürlichen Quellen ist eine schwierige Aufgabe. Zweifellos bieten gekoppelte Techniken wie die Hochleistungs-Dünnschichtchromatographie in Kombination mit der wirkungsbezogenen Analytik und der Massenspektrometrie beeindruckende Möglichkeiten für die Identifizierung von Naturstoffen ohne vorherige mühsame Isolierung der Verbindungen. Die Auftrennung komplexer pflanzlicher Proben in einzelne Verbindungen und die Untersuchung ihrer Wirkungen ermöglicht es, die potenziellen Auswirkungen von Heilpflanzen auf Konsumenten zu untersuchen. Diese Erkenntnisse können zur Untermauerung des derzeitigen traditionellen medizinischen Wissens und zur Bewertung von dessen Nutzen, Risiken und Grenzen verwendet werden. Die neu entwickelte HPTLC-UV/Vis/FLD-EDA-HESI-HRMS-Methode zur Identifizierung der Wirkungen einzelner Verbindungen in *Abelmoschus moschatus* und *Cinnamomum zeylanicum* aus Sri Lanka umfasste (1) ein nicht-Zielsubstanz-orientiertes Screening, (2) die Zuordnung prominenter bioaktiver Einzelverbindungen und (3) den Vergleich von Produktprofilen zur Überprüfung der Qualität kommerzieller Produkte. Beide Studien brachten nicht nur die phytochemischen, sondern auch die herausragenden bioaktiven Bestandteile oder Fraktionen in den Vielstoffgemischen hervor. Es wurden verschiedene antimikrobielle Stoffe, Antioxidantien und Inhibitoren von Glucosidase, Tyrosinase und Cholinesterase nachgewiesen. Der Einsatz von Referenzmaterialien parallel zu den identifizierten Verbindungen bestätigte die Zuordnungen und biologischen Wirkungen. Die kosteneffiziente und umweltfreundliche HPTLC-UV/Vis/FLD-EDA-Technik kann in Entwicklungsländern für die Erstellung von Profilen und die Bewertung von pflanzlichen Lebensmitteln, pflanzlichen Stoffen und Heilkräuterzubereitungen eingesetzt werden.

Publication bibliography

Abdel-Razek, A. S., El-Naggar, M. E., Allam, A., Morsy, O. M., & Othman, S. I. (2020). Microbial natural products in drug discovery. *Processes*, *8*(4), 470. https://doi.org/10.3390/pr8040470

Abraham, A., Samuel, S., & Mathew, L. (2020). Phytochemical analysis of Pathyashadangam kwath and its standardization by HPLC and HPTLC. *Journal of Ayurveda and integrative medicine*, *11*(2), 153–158. https://doi.org/10.1016/j.jaim.2017.10.011

Agatonovic-Kustrin, S., Kustrin, E., Gegechkori, V., & Morton, D. W. (2019). High-performance thin-layer chromatography hyphenated with microchemical and biochemical derivatizations in bioactivity profiling of marine species. *Marine drugs, 17*(3), 148. https://doi.org/10.3390/md17030148

Agatonovic-Kustrin, S., & Morton, D. W. (2020). Hyphenated TLC as a tool in the effect-directed discovery of bioactive natural products. *Applied Sciences, 10*(3), 1123. https://doi.org/10.3390/app10031123

Agatonovic-Kustrin, S., & Morton, D. W. (2020). The power of HPTLC-ATR-FTIR hyphenation in bioactivity analysis of plant extracts. *Applied Sciences*, *10*(22), 8232. https://doi.org/10.3390/app10228232

Ahmad, A., Amir, M., Alshadidi, A. A., Hussain, M. D., Haq, A., & Kazi, M. (2020). Central composite design expert-supported development and validation of HPTLC method: relevance in quantitative evaluation of protopine in *Fumaria indica*. *Saudi pharmaceutical journal*, *28*(4), 487–494. https://doi.org/10.1016/j.jsps.2020.02.011

Ahmed, S., Al-Rehaily, A. J., Alam, P., Alqahtani, A. S., Hidayatullah, S., Rehman, M. T., Mothana, R. A., Abbas, S. S., Khan, M. U., Khalid, J. M., & Siddiqui, N. A. (2019). Antidiabetic, antioxidant, molecular docking and HPTLC analysis of miquelianin isolated from *Euphorbia schimperi* C. Presl. *Saudi pharmaceutical journal : SPJ : the official publication of the Saudi Pharmaceutical Society*, *27*(5), 655–663. https://doi.org/10.1016/j.jsps.2019.03.008

Amarasiri, S. S., Attanayake, A. P., Arawwawala, L., Jayatilaka, K., & Mudduwa, L. (2020). Acute and 28-day repeated-dose oral toxicity assessment of *Abelmoschus moschatus* Medik. in healthy Wistar rats. *Evidence-based complementary and alternative medicine: eCAM*, 1359050. https://doi.org/10.1155/2020/1359050

Azadniya, E., & Morlock, G. E. (2019). Automated piezoelectric spraying of biological and enzymatic assays for effect-directed analysis of planar chromatograms. *Journal of chromatography. A*, *1602*, 458–466.
https://doi.org/10.1016/j.chroma.2019.05.043
Bailey C. J. (2017). Metformin: historical overview. *Diabetologia*, *60*(9), 1566–1576.
https://doi.org/10.1007/s00125-017-4318-z
Bharti, S. K., Krishnan, S., Kumar, A., Rajak, K. K., Murari, K., Bharti, B. K., & Gupta, A. K. (2012). Antihyperglycemic activity with DPP-IV inhibition of alkaloids from seed extract of Castanospermum australe: investigation by experimental validation and molecular docking. *Phytomedicine : international journal of phytotherapy and phytopharmacology*, *20*(1), 24–31.
https://doi.org/ 10.1016/j.phymed.2012.09.009
Biringanine, G., Chiarelli, M. T., Faes, M., & Duez, P. (2006). A validation protocol for the HPTLC standardization of herbal products: application to the determination of acteoside in leaves of Plantago palmata Hook. f.s. *Talanta*, *69*(2), 418–424.
https://doi.org/10.1016/j.talanta.2005.10.007
Birks J. (2006). Cholinesterase inhibitors for Alzheimer's disease. *The Cochrane database of systematic reviews*, (1), CD005593.
https://doi.org/10.1002/14651858.CD005593
Bonesi, M., Xiao, J., Tundis, R., Aiello, F., Sicari, V., & Loizzo, M. R. (2019). Advances in the tyrosinase inhibitors from plant source. *Current medicinal chemistry*, *26*(18), 279–3299.
https://doi.org/10.2174/0929867325666180522091311
Bräm, S., & Wolfram, E. (2017). Recent advances in effect-directed enzyme assays based on thin-layer chromatography. *Phytochemical analysis: PCA*, *28*(2), 74–86.
https://doi.org/10.1002/pca.2669
Buszewski, B., & Noga, S. (2012). Hydrophilic interaction liquid chromatography (HILIC) a powerful separation technique. *Analytical and bioanalytical chemistry*, *402*(1), 231–247.
https://doi.org/10.1007/s00216-011-5308-5
Chaita, E., Gikas, E., & Aligiannis, N. (2017). Integrated HPTLC-based methodology for the tracing of bioactive compounds in herbal extracts employing multivariate chemometrics. a case study on *Morus alba*. *Phytochemical analysis: PCA*, *28*(2), 125–131.
https://doi.org/10.1002/pca.2670
Cole, J. B., & Florez, J. C. (2020). Genetics of diabetes mellitus and diabetes complications. *Nature reviews. Nephrology*, *16*(7), 377–390.

https://doi.org/10.1038/s41581-020-0278-5
Desmedt, B., Courselle, P., De Beer, J. O., Rogiers, V., Grosber, M., Deconinck, E., & De Paepe, K. (2016). Overview of skin whitening agents with an insight into the illegal cosmetic market in Europe. *Journal of the European Academy of Dermatology and Venereology : JEADV*, *30*(6), 943–950.
https://doi.org/10.1111/jdv.13595
Dewanjee, S., Gangopadhyay, M., Bhattacharya, N., Khanra, R., & Dua, T. K. (2015). Bioautography and its scope in the field of natural product chemistry. *Journal of pharmaceutical analysis*, *5*(2), 75–84.
https://doi.org/10.1016/j.jpha.2014.06.002
Dey, A., Bhattacharya, R., Mukherjee, A., & Pandey, D. K. (2017). Natural products against Alzheimer's disease: pharmaco-therapeutics and biotechnological interventions. *Biotechnology advances*, *35*(2), 178–216.
https://doi.org/10.1016/j.biotechadv.2016.12.005
Dimkić, I., Stanković, S., Nišavić, M., Petković, M., Ristivojević, P., Fira, D., & Berić, T. (2017). The profile and antimicrobial activity of *Bacillus* lipopeptide extracts of five potential biocontrol strains. *Frontiers in microbiology*, *8*, 925.
https://doi.org/10.3389/fmicb.2017.00925
Dubey, N., Dubey, N., & Mehta, R. (2012). Validation of HPTLC and HPLC methods for the quantitative determination of allyl disulfide in some polyherbal oils. *Journal of AOAC International*, *95*(6), 1574–1578.
https://doi.org/ 10.5740/jaoacint.11-492
Ebrahimi-Najafabadi, H., Kazemeini, S. S., Pasdaran, A., & Hamedi, A. (2019). A novel similarity search approach for high-performance thin-layer chromatography (HPTLC) fingerprinting of medicinal plants. *Phytochemical analysis: PCA*, *30*(4), 405–414.
https://doi.org/10.1002/pca.2823
Ekor M. (2014). The growing use of herbal medicines: issues relating to adverse reactions and challenges in monitoring safety. *Frontiers in pharmacology*, *4*, 177.
https://doi.org/10.3389/fphar.2013.00177
Friesen, J. B., McAlpine, J. B., Chen, S. N., & Pauli, G. F. (2015). Countercurrent separation of natural products: an update. *Journal of natural products*, *78*(7), 1765–1796.
https://doi.org/10.1021/np501065h

Frommenwiler, D. A., Kim, J., Yook, C. S., Tran, T., Cañigueral, S., & Reich, E. (2018). Comprehensive HPTLC fingerprinting for quality control of an herbal drug - The case of *Angelica gigas* root. *Planta medica*, *84*(6-07), 465–474. https://doi.org/10.1055/a-0575-4425

Galarce-Bustos, O., Pavón, J., Henríquez-Aedo, K., & Aranda, M. (2019). Detection and identification of acetylcholinesterase inhibitors in *Annona cherimola* Mill. by effect-directed analysis using thin-layer chromatography-bioassay-mass spectrometry. *Phytochemical analysis: PCA*, *30*(6), 679–686. https://doi.org/10.1002/pca.2843

Ganorkar, S.B., & Shirkhedkar, A.A. (2017). Novel HPTLC and UV-AUC analyses: for simple, economical, and rapid determination of Zileuton racemate. *Arabian Journal of Chemistry, 10* (3), 360-367. https://doi.org/10.1016/j.arabjc.2013.05.013

Rajat, G., & Panchali, D. (2014). A study on antioxidant properties of different bioactive compounds. *J. Drug Delivery Ther*, *4*(2), 105-115. https://doi.org/10.22270/jddt.v4i2.772

Gul, M. Z., Bhakshu, L. M., Ahmad, F., Kondapi, A. K., Qureshi, I. A., & Ghazi, I. A. (2011). Evaluation of *Abelmoschus moschatus* extracts for antioxidant, free radical scavenging, antimicrobial and antiproliferative activities using in vitro assays. *BMC complementary and alternative medicine*, *11*, 64. https://doi.org/10.1186/1472-6882-11-64

Gunawardana, S., & Jayasuriya, W. (2019). Medicinally important herbal flowers in Sri Lanka. *Evidence-based complementary and alternative medicine: eCAM*, 2321961. https://doi.org/10.1155/2019/2321961

Gupta, P., Patil, D., & Patil, A. (2019). Qualitative HPTLC phytochemical profiling of *Careya arborea* Roxb. bark, leaves and seeds. *3 Biotech*, *9*(8), 311. https://doi.org/10.1007/s13205-019-1846-x

Hazra, B., Das Sarma, M., & Sanyal, U. (2004). Separation methods of quinonoid constituents of plants used in Oriental traditional medicines. *Journal of chromatography. B, Analytical technologies in the biomedical and life sciences*, *812*(1-2), 259–275. https://doi.org/10.1016/j.jchromb.2004.08.007

Iraji, A., Panahi, Z., Edraki, N., Khoshneviszadeh, M., & Khoshneviszadeh, M. (2021). Design, synthesis, in vitro and in silico studies of novel schiff base derivatives of 2-hydroxy-

4-methoxybenzamide as tyrosinase inhibitors. *Drug development research*, *82*(4), 533–542. https://doi.org/10.1002/ddr.21771

Islam, M. K., Sostaric, T., Lim, L. Y., Hammer, K., & Locher, C. (2021). Development of an HPTLC-based dynamic reference standard for the analysis of complex natural products using Jarrah honey as test sample. *PloS one*, *16*(7), e0254857. https://doi.org/10.1371/journal.pone.0254857

Itankar, P. R., Sawant, D. B., Tauqeer, M., & Charde, S. S. (2015). High performance thin layer chromatography fingerprinting, phytochemical and physico-chemical studies of anti-diabetic herbal extracts. *Ayu*, *36*(2), 188–195. https://doi.org/10.4103/0974-8520.175546

Jamshidi-Aidji, M., Macho, J., Mueller, M.B., Morlock, G.E. (2019). Effect-directed profiling of aqueous, fermented plant preparations via high-performance thin-layer chromatography combined with in situ assays and high-resolution mass spectrometry. *Journal of Liquid Chromatography & Related Technologies 42*(9-10), 266–273. https://doi.org/ 10.1080/10826076.2019.1585631.

Jamshidi-Aidji, M., & Morlock, G. E. (2018). Fast equivalency estimation of unknown enzyme inhibitors in situ the effect-directed fingerprint, shown for *Bacillus* lipopeptide extracts. *Analytical chemistry*, *90*(24), 14260–14268. https://doi.org/10.1021/acs.analchem.8b03407

Jayasinghe, C. D., & Jayawardena, U. A. (2019). Toxicity assessment of herbal medicine using zebrafish embryos: A systematic review. *Evidence-based complementary and alternative medicine: eCAM*, 7272808. https://doi.org/10.1155/2019/7272808

Jugran, A. K., Rawat, S., Devkota, H. P., Bhatt, I. D., & Rawal, R. S. (2021). Diabetes and plant-derived natural products: from ethnopharmacological approaches to their potential for modern drug discovery and development. *Phytotherapy research: PTR*, *35*(1), 223–245. https://doi.org/10.1002/ptr.6821

Kaur, P., Gupta, R. C., Dey, A., Malik, T., & Pandey, D. K. (2020). Validation and quantification of major biomarkers in 'Mahasudarshan Churna'- an ayurvedic polyherbal formulation through high-performance thin-layer chromatography. *BMC complementary medicine and therapies*, *20*(1), 184. https://doi.org/10.1186/s12906-020-02970-z

Khalaf, R.A., Abdulla A,M., Mubarak, M.S., & Taha, M.O. (2011). Discovery of new β-D-glucosidase inhibitors via pharmacophore modeling and QSAR analysis followed by in silico screening. *Journal of molecular modelling*, *17* (3), pp. 443–464.

doi: 10.1007/s00894-010-0737-1.
Kharat, S., Namdeo, A., Mehta, P. (2017). Development and validation of HPTLC method for simultaneous estimation of curcumin and galangin in polyherbal capsule dosage form. *Journal of Taibah University for Science 11* (5), 775–781.
https://doi.org/ 10.1016/j.jtusci.2016.10.004.
Klingelhöfer, I., & Morlock, G. E. (2014). Sharp-bounded zones link to the effect in planar chromatography-bioassay-mass spectrometry. *Journal of chromatography. A, 1360*, 288–295.
https://doi.org/10.1016/j.chroma.2014.07.083
Kostić, M., Ivanov, M., Babić, S. S., Petrović, J., Soković, M., & Ćirić, A. (2020). An up-to-date review on bio-resource therapeutics effective against bacterial species frequently associated with chronic sinusitis and tonsillitis. *Current medicinal chemistry, 27*(41), 6892–6909.
https://doi.org/10.2174/0929867327666200505093143
Kotha, R. R., & Luthria, D. L. (2019). Curcumin: biological, pharmaceutical, nutraceutical, and analytical aspects. *Molecules (Basel, Switzerland), 24*(16), 2930.
https://doi.org/10.3390/molecules24162930
Kroslakova, I., Pedrussio, S., & Wolfram, E. (2016). Direct coupling of HPTLC with MALDI-TOF MS for qualitative detection of flavonoids on phytochemical fingerprints. *Phytochemical analysis: PCA*, *27*(3-4), 222–228.
https://doi.org/10.1002/pca.2621
Krüger, S., Hüsken, L., Fornasari, R., Scainelli, I., & Morlock, G. E. (2017). Effect-directed fingerprints of 77 botanical extracts via a generic high-performance thin-layer chromatography method combined with assays and mass spectrometry. *Journal of chromatography. A, 1529*, 93–106.
https://doi.org/10.1016/j.chroma.2017.10.068
Kunle, O.F., Egharevba, H.O. & Ahmadu, P.O. (2012). Standardization of herbal medicines - A review. *Int. J. Biodvers. Conserv. 4*(3), 101-112.
https://doi.org/10.5897/IJBC11.163.
Kuruppu, A. I., Paranagama, P., & Goonasekara, C. L. (2019). Medicinal plants commonly used against cancer in traditional medicine formulae in Sri Lanka. *Saudi pharmaceutical journal: SPJ: the official publication of the Saudi Pharmaceutical Society*, *27*(4), 565–573.
https://doi.org/10.1016/j.jsps.2019.02.004
Laub, A., Sendatzki, A. K., Palfner, G., Wessjohann, L. A., Schmidt, J., & Arnold, N. (2020). HPTLC-DESI-HRMS-based profiling of anthraquinones in complex mixtures-a proof-of-

concept study using crude extracts of Chilean mushrooms. *Foods (Basel, Switzerland)*, *9*(2), 156.
https://doi.org/10.3390/foods9020156
Liang, X., Nielsen, N. J., & Christensen, J. H. (2020). Selective pressurized liquid extraction of plant secondary metabolites: *Convallaria majalis* L. as a case. *Analytica chimica acta: X*, *4*, 100040.
https://doi.org/10.1016/j.acax.2020.100040
Lobo, V., Patil, A., Phatak, A., & Chandra, N. (2010). Free radicals, antioxidants and functional foods: impact on human health. *Pharmacognosy reviews*, *4*(8), 118–126.
https://doi.org/10.4103/0973-7847.70902
Maldini, M., D'Urso, G., Pagliuca, G., Petretto, G. L., Foddai, M., Gallo, F. R., Multari, G., Caruso, D., Montoro, P., & Pintore, G. (2019). HPTLC-PCA complementary to HRMS-PCA in the case study of *Arbutus unedo* antioxidant phenolic profiling. *Foods (Basel, Switzerland)*, *8*(8), 294.
https://doi.org/10.3390/foods8080294
Marston A. (2011). Thin-layer chromatography with biological detection in phytochemistry. *Journal of chromatography. A*, *1218*(19), 2676–2683.
https://doi.org/10.1016/j.chroma.2010.12.068
Mathon, C., Ankli, A., Reich, E., Bieri, S., & Christen, P. (2014). Screening and determination of sibutramine in adulterated herbal slimming supplements by HPTLC-UV densitometry. *Food additives & contaminants. Part A, Chemistry, analysis, control, exposure & risk assessment*, *31*(1), 15–20.
https://doi.org/10.1080/19440049.2013.861934
Medina-Franco J. L. (2019). New approaches for the discovery of pharmacologically-active natural compounds. *Biomolecules*, *9*(3), 115.
https://doi.org/10.3390/biom9030115
Migas, P., Romańczuk, A., Szumacher, M., & Krauze-Baranowska, M. (2020). Application of targeted 2D planar chromatography in the control of ginkgolic acids in some herbal drugs and dietary supplements. *Acta pharmaceutica (Zagreb, Croatia)*, *70*(2), 201–213.
https://doi.org/10.2478/acph-2020-0004
Mohan, S., Elhassan Taha, M. M., Makeen, H. A., Alhazmi, H. A., Al Bratty, M., Sultana, S., Ahsan, W., Najmi, A., & Khalid, A. (2020). Bioactive natural antivirals: an updated review of the available plants and isolated molecules. *Molecules (Basel, Switzerland)*, *25*(21), 4878.
https://doi.org/10.3390/molecules25214878

Mohotti, S., Rajendran, S., Muhammad, T., Strömstedt, A. A., Adhikari, A., Burman, R., de Silva, E. D., Göransson, U., Hettiarachchi, C. M., & Gunasekera, S. (2020). Screening for bioactive secondary metabolites in Sri Lankan medicinal plants by microfractionation and targeted isolation of antimicrobial flavonoids from *Derris scandens*. *Journal of ethnopharmacology*, *246*, 112158.
https://doi.org/10.1016/j.jep.2019.112158
Moon, K. M., Kwon, E. B., Lee, B., & Kim, C. Y. (2020). Recent trends in controlling the enzymatic browning of fruit and vegetable products. *Molecules (Basel, Switzerland)*, *25*(12), 2754.
https://doi.org/10.3390/molecules25122754
Móricz, Á. M., Lapat, V., Morlock, G. E., & Ott, P. G. (2020). High-performance thin-layer chromatography hyphenated to high-performance liquid chromatography-diode array detection-mass spectrometry for characterization of coeluting isomers. *Talanta*, *219*, 121306.
https://doi.org/10.1016/j.talanta.2020.121306
Morlock, G., & Schwack, W. (2010). Hyphenations in planar chromatography. *Journal of chromatography. A*, *1217*(43), 6600–6609.
https://doi.org/10.1016/j.chroma.2010.04.058
Morlock, G. E., & Heil, J. (2020). HI-HPTLC-UV/Vis/FLD-HESI-HRMS and bioprofiling of steviol glycosides, steviol, and isosteviol in Stevia leaves and foods. *Analytical and bioanalytical chemistry*, *412*(24), 6431–6448.
https://doi.org/10.1007/s00216-020-02618-4
Morlock, G. E., Heil, J., Inarejos-Garcia, A. M., & Maeder, J. (2021). Effect-directed profiling of powdered tea extracts for catechins, theaflavins, flavonols and caffeine. *Antioxidants (Basel, Switzerland)*, *10*(1), 117.
https://doi.org/10.3390/antiox10010117
Mühlberg, E., Umstätter, F., Kleist, C., Domhan, C., Mier, W., & Uhl, P. (2020). Renaissance of vancomycin: approaches for breaking antibiotic resistance in multidrug-resistant bacteria. *Canadian journal of microbiology*, *66*(1), 11–16.
https://doi.org/10.1139/cjm-2019-0309
Mulaudzi, N., Anokwuru, C. P., Tankeu, S. Y., Combrinck, S., Chen, W., Vermaak, I., & Viljoen, A. M. (2021). Phytochemical profiling and quality control of *Terminalia sericea* Burch. ex DC. using HPTLC metabolomics. *Molecules (Basel, Switzerland)*, *26*(2), 432.
https://doi.org/10.3390/molecules26020432

Nile, S. H., & Park, S. W. (2014). HPTLC analysis, antioxidant and antigout activity of Indian plants. *Iranian journal of pharmaceutical research: IJPR*, *13*(2), 531–539.
Ntie-Kang, F. & Svozil, D. (2020). An enumeration of natural products from microbial, marine and terrestrial sources. *Physical Sciences Reviews, 5*(8), 20180121. https://doi.org/10.1515/psr-2018-0121
Ong E. S. (2004). Extraction methods and chemical standardization of botanicals and herbal preparations. *Journal of chromatography. B, Analytical technologies in the biomedical and life sciences*, *812*(1-2), 23–33. https://doi.org/10.1016/j.jchromb.2004.07.041
Osathanunkul, M., Osathanunkul, R., & Madesis, P. (2018). Species identification approach for both raw materials and end products of herbal supplements from *Tinospora* species. *BMC complementary and alternative medicine*, *18*(1), 111. https://doi.org/10.1186/s12906-018-2174-0
Ozaslan, M., & Oguzkan, S. B. (2018). Use of plant extracts in alternative medicine. *Pakistan journal of biological sciences: PJBS*, *21*(1), 1–7. https://doi.org/10.3923/pjbs.2018.1.7
Pham, J. V., Yilma, M. A., Feliz, A., Majid, M. T., Maffetone, N., Walker, J. R., Kim, E., Cho, H. J., Reynolds, J. M., Song, M. C., Park, S. R., & Yoon, Y. J. (2019). A review of the microbial production of bioactive natural products and biologics. *Frontiers in microbiology*, *10*, 1404. https://doi.org/10.3389/fmicb.2019.01404
Pillaiyar, T., Manickam, M., & Namasivayam, V. (2017). Skin whitening agents: medicinal chemistry perspective of tyrosinase inhibitors. *Journal of enzyme inhibition and medicinal chemistry*, *32*(1), 403–425. https://doi.org/10.1080/14756366.2016.1256882
Rab, R. A., Zahiruddin, S., Ibrahim, M., Husain, F., Parveen, R., Khan, W., Ahmad, F. J., Khan, A. A., & Ahmad, S. (2020). HPTLC and UPLC-MS/MS methods for quality control analysis of Itrifal formulations of Unani system of medicine. *Journal of AOAC International*, *103*(3), 649–658. https://doi.org/10.5740/jaoacint.19-0231
Ranasinghe, P., Galappaththy, P., Constantine, G. R., Jayawardena, R., Weeratunga, H. D., Premakumara, S., & Katulanda, P. (2017). *Cinnamomum zeylanicum* (Ceylon cinnamon) as a potential pharmaceutical agent for type-2 diabetes mellitus: study protocol for a randomized controlled trial. *Trials*, *18*(1), 446. https://doi.org/10.1186/s13063-017-2192-0

Ruwizhi, N., & Aderibigbe, B. A. (2020). Cinnamic acid derivatives and their biological efficacy. *International journal of molecular sciences*, *21*(16), 5712. https://doi.org/10.3390/ijms21165712

Sahoo, S., & S, B. (2019). Pharmacogenomic assessment of herbal drugs in affective disorders. *Biomedicine & pharmacotherapy*, *109*, 1148–1162. https://doi.org/10.1016/j.biopha.2018.10.135

Sakkas, H., & Papadopoulou, C. (2017). Antimicrobial activity of basil, oregano, and thyme essential oils. *Journal of microbiology and biotechnology*, *27*(3), 429–438. https://doi.org/10.4014/jmb.1608.08024

Saravanan, D., & Asharani, I. V. (2016). HPTLC analysis and in-vitro antioxidant, anti-inflammatory and anti-diabetic activities of ethanol extract of leaves of *Actinodaphne madraspatana* Bedd. *Pakistan journal of pharmaceutical sciences*, *29*(1), 193–200.

Sen, T., & Samanta, S. K. (2015). Medicinal plants, human health and biodiversity: a broad review. *Advances in biochemical engineering/biotechnology*, *147*, 59–110. https://doi.org/10.1007/10_2014_273

Sharma, A., Flores-Vallejo, R., Cardoso-Taketa, A., & Villarreal, M. L. (2017). Antibacterial activities of medicinal plants used in Mexican traditional medicine. *Journal of ethnopharmacology*, *208*, 264–329. https://doi.org/10.1016/j.jep.2016.04.045

Shewiyo, D. H., Kaale, E., Risha, P. G., Dejaegher, B., Smeyers-Verbeke, J., & Vander Heyden, Y. (2012). HPTLC methods to assay active ingredients in pharmaceutical formulations: a review of the method development and validation steps. *Journal of pharmaceutical and biomedical analysis*, *66*, 11–23. https://doi.org/10.1016/j.jpba.2012.03.034

Shivatare, R. S, Nagore, D.H., & Nipanikar, S.U. (2013). 'HPTLC' an important tool in standardization of herbal medical product: a review. *Journal of Scientific and Innovative Research, 2*(6), 1086-1096.

Simões-Pires, C. A., Hmicha, B., Marston, A., & Hostettmann, K. (2009). A TLC bioautographic method for the detection of alpha- and beta-glucosidase inhibitors in plant extracts. *Phytochemical analysis: PCA*, *20*(6), 511–515. https://doi.org/10.1002/pca.1154

Singh, M., Kamal, Y. T., Khan, M. A., Parveen, R., Ansari, S. H., & Ahmad, S. (2015). Matrix solid-phase dispersion extraction and quantification of alpinetin in *Amomum* seed

using validated HPLC and HPTLC methods. *Indian journal of pharmaceutical sciences*, *77*(1), 49–54. https://doi.org/10.4103/0250-474x.151597

Spangenberg, B., Poole, C.F. & Weins, C. (2011). Quantitative thin-layer chromatography. A practical survey. Berlin, Springer.

Sticher O. (2008). Natural product isolation. *Natural product reports*, *25*(3), 517–554. https://doi.org/10.1039/b700306b

Theiler, B. A., Istvanits, S., Zehl, M., Marcourt, L., Urban, E., Caisa, L. O., & Glasl, S. (2017). HPTLC bioautography guided isolation of α-glucosidase inhibiting compounds from *Justicia secunda* Vahl (Acanthaceae). *Phytochemical analysis: PCA*, *28*(2), 87–92. https://doi.org/10.1002/pca.2651

Tran, N., Pham, B., & Le, L. (2020). Bioactive compounds in anti-diabetic plants: from herbal medicine to modern drug discovery. *Biology*, *9*(9), 252. https://doi.org/10.3390/biology9090252

Trifunović, J., Borčić, V., Vukmirović, S., & Mikov, M. (2017). Assessment of the pharmacokinetic profile of novel s-triazine derivatives and their potential use in treatment of Alzheimer's disease. *Life sciences*, *168*, 1–6. https://doi.org/10.1016/j.lfs.2016.11.001

Ullah, Q., Mohammad, A. (2020). Vitamins determination by TLC/HPTLC—a mini-review. *JPC-J Planar Chromat 33*(5), 429–437. DOI: 10.1007/s00764-020-00051-y.

Urbain, A., Simões-Pires, C.A. (2006), Thin-layer chromatography for the detection and analysis of bioactive natural products, *Encyclopaedia of Analytical Chemistry*, 1-29, John Wiley & Sons Ltd.

Van Andel, T., Scholman, A., & Beumer, M. (2018). Icones Plantarum Malabaricarum: early 18th century botanical drawings of medicinal plants from colonial Ceylon. *Journal of ethnopharmacology*, *222*, 11–20. https://doi.org/10.1016/j.jep.2018.04.033

Vavricka, C. J., Christensen, B. M., & Li, J. (2010). Melanization in living organisms: a perspective of species evolution. *Protein & cell*, *1*(9), 830–841. https://doi.org/10.1007/s13238-010-0109-8

Weiss, S. C., Egetenmeyer, N., & Schulz, W. (2017). Coupling of in vitro bioassays with planar chromatography in effect-directed analysis. *Advances in biochemical engineering/biotechnology*, *157*, 187–224. https://doi.org/10.1007/10_2016_16

Wightman E. L. (2017). Potential benefits of phytochemicals against Alzheimer's disease. *The Proceedings of the Nutrition Society*, *76*(2), 106–112. https://doi.org/10.1017/S0029665116002962

Woehrlin, F., Fry, H., Abraham, K., & Preiss-Weigert, A. (2010). Quantification of flavoring constituents in cinnamon: high variation of coumarin in cassia bark from the German retail market and in authentic samples from Indonesia. *Journal of agricultural and food chemistry*, *58*(19), 10568–10575. https://doi.org/10.1021/jf102112p

Wu B. (2014). Tyrosinase inhibitors from terrestrial and marine resources. *Current topics in medicinal chemistry*, *14*(12), 1425–1449. https://doi.org/10.2174/1568026614666140523115357

Wu, H., Guo, J., Chen, S., Liu, X., Zhou, Y., Zhang, X., & Xu, X. (2013). Recent developments in qualitative and quantitative analysis of phytochemical constituents and their metabolites using liquid chromatography-mass spectrometry. *Journal of pharmaceutical and biomedical analysis*, *72*, 267–291. https://doi.org/10.1016/j.jpba.2012.09.004

Yanakiev S. (2020). Effects of cinnamon (*Cinnamomum* spp.) in dentistry: a review. *Molecules (Basel, Switzerland)*, *25*(18), 4184. https://doi.org/10.3390/molecules25184184

Yang, L., Wen, K. S., Ruan, X., Zhao, Y. X., Wei, F., & Wang, Q. (2018). Response of plant secondary metabolites to environmental factors. *Molecules (Basel, Switzerland)*, *23*(4), 762. https://doi.org/10.3390/molecules23040762

Yang, Z., Zhang, X., Duan, D., Song, Z., Yang, M., & Li, S. (2009). Modified TLC bioautographic method for screening acetylcholinesterase inhibitors from plant extracts. *Journal of separation science*, *32*(18), 3257–3259. https://doi.org/10.1002/jssc.200900266

Zhang, Y., Cao, Y., & Wang, H. (2020). Multi-interactions in ionic liquids for natural product extraction. *Molecules (Basel, Switzerland)*, *26*(1), 98. https://doi.org/10.3390/molecules26010098